Awarded Ph.D.

Veeravadas
16.4.66.

LOW TEMPERATURE CALORIMETRIC STUDIES

OF

SOME TRANSITION METAL PEROVSKITES

PART - I

A THESIS SUBMITTED TO THE
UNIVERSITY OF POONA
FOR THE DEGREE
OF
DOCTOR OF PHILOSOPHY

C. DEENA DAS, M.Sc.
NATIONAL CHEMICAL LABORATORY,
POONA, 8.

1966

C O N T E N T S

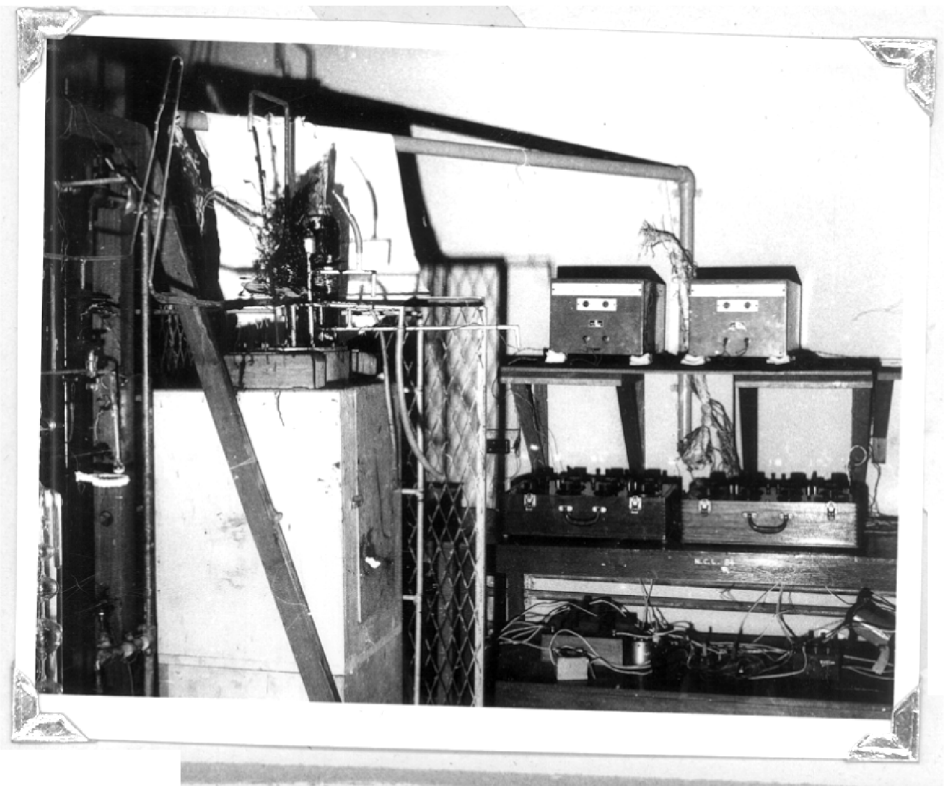

CHAPTER - I

INTRODUCTION

Considerable attention is being given to the investigations of the thermal properties of substances over a broad range of temperatures as they provide basic data for thermodynamic functions for which there is a great demand in many areas of science and technology. Statistical thermodynamic and quantum mechanical analyses of these results provide deeper insight into the details of their molecular structure, electronic energy level pattern and the mechanism of various processes such as order-disorder transitions, phase transformations, occurring in a solid. The experimental findings can often be compared with the theoretical predictions and also be correlated with the results of other solid state electrical, magnetic and lattice dynamical properties.

The production of low temperatures and results of cryogenic investigations are also finding rapid application to commercial and military uses, viz. masers, superconducting computers, high field magnets, cryogenic fuels and isotopic separation.

In this dissertation we are concerned with studies of low temperature heat capacities which provide an extraordinary wealth of information about substances. It may be worthwhile to review briefly developments of some

typical areas of cryogenic calorimetric studies of our interest. No comprehensive survey of these areas has been attempted as these are well described in several recent reviews.[1,2]

There are two principle mechanisms for the absorption of heat by a solid: one, through atomic vibrations and the other, through increased kinetic energy of electrons. The latter factor becomes increasingly important at very low temperatures (below 20°K) but not so at ordinary temperatures since only a fraction of electrons near the Fermi surface are excited. The energy absorption is then predominently through the lattice vibrations. The differential increase of energy with temperature, given by the ratio $(\frac{\partial E}{\partial T})_v = C_v$, is known as the heat capacity at constant volume. Usually C_p, heat capacity at constant pressure, is measured and C_v evaluated from the well known relation $C_p - C_v = \frac{9\alpha^2 VT}{\beta}$, where α is the linear thermal expansion coefficient, V, the specific volume, T, the absolute temperature and β, the compressibility coefficient. Thus the heat capacity as a function of temperature gives considerable insight about the mechanism by which energy is absorbed.

Measurement of C_p, of various phases (x_1, x_2.....x_r) together with enthalpy increments, ΔH_r occurring reversibly at temperatures, T_r permits evaluation of standard enthalpy and entropy (S) of a substance, respectively, by the equations.

$$H_T - H_0 = \int_0^{T_1} C_{p,x_1} dT + \Delta H_1 + \int_{T_1}^{T_2} C_{p,x_2} dT + \Delta H_2 +$$

$$\ldots\ldots + \int_{T_r}^{T} C_{p,x_r} dT$$

$$S_T - S_0 = \int_0^{T_1} \frac{C_{p,x_1}}{T} dT + \frac{\Delta H_1}{T_1} + \int_{T_1}^{T_2} \frac{C_{p,x_2}}{T} dT + \frac{\Delta H_2}{T_2} +$$

$$\ldots\ldots + \int_{T_r}^{T} \frac{C_{p,x_r}}{T} dT$$

Entropy is related to the manner of the arrangement of the entities that make up a system whereas enthalpy is related to the forces holding them together. These functions may be combined to yield the standard Gibbs energy function for the substance.

$$\frac{F_T - H_0}{T} = \frac{H_T - H_0}{T} - S_T$$

The change in Gibbs energy ΔF_T is related to the equilibrium constant K, of a reaction by the equation $\Delta F_T = -RT\ln K$ where R is the gas constant.

The availability of the values of the thermodynamic functions, inter alia, enables generally either to control or predict chemical behaviour, and therefore compilations of such data are being made through the efforts of the International Union of Pure and Applied Chemistry.

According to the classical law of Dulong and Petit, atomic $C_v = 3R$ or 6 cal.deg.$^{-1}$ and is independent of temperature. The first important relation of heat capacity change with temperature of solids, was given by Einstein[3] on quantum mechanical considerations assuming that the system of atoms in a crystal vibrate as independent harmonic oscillators with the same frequency ν. Soon after Debye[4] improved it by assuming that the crystal has a whole spectrum of frequencies from ν_o to ν_m where the ν_m is the maximum frequency allowed. As the temperature is increased, the distribution of frequencies is moved towards the upper end and ultimately at a temperature θ, called the Debye temperature, all the frequencies would be close to ν_m where the Einstein model becomes essentially valid. According to the Debye and Einstein equations C_v tends to vanish at $0^{\circ}K$ is approached and at high temperatures approximates to the Dulong and Petit limit of 3R.

In contrast with the continuum isotropic medium assumed by Debye, Born and Karman[5] gave a complicated treatment based on the periodic boundary condition and near neighbour interactions. Blackman[6] extended these calculations taking into account also the next nearest neighbour interactions. Several reviews[7,8,9] have given exhaustive account of these and related theories. In general, it may be stated that heat capacity behaviour is semiquantitatively explained in terms of the Debye theory and more accurately by the lattice dynamical theories.

Most of the earlier work on heat capacity measurements was concerned with the testing of the third law of thermodynamics which states that the entropy of all substances approaches zero at $0^{\circ}K$ and does so in the case of a perfectly crystalline solid. However, any randomness in the arrangement of molecules at lattice sites would result in a finite entropy even at $0^{\circ}K$. Extreme examples are found in vitreous solids which have the same orientational disorder as liquids. Thus Giauque and Gibson[10] observed a residual entropy of 5.6 $cal.deg.^{-1}mole.^{-1}$ at absolute zero in the glassy state of glycerine.

For crystals whose energy spectra are composed of normal vibrational motion of their constituent atoms, C_v versus T plots are usually characterised by sigmoid shape curves. As typical examples may be mentioned the tetrafluorides of the group IV B elements of the periodic table observed in the range $5-350^{\circ}K$ by Westrum *et al.*[11]

According to the Debye equation C_v at low temperatures would be proportional to the cube of temperature (T^3). However, there are many crystalline substances which are anisotropic due to their lamellar or fibrous structures and thus deviate strongly from the Debye model.

Theoretically Debye-like equations have been developed by Tarasov[12] and by others.[13,14] Tarasov's limiting law predicts $C_v \propto T^2$ for a lamellar crystal and $C_v \propto T$ for a

fibrous crystal. Crystalline molybdenum trioxide and disulphide[15] may be taken as representatives of the lamellar type and selenium and tellurium[16] as those of the fibrous type.

Newell[17] has criticised this law, however, on the grounds that any physically acceptable theory must predict a T^3 law at sufficiently low temperatures. Thus graphite[18] which follows Tarasov's limiting law above 15°K indicates a $T^{2.4}$ dependence at 4°K. Similarly boron nitride[19] shows T^3 dependence at very low temperatures but follows Tarasov's law at slightly higher temperatures. On the basis of these considerations it may be contended that $C_v = aT^x$ where the exponent x gradually decreases from a value of 3 at the lowest temperature region to probably zero at sufficiently high temperatures.

The Electronic Specific Heat

The primary interest in measurement of the electronic specific heat, C_e stems from the fact that it allows an evaluation of the density states, $N(E^*)$ at the Fermi energy, E^*, in the energy band. Usually, studies are confined to metals and the electronic specific heat coefficient γ, is calculated from the equation

$$C_p = C_v = aT^3 + \gamma T$$

where the measurements are done at liquid helium temperatures so that C_e becomes a significantly important fraction of the

total observed C_p. From C_e the number of electrons per atom n_a, can be calculated from the expression.

$$C_e = 3.26 \times 10^{-5} V^{2/3} n_a^{1/3} T \text{ cal./mole.deg.}$$

where V, is the molar volume of the metal, m, the free electronic mass and n_a the number of electrons per $cm.^3$

However, it is necessary to modify the above formulation of C_e when considering the partially bound electrons. In the transition metals contributions to C_e by the electrons in the unfilled d-band are predominant, since due to their tighter binding the d-electrons show a much narrower band than the S electrons and so have a greater number of energy levels per unit energy range. A discussion on the recent developments on the electronic specific heat in metals has been given by Daunt.[20]

The value of γ calculated from low temperature heat capacity measurements, is likely to be in error if there is a contribution to C_p from the excitation process of the Schottky type.[21]

This latter type occurs when the lowest energy state of an ion in a crystal is composed of two or more levels which are separated by a small energy kT'. At temperatures very much below T' the ions cannot be excited to the upper levels and will all be in the lowest state. As temperature T' is approached, some of the ions will be excited to the

higher states. As this requires additional energy there will be extra specific heat in this region. Above T' there is no further excitation and hence specific heat behaves normally. The extra entropy associated with Z number of separate energy levels for an ion is given by

$$S_{Schottky} = R \log_e Z .$$

Such type of an anomaly has been observed by Burns et al.[11] at 6.4°K, in the case of WF_4. Heat capacity of $(NH_4)_2CuCl_4.2H_2O$ has been found[22] to exhibit a maximum at 200.5°K. The extraordinary broadness of the anomaly, as well as a small jump of C_p at the transition point, has been ascribed to the weak interaction between the ammonium ions in this crystal. The broad hump above the transition point is assumed to be due to a Schottky anomaly, based on the population difference of the individual ammonium ion between the two sites of different energies associated with the different chlorine ions, in the disordered state. In one possible orientation of the ammonium ion, all the four protons are directed to the chlorine ions hydrogen bonded with the crystalline water, while in the other all protons are directed to the free chlorine ions.

Order-Disorder Transitions

The recent thermal studies by Suga et al.[23] on potassium cyanide are interesting. The heat capacity shows anomalies at 82.9°, 168.3°K and a small hump at 190°K.

The λ-shaped cooperative transition at 82.9°K with an entropy change of Rln2 is due to the orientational order-disorder rearrangement of the cyanide ion with respect to its head and tail. A perfectly ordered structure for the orientation of the cyanide ions has been suggested.

The crystal undergoes a phase transition at 168.3°K. According to Bijvoet and Lery[24] the cyanide ions either rotate freely or are oriented randomly in eight body diagonal directions in the cubic-phase, while they are all parallel to the b-axis of the orthorhombic lattice of the low temperature phase. After repeated temperature cycles, a broad thermal anomaly was located at about 158°K corresponding to the intermediate monoclinic-orthorhombic transformation previously observed by Ubbelohde and co-workers[25,26] from X-ray studies. The small anomaly at 190°K seems to be associated with some change in higher order structural defects in the transition at 168.3°K.

A phase found below the melting temperature in crystals made up of globulaire, Timmermans[27] named it plastic crystal. They are generally characterised by a low entropy of fusion, high triple-point temperature, easy deformability, high symmetry and one or more energetic transitions in the solid state.

A sharp transition in the heat capacity of triethylene diamine at 351.08°K associated with the transformation to the plastically crystalline state was observed by

Treubridge et al.[28] The entropy of transition was 7.19 e.u. Fusion occurs at 432.98°K with an entropy increment of 4.10 e.u. confirming the classification of the substance under plastic crystals.

Two anomalies in the heat capacity of triethanolamine borate at 466.54°K and 511.86°K were observed.[29] The first transition was attributed to a solid-solid transformation with low entropy of transition and the second to melting with high entropy of fusion (11.26 e.u.) thus indicating that high symmetry alone is not sufficient to ensure the existence of plastic crystal phase.

Ferroelectric Transitions

Since energy must be supplied to destroy the spontaneous polarization of a ferroelectric crystal, the heat capacity is expected to reveal a peak or hump in those regions where the spontaneous polarization is changing with the temperature.

The heat capacity measurement of crystalline potassium ferrocyanide trihydrate by Nakagawa et al.[30] revealed a hump at about 248°K corresponding to the ferroelectric transition temperature, while that of the anhydrous salt exhibits[31] a normal behaviour at this temperature, indicating that water molecules of the hydrate are responsible for the ferroelectric effect.

Magnetic Transitions

Many ionic compounds containing elements with partially filled d or f shells have a pattern of electronic energy levels such that a completely ordered form with more or less zero entropy value at low temperature changes to a nearly random distribution among several electronic states at higher temperature. Because of the magnetic moment accompanying the spin and orbital angular momenta of the electrons, these substances may thus be antiferromagnetic or ferromagnetic in the low temperature and paramagnetic in the higher temperature regions. This change may be called a magnetic transition and the corresponding transition temperature as the Néel or Curie point (T_N or T_C).

It may be mentioned that the number of antiferromagnetic substances is much larger than the corresponding ferromagnetic substances. Thus at present many of the properties appearing when normally paramagnetic substances are cooled down to low temperature, may be explained by assuming the onset of antiferromagnetism below a transition temperature, T_N.

The first theory of antiferromagnetism was suggested by Néel.[32] He divided the crystalline lattices of the magnetic atoms into two sublattices supposing that each magnetic atom in one of the lattices experiences a molecular field proportional to the opposite of the magnetization of

the other sublattice. Néel's original theory has been extended in several respects by Bitter,[33] Van Vleck,[34] Anderson,[35] Nagamiya,[36] Yosida[37] and Slater[38] as well as by Néel himself.[39] There are several recent review articles on antiferromagnetism.[40] Here we shall only mention a few points and typical examples of the behaviour of magnetic salts at low temperatures.

As indicated before, the majority of the substances which show antiferromagnetic properties are ionic crystals in which the magnetic ions are separated from each other by the anions O, S, F etc. and show a strong antiferromagnetic exchange coupling between next to nearest magnetic ions transmitted via the intervening anions. The mechanism of superexchange was proposed by Kramers[41] to explain the magnetic behaviour of paramagnetic salts and Bizette[42] and Neel[39] emphasized the importance of this interaction mechanism in antiferromagnetic substances. The interaction energy may be described as an exchange energy

$$\sum - 2 J_{ij} \vec{S}_i \vec{S}_j$$

where J_{ij} is the exchange integral between the i^{th} and j^{th} atoms and $\vec{S}_i$ and $\vec{S}_j$ are the spin angular vectors measured in units of h. A positive J corresponds to a ferromagnetic interaction and a negative J to an antiferromagnetic interaction.

If the magnetic ion has more than half-filled shell, the transferred electron will set its spin antiparallel

according to the Pauli's principle leading to antiferromagnetic coupling, while that with less than half-filled shell produces parallel orientation according to the Hund rule effect leading to ferromagnetic coupling. Thus MnTe exhibits antiferromagnetic and CrTe ferromagnetic behaviour. Shimizu[43] pointed out that, contrary to prediction, antiferromagnetism is observed in some compounds of magnetic ions with a less than half-filled shell. In such cases the large number of allowed antiparallel configurations may compensate for their energies being higher than those of parallel configurations. Polder[44] suggested that the crystalline field may also lower the energy of the antiparallel configurations.

Several experimental techniques are available for investigating the magnetic structure of compounds : (a) neutron diffraction, (b) X-ray diffraction, (c) nuclear magnetic resonance and paramagnetic resonance absorption, (d) magnetic susceptibility and (e) thermal studies such as heat capacity.

The most direct method of determining the arrangement of spins in a magnetic crystal is that of neutron diffraction. Neutrons are scattered by the nuclei and by the magnetic moment of the atoms. From the diffraction pattern and superstructure lines the direction of positive and negative spins can be ascertained. Shull and coworkers[45] determined the magnetic structures of a large number of compounds such as MnO, MnS, MnSe, CoO, FeO, NiO using this

technique. For MnO, the structure consists of parallel sheets (111 planes) within which all the Mn^{2+} ions are arranged ferromagnetically, but with the antiferromagnetic - coupling between neighbouring sheets. Of the 12 nearest neighbours surrounding any Mn^{2+} one half is oriented parallel to the central ion and the other half antiparallel. Similar structures have been observed in the other compounds.

X-ray analysis also gives an indication of super-structure, though indirectly. Rooksby and Tombs[46] have shown that tetragonal or rhombohedral symmetries may occur in MnO, FeO and NiO which have face centred cubic structures above the Néel temperature. Also anomalous changes of lattice positions without change of the lattice type[47] have been observed. These effects are small and therefore are not of great precision.

Nuclear and paramagnetic resonance absorption techniques can be applied for elucidating magnetic structure but have not yet found wide applications in the study of antiferromagnetics.

Susceptibility is proportional to the effective magnetic moment and hence usually peaks are observed at T_C or T_N. The magnetic susceptibility of $NiCl_2$ increases with decrease of temperature[48] until it reaches a maximum at 50°K, below which it almost remains constant.

Antiferromagnetism is a new domain of research providing scope for many interesting developments. The exact behaviour of these substances at the Neel point T_N where long range order changes to short range order is experimentally as well as theoretically little understood. A study of the specific heat vs temperature behaviour would provide very valuable experimental data for developing or testing theoretical models of order-disorder transition processes. Besides it provides data for evaluation of chemical thermodynamic functions such as entropy, enthalpy and free energy changes associated with such transitions. The calorimetric method is sensitive and precise and compared to susceptibility measurements less subject to being masked by traces of ferromagnetic impurities.

The heat capacity measurements of $NiCl_2$ by Busey and Giauque[49] revealed a maximum at 52.35°K in excellent agreement with the susceptibility data. Stout et al.[50] observed λ-type specific heat anomalies at 37.7°K and 73.22°K respectively for CoF_2 and NiF_2 in accord with the neutron diffraction data of Erickson.[51]

Recently antiferromagnetism at low temperatures has been observed[52] in complex fluorides of the type KMF_3 where M = Mn, Co, Ni, Cu etc., which crystallize in the perovskite-like structures. The divalent magnetic ions are arranged at the body centre of the cubic lattice with F^- in the centre of each two adjacent magnetic ions. $KMnF_3$, $KCoF_3$,

and $KNiF_3$ show the so-called G-type antiferromagnetic structure i.e. the central magnetic ion is coupled anti-parallel to its six neighbours. In $KCuF_3$ A-type antiferromagnetism wherein there is a ferromagnetic coupling within a layer but antiferromagnetic coupling in the successive layers may be observed (fig.1). Such structures have also been observed in several double oxides.[53] Superexchange interaction between adjacent M^{2+} ions via the intermediate F^- ion is considered to play dominant role in the magnetic properties of the compounds.

The magnetic susceptibility measurements by Machin et al.[54] and by Hirakawa et al.[52] revealed a difference by as much as 21°K in the Neel temperatures of $KCoF_3$. Besides, for $KCuF_3$ Machin et al.[54] detected a maximum in the susceptibility at 215°K which is considerably lower than that (243°K) reported by Okazaki et al.[55] from X-ray diffraction measurements. Surprisingly no magnetic ordering has been observed by Scatturin et al.[56] in their neutron diffraction study of the compound.

In view of the current interest in antiferromagnetic compounds and inconsistent results obtained by various techniques, we have been prompted to undertake an investigation on the heat capacity behaviour of these compounds. Such studies have not been reported in the literature so far and are presented in Part II of this thesis.

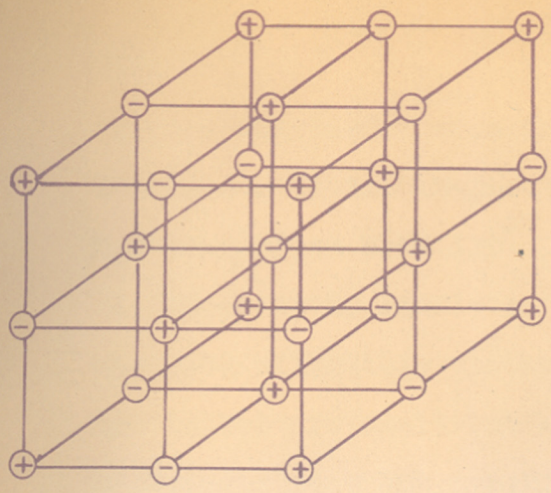

G-TYPE ANTIFERROMAGNETIC STRUCTURE

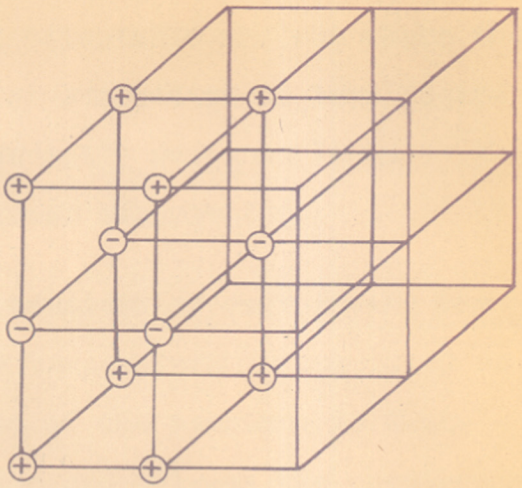

A-TYPE ANTIFERROMAGNETIC STRUCTURE

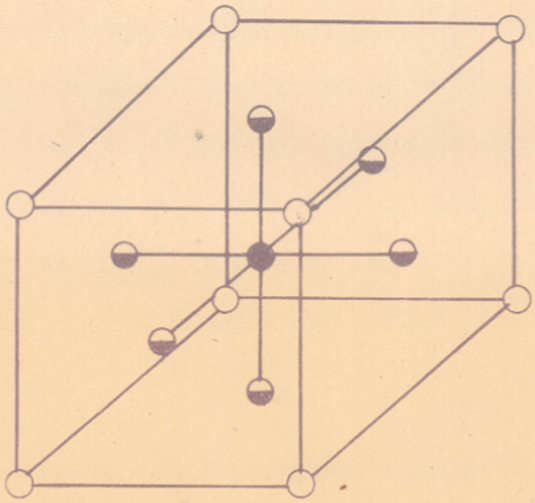

ROOM TEMPERATURE PEROVSKITE CUBIC UNIT CELL

FIG. 1

A review of the more important developments in the techniques of low temperature calorimetry in recent years has been given by Hill.[57] In all types of calorimetry, the accuracy is liable to be limited by heat losses, and one must ultimately choose between an experiment in which the losses are small but not calculable and one where these are significant but capable of evaluation to some degree of approximation. These are generally referred to as (A) adiabatic and (B) isothermal calorimeters.

The adiabatic method consists of surrounding the specimen with a shield whose temperature is regulated so as always to be equal to that of the specimen so that, ideally, there is no heat exchange between the specimen and its shield and the former can be heated adiabatically. In the isothermal type, the temperature of the environment of the calorimeter is maintained a little above the expected mean temperature after the energy input into it. Heat exchange between the calorimeter and its environment (radiation shield) is evaluated from observations of the temperature drift before and after the energy input into the specimen.

In an adiabatic calorimeter, temperature differences between the calorimeter and the shield are detected by a differential thermocouple and regulation to a few millidegrees or better is necessary at all temperatures. Copper-constantan or chromel-constantan thermocouples normally used

for the above purpose are quite insensitive at low temperatures. Further, the thermocouples themselves provide a route for heat exchange and it cannot thus be assumed that strict adiabatic conditions have been achieved. As corrections for heat loss cannot be applied, a good deal of work has been done on thermoregulator to obtain high precision and control. This especially requires lot of instrumentation and automation. On the otherhand, isothermal calorimeter with heat exchange corrections calculable is capable of giving more accurate results particularly at low temperatures. Moreover, this type of calorimeter can be constructed and operated with limited instrumental facilities.

In view of the above, including limited workshop and laboratory facilities available to us, a low temperature isothermal calorimeter has been constructed. In what follows, (Part I) the details of the construction and operation of the same in the range 80-300°K are described.

REFERENCES

(1) Westrum, E.F., J. Chem. Ed. 38, 443-57 (1961);
J. Pure & Appl. Chem. 8, 187 (1964).

(2) Rosenberg, H.M., Low temperature solid state physics, (The Clarendon Press, Oxford) pp.1-35 (1963).

(3) Einstein, A., Ann. Physik. 22, 800 (1907).

(4) Debye, P., Ann. Physik. 39, 782 (1912).

(5) Born, M., and Van Karman, T., Z. Physik, 13, 297 (1912).

(6) Blackman, M., Proc. Roy. Soc. A148, 365-406 (1935).

(7) Launey, J.D., The theory of specific heats and lattice vibrations, Solid State Physics Vol.2 (Academic Press Inc. N.Y.) p.220-306 (1956).

(8) Mitra, S.S., Vibration spectra of solids, Solid State Physics, Vol.13 (Academic Press Inc. N.Y.) pp.1-80 (1962).

(9) Maradudin, A.A., Montroll, E.W. and Weiss, G.H., Theory of lattice dynamics in the harmonic approximation. Supplement.3, Solid State Physics (Academic Press Inc. N.Y.) (1963).

(10) Gibson, G.E. and Giauque, W.F., J. Am. Chem. Soc., 45, 93-104 (1923).

(11) Osborne, D.W., Westrum, E.F.(Jr.) and Lohr, H.R., J. Am. Chem. Soc., 77, 2737-39 (1955);

Burns, J.H., Osborne, D.W. and Westrum, E.F. (Jr.), J. Chem. Phys., 33, 387-94 (1960);

Lohr, H.R., Osborne, D.W. and Westrum, E.F. (Jr.), J. Am. Chem. Soc., 76, 3837-39 (1954); and

Buller, R.D. and Westrum, E.F.(Jr.), J. Phys. Chem., 65, 132-134 (1961).

(12) Tarasov, V.V., Dokl. Akad. Nank. SSSR. 46, 20, 110 (1945)
ibid 84, 321 (1952).

(13) Gurney, R.W., Phys. Rev., 88, 465-66 (1952);
Bouman, J.C. and Krumhanse, J.A., J. Phys. Chem. Solids, 6, 367-79 (1958).

(14) Yoshimori, A. and Kitano, Y., J. Phys. Soc. Japan, 11, 352-61 (1956).

(15) Smith, D.F., Brown, D., Dwerkin, A.S., Sasmor, D.J. and Van Artsdalen, E.R., J. Am. Chem. Soc., 78, 1533-36 (1956).

(16) DeSorbo, W., J. Chem. Phys., 21, 764-65 (1953), ibid 21,1144-48 (1953).

(17) Newell, G.F., J. Chem. Phys., 23, 2431-38 (1955).

(18) Dwerkin, A.S., Sasmor, D.J. and Van Artsdalen, E.R., J. Chem. Phys., 22, 837-42 (1954).

(19) Westrum, E.F.(Jr.) and Beale, A.F.(Jr.), Unpublished data; Westrum, E.F. (Jr.), J. Chem. Ed., 39, 443-54 (1962).

(20) Daunt, J.G., The electronic specific heat in metals, Prog. in low temperature physics, Vol.1 (North Holland Publishing Co., Amsterdam) pp.202-223, (1955).

(21) Schottky, W., Z. Physik, 23, 448 (1922).

(22) Suga, H., Sorai, M., Yamanaka, T. and Seki, S., Bull. Chem. Soc. Japan, 18, 1227 (1963).

(23) Suga, H., Matsuo, T. and Seki, K., Bull. Chem. Soc. Japan, 38, 1115-24 (1965).

(24) Bijveot, J.M. and Lery, J.A., Rec. trav. Chem., 59, 908 (1940).

(25) Cimino, A., Parry, G.S. and Wbbelohde, A.R., Proc. Roy. Soc., A252, 445-56 (1959).

(26) Parry, G.S., Acta Cryst., 15, 596-607 (1962).

(27) Timmermans, J., Bull. Soc. Chim. Belg., 44, 17 (1935).

(28) Trowbridge, J.C. and Westrum, E.F., J. Phys. Chem., 67, 2281-85 (1963).

(29) Clever, H.L., Wong, W.K., Wulff, C.A. and Westrum, E.F.(Jr.), J. Phys. Chem., 68, 1967-9 (1964).

(30) Nakagawa, T., Sawada, S., Kawakubo, T. and Nomura, S., J. Phys. Soc. Japan, 19, 576 (1964).

(31) Keer, H.V., M.Sc. Thesis, Bombay University (1964).

(32) Néel, L., Ann. Physik, (10), 18, 5 (1932); (11), 5, 232(1936).

(33) Bitter, F., Phys Rev., 54, 79-86 (1938).

(34) Van Vleck, J.H., J. Chem. Phys., 9, 85-90 (1941).

(35) Anderson, P.W., Phys Rev., 79, 705-10 (1950).

(36) Nagamiya, T., Prog. Theor. Phys., 6, 342 (1951).

(37) Yosida, K., Prog. Theor. Phys., 7, 25 (1952).

(38) Slater, J.C., Quarterly progress reports, M.I.T., 15, 1 (1953).

(39) Néel, L., Ann. Physik, (12), 3, 137 (1948).

(40) Poulis, N.J. and Gorter, C.J., 'Antiferromagnetic Crystals': Progress in low temperature physics, 1, 243-72 (1955);

Lidiard, A.B., 'Antiferromagnetism' Reports on Prog. of Physics, 17, 201-44 (1954).

Nagamiya, T., Yoshida, K. and Kubo, R., Advances in Physics, 4, 1 (1955).

(41) Kramers, H.A., Physica, 1, 182 (1934).

(42) Bizette, H., Ann. Physik, (12), 1, 295 (1946).

(43) Shimizu, M., Proc. Theor. Phys., 8, 416 (1952).

(44) Polder, M.D., Jour. de Phys. Rad., 12, 274 (1951).

(45) Shull, C.G. and Smart, J.S., Phys. Rev., 76, 1256-7 (1949); Shull, C.G., Wollan, E.O. and Koehler, W.C., Phys. Rev., 84, 912-21 (1951).

(46) Tombs, N.C. and Rooksby, H.P., Nature, 165, 442-43 (1950).

(47) Snow, A.I., Rev. Mod. Phys., 25, 127 (1953); Foex, M., Comptes Rendus, 227, 193 (1948).

(48) Starr, C., Bitter, F. and Kaufmann, A.R., Phys Rev., 58, 977-83 (1940).

(49) Busey, R.H. and Giauque, W.F., J. Am. Chem. Soc., 74, 4443-46 (1952).

(50) Catalano, E. and Stout, J.W., J. Chem. Phys., 23, 1284-89 (1955); 1803-8 (1955).

(51) Erikson, R.A., Phys. Rev., 90, 779-85 (1953).

(52) Hirakawa, K., Hirakawa, K. and Hashimoto, T., J. Phys. Soc. Japan, 15, 2062-68 (1960).

(53) Wollan, E.O. and Koehler, W.C., Phys. Rev., 100, 545-63 (1955).

(54) Machin, D.J., Martin, R.L. and Nyholm, R.S., J. Chem. Soc., 1490-1500 (1963).

(55) Okazaki, A., Suemune, Y. and Fuchikami, T., J. Phys. Soc. Japan, 14, 1823-4 (1959); 16, 671-5 (1961).

(56) Scattorin, V., Corliss, L., Elliott, N. and Hastings, J., Acta Cryst., 14, 19-26 (1961).

(57) Hill, R.W., 'Low Temperature Calorimetry' Progress in Cryogenics, 1, 179-206 (1959) (Heywood and Co. London).

P A R T - I

C H A P T E R - II

DESCRIPTION OF THE CRYOSTAT ASSEMBLY

Heat capacity is a complicated function which involves various types of energies of interaction, possible arrangement and motion of atoms in a crystal. Measurements at low temperatures are generally made with a desire to separate non-lattice contributions from the total specific heat, magnetic entropy contribution and to elucidate the electronic energy level pattern. Thus, at temperatures below $20^{\circ}K$ the electronic term is significant, whereas above $20^{\circ}K$, the lattice contributions become predominant. The latter region is of particular interest to the physical chemists as it aims at evaluating the various thermodynamic functions at room temperature. In view of the above, specific heat data are required over a wide range of temperature and as a matter of fact, many of the reported studies cover a range from 5° to $300^{\circ}K$. This requires liquid helium or hydrogen as coolants to cover the lower range. Due to non-availability of such lower boiling refrigerants, the operation of the cryostat assembly described below, has been restricted down to liquid nitrogen temperature ($78^{\circ}K$) only. The cryostat and other parts of assembly are given as in operating condition in fig. II and the constructional details of the various parts are given in this chapter.

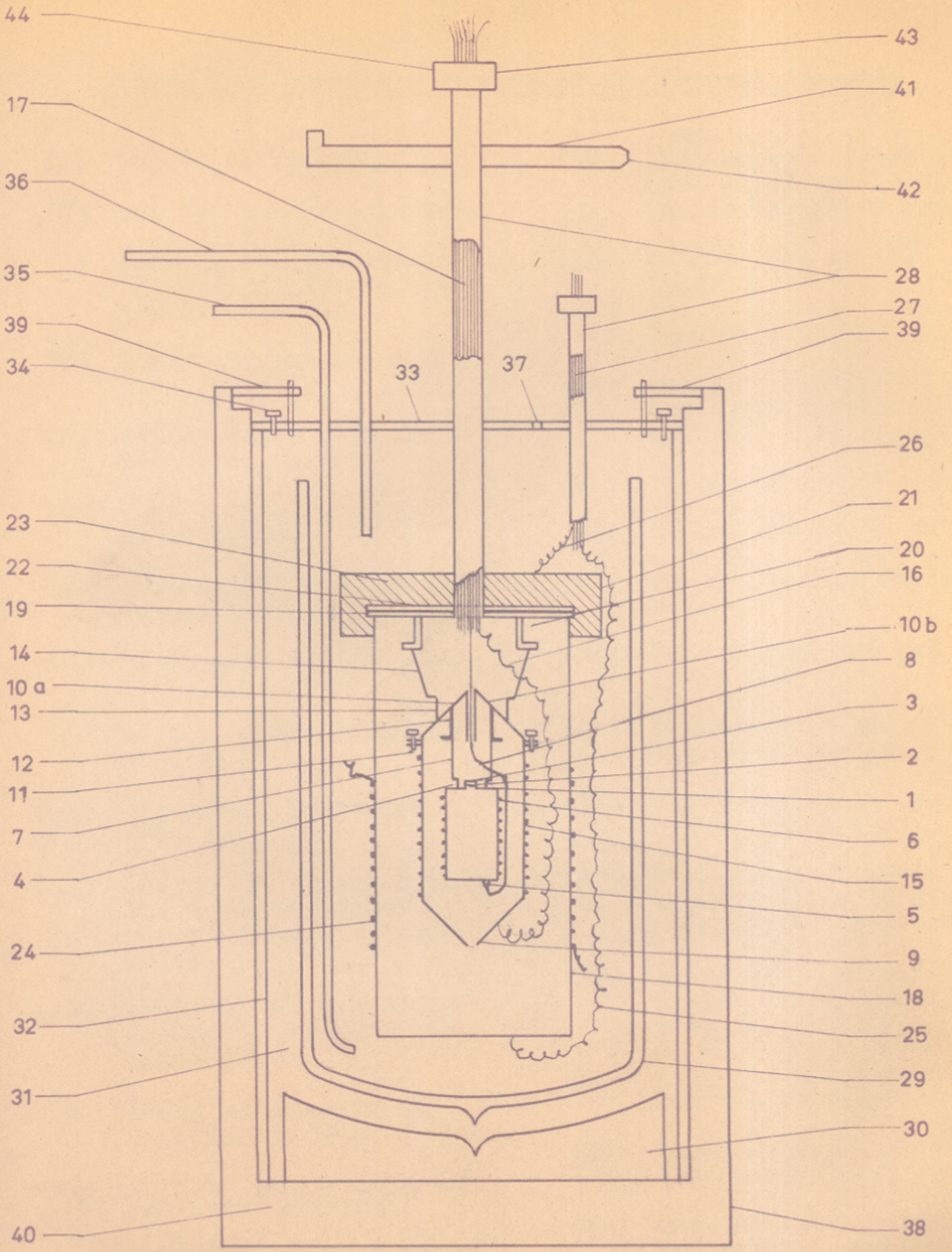
44
43
17
41
36
42
35
28
39
27
34
39
33
37
26
23
21
22
20
19
16
14
10 b
10 a
8
13
3
12
2
11
1
7
6
4
15
5
24
9
18
32
25
31
29
30
40
38

Figure II : Schematic Diagram of the Crystal Assembly

(1) Copper calorimeter;

(2) cap for the calorimeter;

(3) pinhole for introducing the conducting gas into the calorimeter;

(4) hooks for hanging the calorimeter;

(5) thermocouple well for the calorimeter;

(6) heater wire for the calorimeter;

(7) threads for hanging the calorimeter;

(8) thermocouple wires for the calorimeter;

(9) bottom of the radiation shield;

(10) a&b top of the radiation shield;

(11) screws for fixing both the upper and lower parts of the radiation shield;

(12) hooks on the radiation shield for hanging the calorimeter;

(13) hooks for hanging the radiation shield;

(14) threads for hanging the radiation shield;

(15) heater wire for heating the radiation shield;

(16) thermocouple wires for the radiation shield;

(17) thermocouple wires and lead wires leading to inside the inner can;

(18) bottom part of the inner can;

(19) lead gasket;

(20) hooks on the lid of the inner can for hanging the radiation shield;

(21) trough to put the solder;

(22) lid of the inner can;

(23) solder to seal the inner can;

(24) heater wire for the inner can;

(25) thermocouple to the bottom of the inner can;

(26) thermocouple to the top of the inner can;

(27) bunch of lead wires and thermocouples leading to outside the inner can;

(28) brass tubes containing heater wires and thermocouples;

(29) silvered pyrex dewar flask for the refrigerant;

(30) wooden base supporting the dewar flask;

(31) non-conducting felt support for the dewar;

(32) bottom part of the outer can;

(33) lid of the outer can;

(34) screws for fixing the bottom and top of the outer can in position;

(35) transfer tube for transferring the liquid refrigerant to the bottom of the inner can;

(36) transfer tube for transferring the liquid refrigerant to the top of the inner can;

(37) hole in the top of the outer can for introducing solid carbon dioxide;

(38) wooden box to hold the outer can;

(39) clamps to fix the outer can in position;

(40) heat insulating material in the wooden box;

(41) brass tube connection for the vacuum line;

(42) b-19 male joint connecting the vacuum system;

(43) picein sealing wax for high vacuum; and

(44) cup fitted with rubber cork and closed with picei

The Calorimeter

One major consideration in the construction of a calorimeter is to secure a favourable ratio between the heat capacities of the specimen and that of its container. In addition it has to be made sufficiently robust to withstand a differential pressure of one atmosphere; this limits the extent to which the heat capacity of the empty calorimeter can be reduced as the built-up assembly will also contain appreciable quantity of insulating adhesives, solders etc. As a rough rule, it should be aimed that the ratio of the heat capacities of the container to that of non-metallic specimens be nearly one at a temperature of $\theta/50$ where θ is the effective Debye temperature of the specimens.

The present calorimeter (1) is made out of a cylindrical copper tubing of thickness 0.05 cm, outer diameter 4.0 cm. and a height of 6.0 cm. A tubing of 1.0 cm. diameter and height of 1.5 cm. is soldered into a hole drilled in the top cover of the calorimeter to facilitate the introduction and removal of substances into and from the calorimeter. A cap (2) sits firmly on the ring-seal of this tubing so that it can be soldered to make a vacuum-tight joint. A pin-hole (3) on this cap helps evacuation and filling with hydrogen(or helium) gas employed to facilitate thermal equilibrium during a heat capacity measurement. Two small copper tubes (5)

soldered to the bottom surface of the calorimeter are used to attach the thermocouple (8). To give a good thermal contact[1] the thermocouple is wrapped around the calorimeter, care being taken not to produce any kink or strain on it. All the joints in the calorimeter are silver soldered except at the cap where soft solder is used.

Over the cylindrical surface of the calorimeter, a thin coating of tar is given for insulation and enamelled copper wire (6) (S.W.G. 44) of about 160 ohms resistance is wound on it uniformly leaving a space of 0.5 cm. on either side. Over it another thin coating of tar is given and air-dried. This ensures the thermal contact as well as the electrical insulation between the wire and the calorimeter. Thin coatings of silver followed by gold are then vacuum-deposited over it. Finally thin gold leaves of negligible heat capacity are wrapped around to reduce the radiation effects to a minimum.

The total weight of the empty calorimeter together with heater wire is 38.10 grams.

The Radiation Shield

The radiation shield is a heavy copper block compared to the calorimeter and weighes about 650 g. This block is used to maintain an environment of constant temperature for the calorimeter. It has two parts, of which the upper one is shaped like a cone and consists of

two halves which are fixed in position by screws (10a,b). The lower part (9) is cylindrical with a cone at one end. The cylindrical part has a diameter of 6.0 cm. and a height of 13.0 cm. Both the cone ends have holes to take out thermocouple and lead wires of the calorimeter. The detachable parts of the radiation shield are connected by screws (11), which make the assembling and dismantling process easy.

As in the case of the calorimeter an enamelled copper wire (15) (S.W.G. 40) of about 300 ohms resistance is wound on the cylindrical part of the radiation shield. Thick coatings of silver followed by gold vacuum-deposited on the entire surface of the radiation shield, help to minimize the radiation effects. A thermocouple (16) is directly soldered to the radiation shield. The upper conical part contains hooks inside and on the top for hanging the calorimeter (12) and the radiation shield (13), respectively.

The Inner and Outer Cans

The inner can (18) is a heavy brass vessel with a diameter of 13 cm. and a height of 23 cm. It has a flange at the top with a circular groove in it. Brass is used as the material of construction for the inner can as it can be readily fixed with solder. A trough (21) of brass, brazed at the top of the inner can, has a height

of 3.5 cm. and can accommodate about 10-12 lbs. of soft-solder. The large amount of solder (23) serves a three-fold purpose: (1) It gives enough mechanical strength as this alone holds together the lid and the bottom part of the can. (2) It offers resistance to leakage of gases and relieves any strain produced[2] when the can is cooled to low temperatures; and (3) it stabilizes the temperature of the can. In addition, heavy lead blocks (weighing about 6-8 lbs.) kept on the can also help in stabilizing the temperature of the inner can. A thin lead foil (19) kept in the circular groove of the flange and pressed against the lid (22) prevents the passage of solder inside while soldering the can.

A long brass tube is brazed at the centre of the lid which closes the inner can. At a height of 18 cm. from the lid another one (33) of 26 cm. diameter is welded to the brass tube so that the outer can (32) can be closed simultaneously along with the inner can. An enamelled constantan wire (24) of about 300 ohms resistance is wound on the inner can for heating, whenever necessary. Two thermocouples (25,26) are soldered to the top and bottom of the inner can to indicate their temperatures, whenever necessary.

The outer can (32) is a large cylindrical brass vessel with a height of 60 cm. and an outer diameter of 26 cm. At the top it has a flange of 1.5 cm. pointing

inwards with an O-ring and a row of projected screws to keep the lid pressed tightly in position. The lid of the outer can has holes at corresponding positions so that the inner can can be put in a fixed position in the enclosed dewar flask (29). Two tubes (35,36) of 0.5 cm. diameter are welded through the lid of the outer can. One of them extends down to the bottom of the inner can and the other to the top. These are used to pump the coolant liquid to cool the apparatus to low temperatures. There is also an opening (37) on the lid of the outer can which can be closed at will, through which solid carbon dioxide can be introduced, if required, to obtain the temperatures in the corresponding region.

The outer can holds a glass dewar flask that rests on felt pads supported by an wooden-base (30). Non-conducting felt (31) prevents the dewar from coming into direct contact with the outer can. A double-walled wooden box (38) packed with heat insulating material (40), houses the entire cryostat and ensures mechanical stability for the whole system, such that the latter does not rock once locked inside the box with clamps (39). This is necessary as the side tube (41) of the inner can is directly connected to the high vacuum glass system through a B-19 joint.

All the thermocouples and lead wires (17) of the calorimeter and radiation shield with a few spare wires

are drawn through a cup (44) at the end of the long tube (of the inner can) and sealed with Apiezon wax W.100 (43) to stand high vacuum. Similarly the thermocouples (27) and lead wires for the inner can are brought through a side tube (28) and sealed.

Having described the apparatus used for the measurements, in the next chapter, the calibration of thermocouples at fixed temperatures in an all-glass apparatus, specially constructed for this, is described.

C H A P T E R - III

CALIBRATION OF THERMOCOUPLES

Selection of Thermocouples

It is now generally accepted that only the platinum thermometer is capable of the reproducibility and accuracy required for temperature measurements in cryogenic calorimetric studies. A suitably designed platinum resistance thermometer and carefully calibrated against the standard gas thermometers by N.B.S. has been accepted as a standard temperature scale by many workers, in this field. However non-availability of such a thermometer or any thermocouple calibrated against such a standard necessitated the use of an easily available sensitive and stable thermometer for our experiments. Reliable performance over a number of years of copper-constantan thermocouples has been reported and those have been extensively used in the low temperature calorimetric work.[3] Giauque and coworkers[4,5,6] used these thermocouples down to 12°K and found that the reproducibility is within ± 0.05°K over many years, especially above 75°K.

Such a thermocouple may also be calibrated by measuring the e.m.f. produced at a number of fixed points the temperatures of which are known on the international

scale. Scott[7] showed that sufficient accuracy can be obtained by calibrating the thermocouple at oxygen boiling point and carbon dioxide sublimation point. Calibration at intervals of 50°K or less gives results with an accuracy of ± 1 μV.

The accuracy with which copper-constantan thermocouples may be calibrated is usually limited by lack of homogeneity of the wires i.e. irregularities in chemical composition or physical condition of the wires in regions where temperature gradients exist cause spurious e.m.fs. to appear, which change if the temperature gradient is shifted along the wire. In copper-constantan thermocouple the copper being relatively uniform the constantan is usually the element responsible for most of the spurious e.m.fs. Three constantan wires are used in parallel with a single copper wire so that any errors due to irregularities in different constantan wires are averaged out.[8]

Taking all the factors into consideration several copper-constantan thermocouples of 150 cm. length each were prepared. The materials specially meant for making thermocouples were obtained from Johnson Matthey & Co. Ltd., London. They are annealed by alternate heating to temperatures above 400°K and cooling to liquid nitrogen temperatures several times. The composition of the constantan wire is 56 copper to 44 nickel by weight. The gauge of the wire is B and S 30. It has a resistance of 0.0866 ohm per cm. and is diamel-coated for insulation.

Apparatus for Calibration

An all-glass apparatus (fig.III) has been constructed for calibrating the thermocouples at some selected fixed points. A copper block (1) weighing about 1 Kg. and having six thermocouples soldered to it has a central cavity of approximately 6 mm. into which a glass tube (17) fits in neatly. Around this glass tube which can be connected to a vacuum system as well as to a pure oxygen source, is an evacuated jacket (4) which prevents the bath from coming into direct contact with the pressure transmitting tube so that cold spots are avoided. Manometer I (15) indicates the vapour pressure of the liquid refrigerant. Manometer II (5) reads the oxygen vapour pressure. Pure oxygen at a pressure of 900 mm. mercury prepared by heating pure potassium permanganate is used for vapour pressure measurements. The outer jacket (18) is kept in a big dewar vessel and the intermediate space between the dewar vessel and the glass jacket is packed with thermocole and asbestos powder for heat insulation.

All the thermocouples calibrated several times at the fixed points[7,9,10] (Table 1) showed reasonably good agreement with a reproducibility of $\pm$ 1 μV. All the chemicals used were at least of 99.5% purity and distilled water ice was used as the reference temperature.

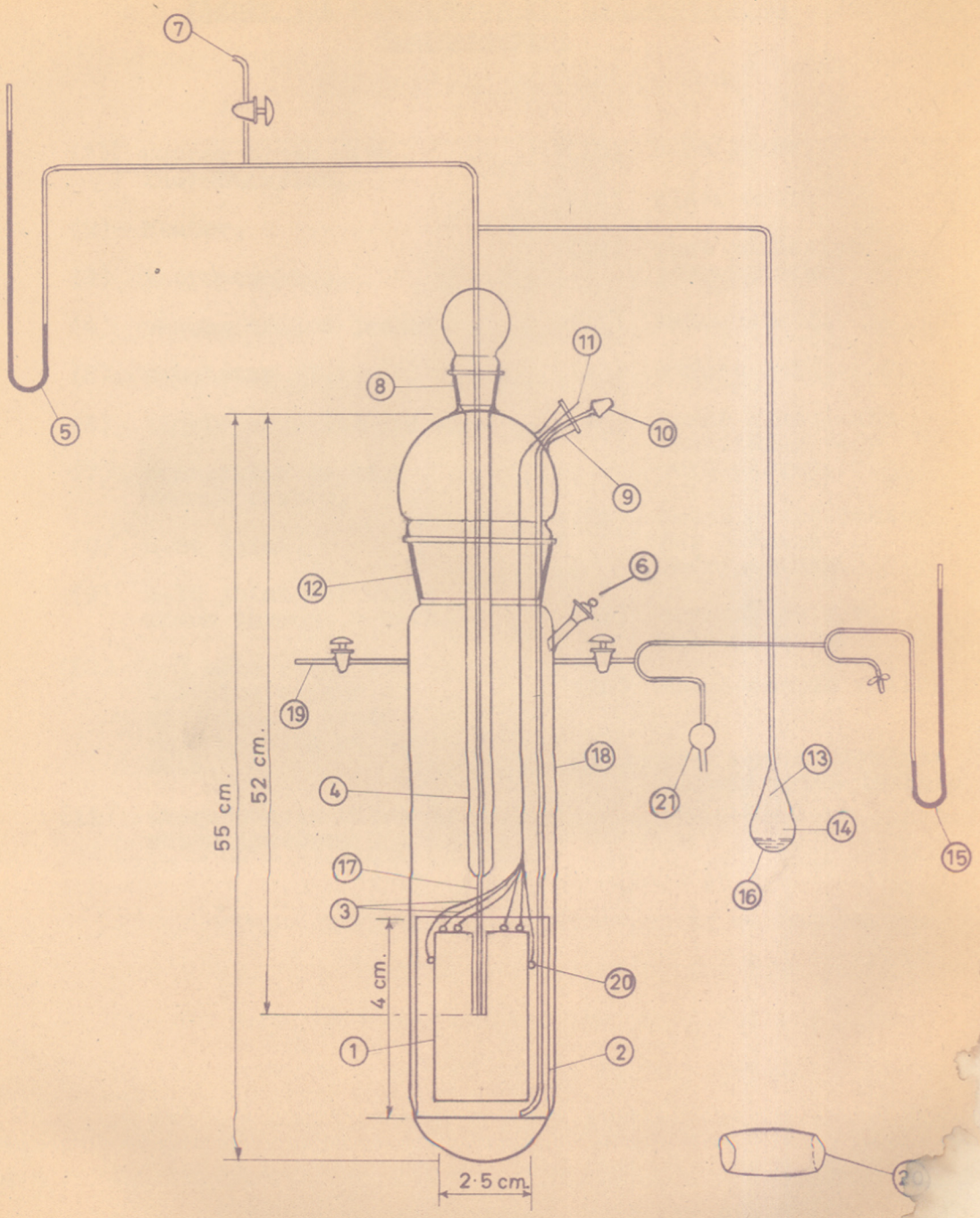

FIG. 3 - APPARATUS FOR CALIBRATION OF THERMOCOUPLES

Figure III : Apparatus for Calibration of Thermocouples

(1) Copper block with thermocouples,

(2) heater,

(3) thermocouples,

(4) vacuum sealed jacket,

(5) manometer II,

(6) liquid or solid inlet,

(7) connection to high vacuum system,

(8) B-24 joint,

(9) B-14 joint for wires drawn through a cork,

(10) B-7 male joint for bubbling oxygen or nitrogen to avoid superheating of the bath,

(11) thermocouple wires to potentiometer,

(12) B-55 joint,

(13) glass wool,

(14) pure potassium permanganate,

(15) manometer I,

(16) oxygen bulb,

(17) inner glass tube containing very pure oxygen,

(18) outer glass jacket for keeping refrigerants,

(19) connection for rotary pump,

(20) thermocouple wells,

(21) pressure indicating safety valve (a thin balloon).

Table I

Thermocouple calibration data

Substance	Temperature (^{o}K)	e.m.f. ($\mu V \pm 1$)	$\frac{dE}{dT}$	$\frac{dR}{dT}$
Liquid nitrogen	77.18 (b.p.)	5524	17	0.63
Liquid oxygen	89.06 (b.p.)	5317	18	0.63
Carbon disulphide	161.56 (f.p.)	3652	26	0.58
Toluene	178.06 (f.p.)	3190	28	0.56
Solid carbon dioxide	193.92 (s.p.)	2730	29	0.55
Carbon tetrachloride	250.26 (f.p.)	863	37	0.53
Ice	273.15 (m.p.)	0	38	0.52

b.p. - boiling point
f.p. - freezing point
m.p. - melting point
s.p. - sublimation point

Calibration at Fixed Points

Oxygen and nitrogen boiling points :- Generally liquid oxygen and nitrogen supplied by the commercial firms are not pure and hence to know the exact boiling points it is necessary to use an oxygen vapour pressure thermometer in which a small amount of very pure oxygen is used. Pure potassium permanganate has been suggested as a source material for very pure oxygen[9] and hence a recrystallized sample of potassium permanganate was used. After discarding the gas evolved by heating potassium permanganate

upto 200°C, the oxygen was collected till the manometer showed a pressure of 900 mm. Hg. From the vapour pressure measurements of oxygen the corresponding temperatures of liquid oxygen and nitrogen were read directly from the tables of Hoge.[11]

Carbon dioxide point :- Solid carbon dioxide, crushed in presence of air, becomes colder because the air reduces the partial pressure of CO_2 in contact with the solid. This has the effect of lowering the sublimation point. So to maintain an atmosphere of carbon dioxide vapour around the solid, a thin copper cylinder (hollow) was wound with an enamelled copper wire of about 40 ohms resistance and this heater was embedded in the solid carbon dioxide. In the beginning heating was maintained with about 30 watts for about 15 minutes to obtain a steady condition. The sublimation point was calculated by using the following equation.[12]

$$\log_{10} P = 9.81137 - \frac{1249}{T}$$

where P is the pressure in mm. Hg. and T is the temperature in °K.

Freezing point of carbon disulphide :- The carbon disulphide was introduced into the glass jacket through the inlet tube B.24 and was cooled with liquid air. As it was being cooled the e.m.f. of the thermocouple increased until the freezing point and the steady e.m.f.

reached at this point was noted. Then it was cooled to about 10 degrees below the freezing point. The dewar containing the liquid air was taken out and the solid carbon disulphide was heated slowly until some liquid was formed. The steady e.m.f. was again measured at the melting point. The procedure was repeated at least five times and an average of the steady e.m.f. values was taken.

The e.m.fs. at the freezing points of toluene and carbon tetrachloride were measured similarly.

Ice point :- Ice made from distilled water was used for the ice point.

All the e.m.fs. were measured in the conventional way with a vernier potentiometer and a sensitive galvanometer with a sensitivity of 1 μV/div. A smooth curve was drawn through the points and a table of the rate of change of e.m.f. with temperature from 74° to 300°K with 2° interval was prepared (Appendix I). Relevant data for the observation of temperatures are given in Table-I for a representative thermocouple labelled T.C.2 .

The present apparatus can also be used for calibration of thermocouples at still lower temperatures e.g. triple points of nitrogen and oxygen. In this case the cork used for clipping thermocouples as well as the B7 gas bubbler (10) should be closed with sealing wax such as piecein. The liquid refrigerant has to be pumped through the wide-bore stop cock (19) till it solidifies.

C H A P T E R - IV

OPERATION OF THE CALORIMETER

In the preceding chapter the details of the apparatus and the calibration of the thermocouples were described. This chapter deals with the details of the operation of the calorimeter including experimental procedure, electrical equipment, method of operation and the calculations of heat capacities from the measured data.

Experimental procedure

Filling the calorimeter with heat exchange gas :- The calorimeter was filled with the specimen whose thermal properties are to be studied and the cap closed with solder leaving a pinhole on the top. It was then placed in a glass chamber connected to a manometer, a hydrogen gas reservoir and a high vacuum pump. After evacuating the calorimeter chamber to a good vacuum, some hydrogen gas was repeatedly introduced and evacuated and finally filled to a pressure of 10-20 mm. above the atmosphere. The lid of the glass chamber was then removed and the pin hole immediately closed by soldering. This required less than a minute and as the excess pressure inside caused the hydrogen to stream out entry of air into the calorimeter was excluded. It was assumed that the pressure of hydrogen gas in it was one atmosphere.

Cooling the calorimeter to low temperatures :- After assembling the calorimeter and radiation shield as shown in fig.2 the inner can is closed by soft solder in position to stand high vacuum. Before connecting the cryostat to the high vacuum system the inner can is tested for leaks, if any, through the soldered region by pressurising the interior of the system with nitrogen gas and immersing in water. The method can locate leaks as small as 0.1 micron litre per second.[13] Generally high vacuum is obtained once the can stands to this test. The high vacuum system consists of a mercury diffusion pump backed by a high capacity two stage rotary vacuum pump. It takes about 24 hours of pumping to get the required vacuum as generally sizable quantities of water vapour and gases adsorbed on the surface of the can are slowly released. The evacuation process is facilitated by heating the can with a small current through the heater wire. The pressures are read with a calibrated McLeod guage.

A liquid nitrogen trap constitutes a part of the high vacuum connecting line between the diffusion pump and the calorimeter assembly to capture any readily condensible vapours. Also it avoids the possibility of mercury vapours diffusing into the assembly.

Liquid nitrogen is pumped on to the top and bottom of the inner can through the inlet tubes provided. When the can is cooled then sometimes the vacuum may fail.

This may be due to the drastic differential contraction of the can and the solder producing a bad contact between the surfaces or the flux used for soldering which might have closed a pin hole to give vacuum at room temperature, cracked on cooling. In such cases the can is resoldered to obtain the desired vacuum. When the thermocouples on the top and bottom of the inner can show the lowest expected temperature, helium gas is introduced into the insulating space between the inner can and the calorimeter to facilitate cooling of the calorimeter and radiation shield to the required extent. When this is attained, helium gas is pumped out and high vacuum obtained once again. The high vacuum in the calorimeter assembly minimizes heat leak due to conduction and convection. It also removes any possible condensation of water vapour and other condensible materials on cooling the system. Before actual measurements are started a small current is passed through the calorimeter heater wire for 1 or 2 minutes to remove any 'backlash'.

Electrical equipment

The operation of the calorimeter requires the accurate determination of initial and final temperatures and electrical energy input. The latter quantity is evaluated from the measurement of current, voltage and heating time.

The calorimeter heater wire is connected in series with a standard 1 ohm resistance. Several Edison alkaline batteries are connected in series through a switch and a high resistance of 12,000 ohms with the calorimeter heater wire (current supply batteries). Another set of Edison alkaline cells (energy supply batteries) provides current which passes all the time either through the heater wire of the calorimeter or an equal dummy resistance, thereby stabilizing the current when the energy is not being put into the calorimeter. The energy voltage is adjusted to give a current of about 0.08-0.1 ampere by increasing or decreasing the number of cells and using a variable resistance included in the circuit. The energy input is timed by presetting an automatic timer included in the circuit. This disconnects the energy circuit automatically once the present period is over.

The radiation shield heater wire in series with a 100 ohms rheostat is connected to a set of acid batteries through a rotary switch which enables to vary the voltage required to heat the radiation shield whenever necessary. The rheostat included also helps to increase or decrease the current passing through the radiation shield heater wire thereby regulating the heating rate. Similarly the inner can heater wire is connected to an A.C. source through a dimmerstat so that the can also can be heated whenever necessary.

A Weston standard cell is used to calibrate the potentiometers. The e.m.fs. are measured with two vernier potentiometers with an accuracy of $\pm$ 1 μV in conjunction with two galvanometers having a sensitivity of 8 x 10^{-8} A/mm. and a damping resistance of 30.0 ohms.

Method of measurement

It has been pointed out earlier that s.w.g. 44 copper wire was wound on the calorimeter, which following Eucken,[14] Giauque and co-workers[15,16,17] is used as a thermometer-heater. As the calorimeter is made out of copper, copper wire only is used to make the thermometer as strain free as possible.[18] It has a resistance of about 160 ohms at room temperature and about 30 ohms at liquid nitrogen temperatures.

The size and design of the thermometer prevents any direct calibration of it. Though only a copper wire is used it will not be possible in practice to get a completely strain free thermometer. Hence it is necessary to calibrate it against a platinum resistance thermometer or a calibrated thermocouple. In the present case it is calibrated against a thermocouple calibrated according to the procedure described before. It may be noted that the accuracy of the resistance thermometer is in fact better because the high rate of change of resistance with temperature permits more precise measurements. The resistance of the thermometer is continuously calibrated against thermo-

couple as heat capacities are measured in the range 80-300°K. A graph is plotted between resistance and temperature and the rate of change of resistance with temperature (Table I) is calculated.

A small current of about 500 micro amperes passing through the thermometer-heater wire enables the resistance measurement. The resistance of the thermometer can be estimated by measuring the potential drop against the standard 1 ohm resistance and the calorimeter heater wire. As the current is too small to produce any heating effects it is allowed to pass through the heater-wire all the time, except during energy measurements, when this is disconnected. Since a very high resistance is included in the circuit slight changes in the thermometer-heater wire due to heating produce negligible effect on the total resistance and the current remains practically constant. Thus only two current readings, taken just before and after the energy input are quite sufficient for each heat-capacity measurement.

The heating current during energy input is calculated from the potential drop across 1 ohm resistance. A high resistance of 10,000 ohms connected in parallel to the calorimeter heater wire helps to measure the voltage of energy current. As the total potential drop across this high resistance is too large to be measured on the potentiometer, the voltage across a small known fraction is measured and the potential multiplied by the fraction (factor) to

get the actual potential. The factor in the present case is 40.07. A correction was made for the fraction of the heating current which passed through the resistance. The parallel resistance was disconnected during temperature measurements. The energy input is timed with an accurate stopwatch with a precision of ± 0.2 sec. corresponding to an error of 0.03 % in a ten minute time period.

The radiation shield is heated approximately $\frac{1}{2}X$ °K, where X is the anticipated rise in the temperature of the calorimeter after energy input. The energy is then put into the calorimeter for a definite time of 6, 8 or 10 minutes by passing a current of about 0.1 ampere. As the radiation shield is massive, its temperature remains practically constant, while that of the calorimeter becomes $\frac{1}{2}X$° higher. Both the preheating as well as the cooling rates of the calorimeter are measured for about 10-30 minutes depending upon the time taken for equilibrium. In general, about 15-20 minutes are required for attaining the same. Temperatures are measured by the change in the resistance thermometer of the calorimeter as well as by the change in e.m.fs. of the thermocouple. In general about 60-80 minutes are taken for each heat capacity measurement. Also the temperatures of various relevant parts such as the top and bottom of the radiation shield and inner can are taken. Distilled water ice is taken as the reference point for all thermocouple measurements. If the inner can starts

heating up affecting the temperature of radiation shield it has to be cooled with liquid nitrogen, and if the liquid nitrogen is in excess the inner can has to be heated to boil off the excess liquid nitrogen.

Calculation and Corrections

The method adopted for calculation of heat capacities is essentially the same as that given by Giauque and co-workers.[15,17,19] Cole et al.[20] have discussed in detail the various corrections to be applied.

The expression for obtaining the heat capacities from experimental data can be written as

$$C_{p(\text{at } T)} = \frac{\left(\frac{E.I.t}{T} \cdot A\right) - C_E}{B}$$

where C_p - heat capacity of the substance in cal. per gram per deg.

E - voltage across heater terminals during energy input

I - amperes (current) through heater during energy input

t - time of energy input

A - factor converting Joules to calories

C_E - heat capacity of the empty calorimeter

B - amount of material present in the calorimeter.

Since the applied voltage from energy batteries remains practically constant during measurement, a single reading taken at (t/2), where 't' is the total time of

energy input, is sufficient for the calculations. The resistance of the thermometer-heater increases while energy is being introduced. This causes a continuous drop in current since the applied voltage is constant. In order to avoid a tedious graphical process of evaluation the method of Gibson and Giauque[15] for obtaining the average value of current has been followed.

The change of current with time is found to be nearly constant and the current can be represented very accurately as a quadratic function of time.

$$I = A + Bt + Ct^2$$

Let 'I_1' be the current after 't_1' seconds; 'I_2' the current after 't_2' seconds; 'I_{av}' the average value of the current, and 't' the total time of energy input.

Make $t_1 + t_2 = t$ and $\frac{I_1 + I_2}{2} = I_{av}$

Then

$$I_{av} \cdot t = \int_0^t I.dt$$

$$= At + \tfrac{1}{2}Bt^2 + \tfrac{1}{3}Ct^3$$

$$\therefore \quad I_{av} = A + \tfrac{1}{2}Bt + \tfrac{1}{3}Ct^2 \qquad \ldots\ldots (1)$$

and $$\frac{I_1 + I_2}{2} = I_{av} = A + \tfrac{1}{2}B(t_1 + t_2) + \tfrac{1}{3}C(t_1^2 + t_2^2)$$

$\ldots\ldots$ (2)

Comparing equations 1 and 2 we get

$$\frac{t_x^2}{3} = \frac{1}{2}(t_1^2 + t_2^2)$$

$$= \frac{1}{2}\left\{(t_s - t_2)^2 + t_2^2\right\} \quad (\because t_s = t_1 + t_2)$$

$$= \frac{1}{2}(t^2 - 2tt_2 + 2t_2^2)$$

i.e. $6t_2^2 - 6tt_2 + t^2 = 0$

So $t_2 = t\left(\frac{1 \pm \sqrt{1/3}}{2}\right) = 0.79t$ or $0.21t$

$\therefore$ $t_1 = 0.21t$ or $0.79t$.

Hence the arithmatic mean of energy current readings taken at 0.21 t and 0.79 t minutes where 't' is the total period of energy input gives the average value of current. Frequent readings in addition to these are also taken as a precautionary measure.

Heat interchange between the radiation shield and calorimeter :- Newton's Law of cooling which states that the heat transfer is proportional to the temperature difference is used in calculating the heat interchange. This requires the knowledge of temperatures of both the calorimeter and the radiation shield at all times during a measurement. The energy measurements furnish sufficient data for obtaining the external temperature of the calorimeter during the energy input. The temperature can

be considered to increase linearly with time within the limits of necessary accuracy, since firstly, the energy is put rather slowly; and secondly, by using over 50 meters of wire in the calorimeter thermometer heater, a small amount of energy is developed per unit length which is almost instantaneously delivered to the calorimeter. The radiation shield is comparatively heavy and hence only two readings during a heat capacity measurement are considered sufficient for calculations. The correction is found to be 1-2 %.

Energy correction :- During energy input the heater wire is hotter than the calorimeter. After a initial brief period following the begining of energy input this temperature difference remains the same (approximately constant). A correction to the energy is necessary to account for the rapid change in current or voltage in the transient period before a steady state is reached. This is related to the thermal relaxation time between the heater wire and the calorimeter, and can be calculated from the resistance of the heater wire and the resistance corresponding to the mean calorimeter temperature both at the mid point of the heating period.

The heat energy developed in the lead wires during energy input is included in the measured energy. Half of this energy goes to the calorimeter and half to the shield.

The correction to heat capacity is negligible compared to the accuracy of measurements. Similarly, the hydrogen gas filled in the calorimeter and the amount of solder used for sealing purposes are kept the same within practical limitations. Hence the corrections due to slight changes are assumed to be negligible.

The heat capacity of the empty calorimeter is measured over the entire range of temperature study in different series. A graph of heat capacity against temperature is plotted and smoothened values are taken from it as these are necessary for the further investigations.

C H A P T E R - V

HEAT CAPACITY OF STANDARD BENZOIC ACID

The importance of reproducibility within a laboratory and also between laboratories has been recognised and stressed in several recent international conferences on Calorimetry and Thermodynamics, so that the results of different laboratories for the same specimen can be compared and systematic errors located. Accordingly it is necessary for us initially to measure the heat capacity of a standard substance in order to check the temperature scale, accuracy of heat capacity measurements and overall efficiency of performance of our apparatus.

Since the begining of calorimetry, water has been used as a standard for heat capacity measurements, partly because it is universally available in high purity. However, as measurements are extended below 0°C the large expansion of water on freezing made it impracticable to use in many calorimeters. Above 100°C the high vapour pressure of water is a serious drawback because of the complications of accounting for the change with temperature of the relative amounts in the two phases. Due to such considerations, at the meeting of the Low Temperature Calorimetry Conference on 21st April 1948 organised for the purpose of promoting improved calorimetric techniques and setting up standards for

testing and calibrating calorimeters of various designs, benzoic acid, α-aluminium oxide and normal heptane were selected as standards in the temperature ranges 10-350°K, 10-1800°K and 10-300°K respectively.

In low temperature calorimeters, benzoic acid was chosen as a standard for the solid state whereas n-heptane was chosen where it is desirable to introduce the substances in the liquid form. Aluminium oxide was considered suitable as a standard substance because of its chemical stability even up to its melting point. Benzoic acid has a lower molal heat capacity than n-heptane but higher than aluminium oxide. It has been preferred for the present measurement as it is available in high purity and as the calorimeter is constructed for the study of solid substances. It is, however, not suitable as a heat capacity standard[21] above 350°K due to its corrosive nature especially since the calorimeter is made of copper. This is particularly so in the liquid state. But as the present measurements extend only up to 300°K there is little possibility of benzoic acid reacting with the container vessel.

Benzoic acid (A.R.) was recrystallised and the purity of the sample is better than 99.9%. The calorimeter was filled with 31.310 grams of benzoic acid and the remaining space was filled with hydrogen gas to one atmosphere. Heat capacity of the compound was measured from 80-300°K in

different series. The data are converted for one mole of the substance and the values are given for every 5°K in Table II, from a smoothened graph of heat capacity versus temperature, following the convention of the National Bureau of Standards. The values are given in calories (1 calorie ≡ 4.184 abs. joules). Percentage deviations of the smoothened values from N.B.S. values[22] are also given in the Table. The ratio of the heat capacity of the empty calorimeter to that of filled calorimeter is 0.43 at 100°K, 0.38 at 200°K and 0.43 at 300°K.

The precision of the present data has been estimated from the scatter of the values from their own mean, the maximum deviation being ± 2.0% for measurements between 80-300°K. It may be noted that at a temperature of 200°K the values of heat capacity determined with the present equipment are scattered both on the higher as well as on the lower side of the N.B.S. values, whereas at temperatures higher as well as lower than 200°K, the observed values are scattered only on the higher side of the N.B.S. values. The maximum deviation is about 3% in the range 80-150°K and this gradually becomes less than 1% at about 300°K.

Thermodynamic Functions

The thermodynamic functions viz. entropy and heat content of benzoic acid are calculated from the smoothened values of heat capacity. They are given for every 5°K

Table II : Comparison of the Heat Capacity (C_p) Values of Benzoic Acid (Mol. Wt. 122.13) determined with the Present Apparatus with NBS Data

Temperature °K	C_p cal./mole.deg.		Deviation from NBS values %
	Present expt.	NBS values	
80	13.64	13.35	+ 2.25
85	14.17	13.90	1.94
90	14.70	14.37	2.30
95	15.18	14.83	2.39
100	15.66	15.28	2.48
105	16.14	15.73	2.61
110	16.60	16.17	2.65
115	17.04	16.63	2.46
120	17.48	17.09	2.28
125	17.93	17.54	2.22
130	18.40	17.99	2.28
135	18.83	18.45	2.06
140	19.23	18.90	2.28
145	19.77	19.36	2.12
150	20.30	19.82	2.42
155	20.70	20.27	2.12
160	21.13	20.73	1.93
165	21.60	21.20	1.89
170	22.04	21.68	1.66

contd...

Temperature °K	C_p cal./mole.deg.		Deviation from NBS values %
	Present expt.	NBS values	
175	22.50	22.15	+ 1.58
180	22.92	22.63	1.28
185	23.42	23.12	1.30
190	23.85	23.60	1.06
195	24.29	24.08	0.87
200	24.65	24.59	0.24
205	25.03	25.09	- 0.24
210	25.56	25.60	- 0.16
215	26.18	26.11	+ 0.27
220	26.74	26.62	0.45
225	27.29	27.14	0.55
230	27.86	27.67	0.68
235	28.40	28.20	0.71
240	28.89	28.73	0.56
245	29.42	29.27	0.51
250	29.96	29.80	0.54
255	30.49	30.35	0.46
260	30.98	30.89	0.29
265	31.49	31.43	0.19
270	32.02	31.99	0.09
273.15	32.38	32.33	0.15

contd...

Temperature °K	C_p cal./mole.deg.		Deviation from NBS values %
	Present expt.	NBS values	
275	32.60	32.53	+ 0.22
280	33.24	33.09	0.45
285	33.87	33.62	0.74
290	34.38	34.18	0.58
295	34.89	34.73	0.46
298.15	35.29	35.09	0.57
300	35.54	35.30	0.68

along with N.B.S. values in Table III. In these calculations the values up to 80°K are taken from N.B.S. data and above 80°K are calculated from the present data.

Table III : Thermodynamic Functions of Benzoic Acid and comparison with N.B.S. values

$T^{\circ}K$	S_T-S_0 (present)	S_T-S_0 N.B.S.	H_T-H_0 (present)	H_T-H_0 N.B.S.
80	11.75	11.75	551.2	551.2
85	12.59	12.45	626.7	618.0
90	13.42	13.36	698.7	690.1
95	14.23	14.15	773.2	763.2
100	15.02	14.91	850.2	838.5
105	15.79	15.67	929.5	915.8
110	16.55	16.42	1011	995.6
115	17.30	17.14	1095	1075
120	18.03	17.86	1181	1162
125	18.76	18.57	1270	1248
130	19.47	19.27	1360	1338
135	20.17	19.95	1453	1429
140	20.87	20.64	1549	1522
145	21.55	21.30	1647	1617
150	22.23	21.97	1747	1715
155	22.90	22.62	1849	1816
160	23.57	23.28	1954	1918
165	24.22	23.92	2061	2023
170	24.88	24.56	2170	2130
175	25.52	25.20	2281	2240
180	26.16	25.83	2394	2352

contd...

$T^{o}K$	S_T-S_0 (present)	S_T-S_0 N.B.S.	H_T-H_0 (present)	H_T-H_0 N.B.S.
185	26.79	26.44	2510	2466
190	27.42	27.08	2628	2583
195	28.05	27.70	2748	2704
200	28.67	28.33	2871	2824
205	29.28	28.92	2995	2941
210	29.89	29.54	3121	3075
215	30.50	30.14	3250	3204
220	31.11	30.76	3382	3336
225	31.71	31.35	3517	3470
230	32.32	31.96	3655	3606
235	32.93	32.55	3795	3747
240	33.53	33.16	3939	3886
245	34.13	33.75	4085	4035
250	34.73	34.34	4233	4170
255	35.33	34.95	4383	4333
260	35.92	35.55	4537	4485
265	36.52	36.14	4693	4640
270	37.11	36.74	4852	4798
275	37.71	37.33	5013	4963
280	38.30	38.50	5178	5125
285	38.89	39.09	5346	5291
290	39.49	39.68	5516	5462
295	40.08	40.05	5689	5633
300	40.67	40.18	5765	5809

REFERENCES

(1) Johnston, H.L., Clarke, J.T., Eliss, B. and Kerr, E.C., J. Am. Chem. Soc., 72, 3933-38 (1950).

(2) Scott, R.B., 'Cryogenic Engineering' D. van-Nostrand Company, Inc. Princeton, N.J. (1950).

(3) Aston, J.G., 'Temperature-its measurement and control in Science and Industry' Reinhold Publishing Corporation, N.Y., pp.219-27 (1941).

(4) Giauque, W.F. and Egan, C.J., J. Chem. Phys., 25, 45-54 (1937).

(5) Giauque, W.F., Buffington, R.M. and Shulze, W.A., J. Am. Chem. Soc., 49, 2343-54 (1927).

(6) Stephenson, C.C. and Giauque, W.F., J. Chem. Phys., 5, 149 (1937).

(7) Scott, R.B., 'Temperature-its measurement and control in Science and Industry' Reinhold Publishing Corporation, N.Y., pp.206-18 (1941).

(8) Hovorka, F. and Rodebush, W.H., J. Am. Chem. Soc., 47, 1614-24 (1925).

(9) Hoge, H.J., 'Temperature-its measurement and control in Science and Industry' Reinhold Publishing Corporation, N.Y., pp.141-56 (1941).

(10) "Handbook of Chemistry and Physics" Chemical Rubber Publishing Co., Cleveland, Ohio, p.2416 (1962-63).

(11) Hoge, H.J., J. Res. Nat. Bur. Stands., 44, 321-45 (1950).

(12) Mayers, C.H. and Van Dusen, M.S., J. Res. Nat. Bur. Stands., 10, 381-412 (1933).

(13) Scott, R.B., 'Cryogenic Engineering' D. van-Nostrand Company, Inc. Princeton, N.Y., (1959).

(14) Eucken, A., Z. Physik, 10, 586-89 (1909).

(15) Gibson, G.E. and Giauque, W.F., J. Am. Chem. Soc., 45, 93-104 (1923).

(16) Blue, R.W. and Giauque, W.F., J. Am. Chem. Soc., 57, 991-97 (1935).

(17) Giauque, W.F. and Johnston, H.L., J. Am. Chem. Soc., 51, 2300-21 (1929).

(18) Onnes, K. and Holst, Comm. Phys. Lab. Leiden, 142A, (1914).

(19) Giauque, W.F. and Wiebe, R., J. Am. Chem. Soc., 50, 101-22 (1928).

(20) Cole, A.G., Hutchens, J.O., Robie, R.A. and Stout, J.W., J. Am. Chem. Soc., 82, 4807-13 (1961).

(21) Ginnings, D.C. and Furukawa, G.T., J. Am. Chem. Soc., 75, 522-7 (1953).

(22) Furukawa, G.T., McCoskey, R.E. and King, G.J., J. Res. Nat. Bur. Stands., 47, 256-61 (1951).

P A R T - II

C H A P T E R - VI

PREPARATION AND HEAT CAPACITY MEASUREMENTS OF COMPOUNDS

In the earlier part the construction, calibration and operation of the cryostat assembly was described. In what follows, the preparation and measurement of heat capacities of a series of compounds with formula KMF_3 where M = Mn, Co, Ni and Cu have been described.

Preparation of Compounds

The double fluorides can be prepared by reaction of gaseous hydrogen fluoride with the respective chlorides or by reacting alkali metal fluorosilicates with the sulphates of the desired metal. The method more commonly adopted is by mixing the potassium fluoride solution with the respective divalent transition metal salt solution of appropriate quantity. We have essentially followed this procedure as described by Hirakawa et al.[1]

Potassium manganese trifluoride :- Appropriate quantities of potassium fluoride and manganese chloride tetrahydrate are mixed in aqueous solution at room temperature. The precipitated compound is filtered, dried, packed in a carbon boat and melted in argon atmosphere. The resulting compound is white in colour with a shade of pink.

Potassium cobalt trifluoride :- Concentrated solutions of cobalt chloride and potassium bifluoride are mixed and evaporated on a water-bath at 90°C, when $KCoF_3$ precipitates out. The compound is filtered and washed with hot distilled water to remove traces of potassium chloride and hydrofluoric acid. It is then dried by heating to 200°C in vacuum. Potassium nickel trifluoride is also prepared in the similar way, starting with nickel chloride and potassium bifluoride solutions.

Potassium copper trifluoride :- The procedure adopted for $KCuF_3$ is slightly different. Copper carbonate is dissolved in excess of hydrofluoric acid. Then an adequate quantity of potassium fluoride is added and the solution heated at 90°C to evaporate off the excess water and hydrofluoric acid.

All the chemicals used for the preparations are A.R. or E. Merck quality.

X-ray Analysis

The compounds are analysed by X-ray powder diffraction at room temperature, using a 14 cm Debye-Scherrer camera and MoK_α ($\lambda = 0.709$ Å) radiation filtered through Zirconium foil. No extra line due to any of the components was observed. The compounds show cubic perovskite-like patterns. $KCuF_3$ however, has a tetragonal structure distorted from cubic symmetry. The calculated lattice constants agreed well with those reported in the literature[1,2,3] (Table IV).

Table IV

Comparison of the Lattice Constants of the compounds with those reported in the literature

Compound	Crystal symmetry	Lattice constant 'a' in Å	
		Present	Others[1,23]
$KMnF_3$	Cubic	4.191 ± 0.002	4.191; 4.186
$KCoF_3$	Cubic	4.060 ± 0.002	4.069; 4.070
$KNiF_3$	Cubic	3.980 ± 0.003	4.015; 4.010
$KCuF_3$	Tetragonal	a = 4.140 ± 0.002	4.140
		c = 3.930 ± 0.002	3.926

Heat Capacity Measurements

The calorimeter (with laboratory designation) No.102L with vanes soldered to the bottom surface of the calorimeter to facilitate thermal equilibrium was used. This weighes 137.78 g. The radiation shield used was also correspondingly heavy and weighes about 1,800 g. The heat capacities are measured in the range 80-300°K. In general, each series of experiments was done at least twice throughout the range for checking the reproducibility. The ratio of the heat capacity of the samples to that of the calorimeter varies from 0.70-0.85 in the relevant temperature ranges.

In calculating the heat capacities the defined calorie was taken as equal to 4.184 abs. joules. The ice from distilled water is used for reference point, 273.15°K. The temperatures T listed are the arithmatic means of the initial and final temperatures. The heat capacities reported are the ratios of increase in enthalpy ΔH to the rise of temperature ΔT. In the neighbourhood of transition shorter runs with a temperature rise of about 1°K are taken. As the temperature differences are not quite small, it is not possible to decide whether the heat capacity versus temperature curve near the maximum is smooth or any discontinuity exists in the same. However, a smooth curve is assumed near the maximum.

At the end of the experiments, the recalibration of the thermocouples at fixed points of liquid N_2, liquid O_2 and solid CO_2 gave results in good agreement with the previous measured values.

C H A P T E R - VII

POTASSIUM MANGANESE TRIFLUORIDE

Antiferromagnetic ordering has been observed in many manganese salts. Bizette et al.[4] found by magnetic susceptibility measurement, the Neel temperature in MnO to be 122°K. Neutron diffraction study by Shull et al.[5] and by Roth[6] confirmed the magnetic ordering in this compound at low temperature. Miller[7] and Todd et al.[8] measured the heat capacity behaviour of MnO in the temperature range 50-300°K and noted an anomaly around 116°K. The same type of ordering at low temperature was also observed in MnS, MnSe, MnTe, MnF_2, $MnCl_2$, $MnBr_2$ and MnI_2 with the help of these techniques.[9,10,11]

Hirakawa et al.[1] reported an antiferromagnetic transition in $KMnF_3$ at 88°K from susceptibility measurements. A neutron diffraction study of this compound at 4.2°K by Scatturin et al.[12] confirmed this type of spin ordering. As stated earlier, heat capacity-temperature study in the relevant range would detect such a transition and also provide valuable thermodynamic data for elucidating the mechanism of the process. No such studies have so far been reported in the literature, except a preliminary account of the results in a note by us.[13] In what follows,

heat capacity measurements of this compound over the temperature range 80-300°K have been presented in more detail.

Experimental

The calorimeter was filled with 46.711 g. (0.3905 mole) of the compound and sealed after filling with hydrogen gas as described earlier. The several series of measurements are given in chronological sequence in Table V and represented graphically in fig.4.

In the first series, the calorimeter was cooled to 144°K and measurements were extended up to 240°K, when an anomaly was observed at about 180°K. After allowing the calorimeter to heat up to room temperature, it was cooled to 78°K. The measurements were again continued when another anomaly was noticed around 85°K. When the temperature reached 117°K the calorimeter was recooled to 80°K and the series repeated for measurement of the transition at closer intervals. The fifth series was done with the same view for the anomaly observed in the first series. The fourth and sixth series were done in the high temperature range covering the interval up to 300°K. No dependence of the heat capacity on the thermal history of the sample was found.

Results

In fig.4 it can be seen that the compound shows two peaks in the heat capacity versus temperature graph.

Table V : Heat Capacity of Potassium Manganese Trifluoride (cal./mole.deg.)

Molecular weight : 151.04 $0^{\circ}C$: $273.15^{\circ}K$

T	C_p	T	C_p
SERIES - I		SERIES - II	
144.30	20.02	79.45	19.56
149.04	20.53	81.27	20.53
153.00	20.44	82.90	24.41
157.36	20.50	83.94	22.35
162.51	21.24	85.85	19.14
166.57	22.15	87.50	17.62
170.36	22.31	89.55	15.75
173.20	23.57	93.14	15.88
178.26	25.09	96.92	15.62
181.60	24.74	106.12	16.20
184.30	24.25	109.76	16.85
192.15	23.45	112.99	17.17
198.16	23.09	115.88	16.78
208.45	23.93	SERIES - III	
214.68	24.22	79.58	18.95
220.69	24.51	81.19	21.02
226.61	24.67	83.16	24.35
232.42	24.77	84.34	21.99
238.35	25.48	86.26	18.11

contd...

T	C_p	T	C_p
88.14	16.97	235.24	25.00
90.18	16.07	245.69	25.23
93.45	15.84	255.41	26.77
95.97	15.81	259.97	26.19
98.21	15.88	269.04	27.00
100.64	15.78	272.77	27.23
102.47	15.65	276.08	26.59
105.14	16.33	282.82	27.77
120.22	17.01	286.38	27.43
123.04	17.95	289.60	27.62
127.64	18.40	292.72	27.62
133.57	18.95	295.93	27.13
139.03	19.34	299.05	27.68
144.45	19.72	302.10	27.60
149.77	20.21	305.10	27.65
SERIES - IV		307.53	28.00
208.15	24.41	310.67	28.00
209.59	23.77	SERIES - V	
214.12	24.32	165.36	21.27
217.82	24.32	168.00	22.38
220.20	24.41	170.13	22.48
222.85	24.25	171.86	23.28
225.88	24.44	174.03	23.44
227.40	25.02	179.29	26.28
231.10	25.35	181.92	24.71

contd...

T	C_p	T	C_p
184.63	23.31	SERIES - VI	
188.22	23.28	239.12	25.30
192.15	23.51	241.42	25.16
195.78	23.21	243.90	25.55
199.03	23.63	246.44	25.64
202.76	23.37	250.24	25.77
209.75	24.18	254.30	25.87
214.25	24.41	258.23	26.19
218.08	24.39	261.89	26.19
222.44	24.47	266.55	27.01
226.15	24.61	267.97	26.84
230.26	24.47	270.99	26.73
234.33	24.86	274.10	26.84
238.27	25.48	277.41	27.19
241.99	25.32		
245.23	25.77		
248.55	25.33		

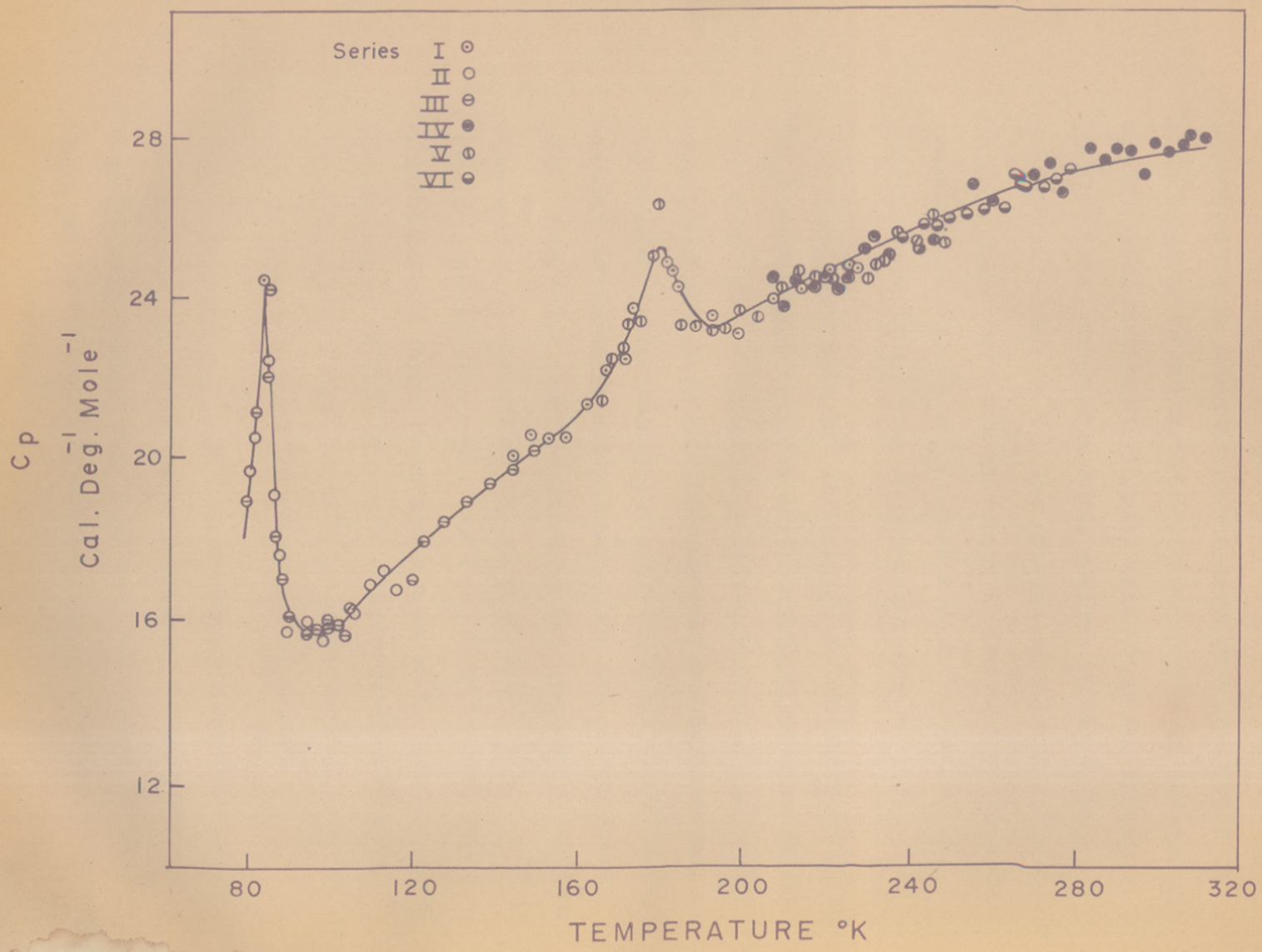

FIG 4 - HEAT CAPACITY OF POTASSIUM MANGANESE TRIFLUORIDE.

By comparison with the magnetic and neutron scattering results of this compound the anomaly at 83.3 ± 0.2°K is attributed to an antiferromagnetic ordering of the moments of Mn^{2+} ions below this temperature. Further, Suemune et al.[14] also observed a broad minimum in the thermal conductivity near 85°K. The torsion measurements by Heeger et al.[15] have shown the existence of yet another magnetic transition at 81.5°K below which a weak ferromagnetic moment caused by canting of spins has been noticed.

Mn^{2+} ion with $3d^5$ electronic configuration is in the $^6S_{5/2}$ state which excludes any possibility of Jahn-Teller type distortion. Hence little distortion from the cubic symmetry observed at room temperature, can be expected. The neutron diffraction pattern at 4.2°K revealed[12] a small movement of fluorine and potassium but not of manganese ions, from their ideal position in the perovskite lattice. Such a kind of distortion was also observed by Geller[16] in several similar compounds. By X-ray diffraction[2] the distortion was found to be maximum at 65°K, which was less pronounced at 84°K in the pure antiferromagnetic state. The paramagnetic state at 95°K is characterized by a tilting only of the octahedron formed by the fluorines.

Theoretically, Mn^{2+} ions with spin quantum number $S = \frac{5}{2}$ are expected to give a magnetic entropy contribution of $R\ln(2S+1) = R\ln 6$ i.e. 3.56 cal./deg.mole. In practice, this can be evaluated by subtracting the lattice contribution

from the measured heat capacities over the relevant range of temperature. As the present studies could not be extended to temperatures much below the transition point an evaluation of the magnetic contribution to the observed heat capacity was not possible.

The second anomaly observed at 179°K is shown as a small hump (fig.4). This is due to a structural change which is in agreement with the crystallographic results reported by Beckman and Knox.[2] The room temperature cubic structure was found to change at 184°K to a tetragonal pseudocell with $\frac{c}{a} > 1$ in which the fluorine octahedra around Mn^{2+} ion remain essentially regular but tilt relative to crystal axis. At 84°K also it formed tetragonal pseudocell but with $\frac{c}{a} < 1$, the regular octahedra being rotated and twisted.

The instability of the $KMnF_3$ perovskite lattice is also indicated by the value of Goldschmidt tolerance factor 't' in the relation $r_{K^+} + r_{F^-} = t\sqrt{2}\,(r_{Mn^{2+}} + r_{F^-})$ where r's denote the radii of the respective ions. Ideally the value of t = 1 and deviations from the same indicate instability of the lattice. The low value (t = 0.88) implies that the Mn^{2+} and F^- are touching one another while K^+ ions are rather free to move. This situation might be responsible for the structural change noted above and consequently, the anomaly in heat capacity at 179°K.

Above this transition the C_p changes slowly and reaches a value of 27.50 cal./mole.deg. at 298.15°K. The corresponding values of entropy, enthalpy and Gibbs free energy, are 38.02 cal./mole.deg. and 5399 and -5938 cal./mole respectively. The method of extrapolation of C_p below 80°K and the evaluation of these thermodynamics functions are described in Chapter XII. The data given above are the redetermined values of $KMnF_3$, since some inaccuracies due to non-equilibrium were observed in our earlier study.[13]

The Néel temperature may be taken as a measure of the strength of the exchange coupling between the magnetic ions through the intervening anions. It would be of interest to compare these temperatures reported for a number of manganese compounds. These have been compiled in Table VI for this purpose.

The existence of super-exchange coupling in antiferromagnetic substances was proposed by Kramers.[17] Anderson[18] and Van Vleck[19] presented a detailed theoretical explanation of the mechanism. Anderson[18] suggested that if one of the 2p electrons of the O^{2-} ion is transferred to the Mn^{2+} ion in an arrangement Mn - O - Mn , the resulting excited ions will have the same spin directions. The unpaired electron left in the oxygen ion can couple antiparallel with another Mn^{2+} ion leading to an antiferromagnetic interaction. Thus a strong superexchange between

Table VI : Comparison of Néel Temperatures of Divalent Manganese Compounds

Compound	Crystal type	Lattice constants a, c Å; α	Transition temperature °K		
			Heat capacity	Susceptibility	Other methods
MnO	NaCl	4.4345	116; 117.8	122	116 (D)
MnS	NaCl	5.2120	139; 147	165	-
MnSe	NaCl	5.448	247	-	-
MnTe	NiAs	4.124; 6.698	307	307	323 (E)
MnF_2	Rutile	4.8734; 3.3103	66.5	72; 70	75 (N)
$MnCl_2$	$CdCl_2$	6.20; 34°35'	1.81; 1.96	1.9	-
$MnBr_2$	CdI_2	3.82; 6.19	2.16	2.16	-
MnI_2	CdI_2	4.16; 6.82	-	3.4	-
$KMnF_3$	Cubic Perovskite	4.191	83.3	88 88.5 (A)	88 (C)
$KMnCl_3$	Tetragonal $\frac{c}{a}$ = 1.005		-	-	100 ± 3 (P)

D = Dialatometric measurements; E = Electrical conductivity;
N = Neutron diffraction; C = Thermal conductivity;
A = Anisotropic measurements; P = Paramagnetic resonance.

two neighbouring Mn^{2+} ions with the paired electrons of the same p orbital of the intervening O^{2-} ion takes place.

Slater,[20] proposed another mechanism of super-exchange that the polarization or deformation of the anion such as O^{2-} stabilizes the energy of the antiferromagnetic state. Again considering MnO as an example, in the antiferromagnetic configuration of Mn-O-Mn, the spins of one Mn^{2+} ion point in one direction while those of the other Mn^{2+} ion point in the opposite direction. The electrons of the O^{2-} ion with plus and minus spins will be pulled each towards that Mn^{2+} ion which has the same spin direction. Thus the oxygen ion is polarized and antiferromagnetic state is stabilized.

In addition to exchange interaction we need sometimes to take into account other factors such as the nature of crystalline field, anisotropy energy and dipolar interactions in this connection.

In the light of the above, we compare the T_N of the related series MnO, MnS, MnSe and MnTe (Table VI). It is evident that T_N increases steadily with polarizability of the anions. This may be attributed to a greater overlap of the cation-anion orbitals due to increasing polarizability of the anion producing stronger coupling between the magnetic ions. Even though MnTe has a little different crystal structure, this still follows the regular trend.

However, if we similarly compare the halides of Mn, the same regularity is not observed, but on the contrary T_N decreases considerably in going from fluoride to other halides of the series. Here the difference in crystal structure is perhaps playing a major role in reducing the coupling interactions apart from the fact that the coupling mechanism is very complex in all the cases except in fluoride.

The structure of MnF_2 is of the rutile type in which the metallic ions constitute a body-centred tetragonal lattice and each is surrounded octahedrally by six negative ions. The crystalline field at each Mn^{2+} ion is therefore orthorhombic, which will produce a different electrostatic potential and therefore a different exchange interaction energy from that in the NaCl type of lattice formed by MnO etc. Further F^- is more electronegative, deformable and produces a weaker electrostatic field than O^{2-}. Accordingly, the exchange coupling will be weaker and therefore T_N (= 66°K) is lower than that of MnO (T_N = 116°K). (Incidentally, we may compare the T_N of MnO_2 (92°K) which has the same rutile type of structure. However, the manganese ions in MnO_2 are Mn^{4+} and the free Mn^{4+} is in the state ^4F. The dipolar interactions would make a significant contribution here.)

$MnCl_2$ has the $CdCl_2$ structure consisting of hexagonal layers of metal ions separated by two layers of chloride ions. $MnBr_2$ is of the CdI_2 type with layers of Mn^{2+} ions arranged in a plane triangular net, with two layers of bromide ions in between the magnetic ions. MnI_2 has also CdI_2 type of structure. In view of the large distances between the magnetic ions (Mn^{2+}) lying in adjoining layers in such a structure, the coupling interactions responsible for antiferromagnetic ordering via the two intervening anions should be relatively very weak. Hence very low T_N ($\sim$ 1-4°K) are observed in these cases. Since $MnCl_2$, $MnBr_2$ and MnI_2 have similar type of structures, their T_N values can be correlated. It is again seen in Table VI that the indirect exchange interactions and therefore T_N values tend to increase with anion polarizability, even though the change is very much smaller than in the case of the oxide-telluride series.

Finally, we may compare the Néel temperatures of MnF_2 (orthorhombic) and $KMnF_3$ (cubic). Because of the difference in the symmetry of ligand field and directional character of the interaction energy, a stronger coupling is facilitated in $KMnF_3$ structure and hence the higher Néel temperature (88°K) is observed in this case than in MnF_2 (66°K). Similarly $KMnCl_3$ has a higher Néel temperature than $KMnF_3$, which may be due to more polarizability of the chlorine ion compared to that of fluorine ion.

C H A P T E R - VIII

POTASSIUM COBALT TRIFLUORIDE

In recent years the magnetic properties of CoO and CoF_2 have been investigated in detail both theoretically and experimentally.[21-24] The magnetic susceptibility measurements by La Blanchetais[25] showed the Néel temperature of CoO to be 292°K. The thermal data of King[26] is in close agreement with this observation. The earlier susceptibility measurements of Bizette et al.[27] did not indicate any evidence of antiferromagnetic ordering in CoF_2 down to 25°K. But later studies by Stout et al.[28] and Erickson[10] showed the compound to be antiferromagnetic below 37.7°K. Such an ordering in several other cobalt compounds has also been noticed by various techniques.

Hirakawa et al.[1] and Machin et al.[29] reported the Néel temperatures of $KCoF_3$ at 114° and 135°K respectively by magnetic susceptibility experiments. The antiferromagnetic ordering in this compound has been confirmed by a neutron diffraction study.[12] In what follows, is a report of a study of the heat capacity of $KCoF_3$ undertaken to investigate the magnetic transition and to evaluate the thermodynamic functions at regular intervals in the range 80-300°K.

Experimental

The calorimeter was loaded with 55.274 g. (0.3566 mole) of the compound and as before sealed after filling with heat exchange gas. The heat capacity values are listed in Table (VII) in the chronological sequence and are represented graphically in fig.5. Initially two series of measurements were taken in the ranges 217-280°K and 180-250°K prior to cooling the calorimeter to liquid nitrogen temperature. The calorimeter was allowed to heat up to room temperature and then cooled to 100°K to start the third series which was extended up to 170°K. It was recooled to 85°K to study at closer intervals the transition noticed near 110°K in the previous series. The fifth and the last series was done in the range 235-205°K to cover the entire range of measurements (80-300°K). The thermal history was observed to have no effect on the heat capacity of the compound.

Results

In $KCoF_3$ a maximum at 109.5°K reaching a value of 22.90 cal./mole.deg. has been observed in the heat capacity versus temperature graph. The shape of λ in the curve and the rapid drop in the heat capacity above this temperature indicate that the transition is of a cooperative type. The susceptibility values below 114°K decrease monotonically with lowering of temperature. The paramagnetic Curie temperature has been reported as 125°K. The lowest value

Table VII: Heat Capacity of Potassium Cobalt Trifluoride (cal./mole.deg.)

Molecular weight : 155.04 $0^{\circ}C$: $273.15^{\circ}K$

T	C_p	T	C_p
SERIES - I			
217.80	25.50	215.70	26.00
222.35	26.43	220.30	26.15
228.25	26.82	225.17	26.66
232.76	26.64	230.00	26.60
238.16	26.60	234.50	26.56
243.47	27.40	244.00	27.16
248.00	27.26	249.20	27.72
252.66	28.00	254.70	27.67
256.00	27.91	SERIES - III	
263.67	28.41	100.85	18.47
266.83	28.24	102.95	19.41
272.40	28.20	105.39	21.30
276.62	28.33	107.78	22.25
SERIES - II		110.17	22.14
180.10	23.71	111.02	21.10
183.20	24.27	112.72	19.52
186.70	24.72	114.58	18.87
190.80	24.70	117.65	18.70
194.40	24.69	121.88	19.07
198.60	25.20	125.77	19.41
203.10	25.50	131.42	20.42
211.00	25.50	143.60	21.17

contd...

T	C_p	T	C_p
147.43	21.71	122.70	19.72
151.18	22.05	129.35	19.87
154.88	22.19	134.57	20.57
158.55	22.47	139.39	20.92
162.42	22.92	144.02	21.32
167.78	22.78	148.20	21.17
171.22	23.20	SERIES - V	
SERIES - IV		236.40	26.85
86.00	14.22	241.35	26.82
89.20	14.90	246.17	27.16
91.85	15.40	250.96	27.38
95.39	16.59	255.35	27.44
96.83	17.09	259.04	27.49
99.01	17.93	264.23	27.90
101.39	18.74	268.77	28.76
103.59	19.78	273.00	27.81
105.73	20.80	277.04	27.91
107.92	22.53	281.08	28.21
109.50	22.90	285.84	28.30
111.63	20.80	291.51	28.70
115.08	18.77	296.30	28.73
116.63	18.71	302.50	29.00
120.22	18.85	305.22	29.20

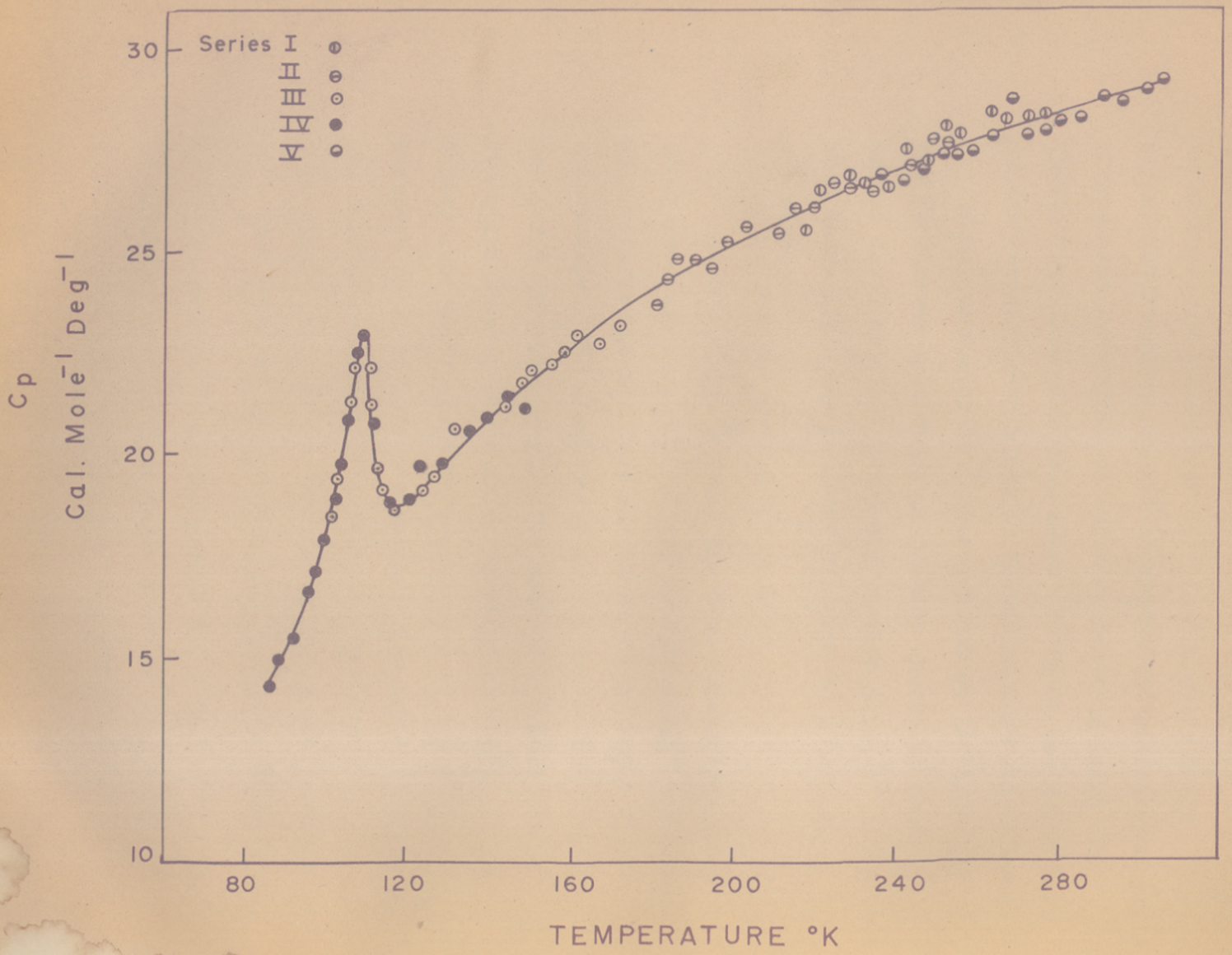

FIG. 5- HEAT CAPACITY OF POTASSIUM COBALT TRIFLUORIDE.

of $\frac{\theta}{T_N} = 1.09$ has been attributed as due to the effect of residual orbital moment of Co^{2+} in the cubic field.[1] The neutron diffraction study[12] confirmed the antiferromagnetic arrangement consisting of spins alternating along the three directions of a cube whose 'a' value was twice that of the perovskite unit cell. The transition was observed in thermal conductivity[14] measurements at 114°K due to the incoherent scattering of phonons caused by phonon magnon interactions. X-ray diffraction studies[30] indicated that below 112°K the compound distorts to a tetragonal symmetry.

Machin et al.[29] found the Néel temperature to be 135°K from their susceptibility measurements. Our present measurements did not show any anomaly near about this temperature. The discrepancy may be due to the sample used, for Hirakawa et al.[1] also noticed a transition at 134°K for some of the samples prepared by them. It is likely that the transition temperature at 109.5°K observed by us is more preferable. The crystallographic[30] and thermal conductivity[14] experiments are also in consistence with our observation of the anomaly rather than that reported by Machin et al.[29] around 135°K.

In free Co^{2+} ion the ground level is $3d^7\ ^4F$. In an electrostatic field of cubic symmetry this level, together with some admixture of the excited level $3d^7\ ^4P$

gives rise to a twelve-fold degenerate ground level and excited levels, which are separated by about 10,000 cm^{-1} or higher in energy. Therefore, the excited levels contribute nothing to entropy at room temperature. The ground level is further split by the combined action of the crystal field of symmetry lower than cubic and of spin-orbit coupling into six levels whose energy spacings are of the order of 100 cm^{-1}.

When there is an odd number of electrons, however, Kramers' theorem states that under the influence of the crystal field and spin orbit coupling each energy level is at least doubly degenerate. So a magnetic entropy of Rln2 or an integral multiple of it is expected. In $KCoF_3$ the resonance experiments indicate that the ground state is split with $J = \frac{1}{2}, \frac{3}{2}$ and $\frac{5}{2}$. As the separations are of the order of kT there may be some population in the higher levels.

Following the procedure used by Stout et al.[21] an experimental evaluation of the magnetic behaviour of the magnetic heat capacity could have been made if the data on the isomorphous diamagnetic salt ($KZnF_3$) were known.* Since our data has thus been limited, it is not possible to evaluate the magnitude of magnetic contribution.

---

* A study on the heat capacity temperature behaviour of $KZnF_3$ is under progress in this laboratory.

However, using a Debye-Einstein function to represent the heat capacity over the relevant temperature range and assuming it to be equal to that of the lattice contribution the magnetic entropy has been estimated approximately. At 110°K it is equal to 0.82 e.u. and at 115°K it equals to 0.84 e.u. Though the theoretically expected value of Rln (2S+1) is much higher than what is evaluated above, this indicates at least the persistence of short range order above the Néel temperature. The heat capacity rises very slowly after about 230°K and reaches a value of 28.84 cal./deg.mole. at 298.15°K. The thermodynamic functions, entropy, enthalpy and free energy calculated from the smoothened values of heat capacities are reported in Chapter XI. The values at 298.15°K are 39.40 cal./mole.deg.; 5669 and -6040 cal./mole. respectively.

A comparison of the Néel temperatures and hence the strength of exchange interaction of several other cobalt salts in the same lines as was done for manganese in the earlier chapter is worth considering. In Table VIII the T_N are listed for such a purpose. As mentioned earlier, in Co^{2+} both the crystalline field and spin-orbit coupling interaction play an important role in influencing the magnetic ordering temperature.

In the oxide series CoO has a Néel temperature of 298.15°K. In contrast with the MnTe it is surprising to note that in CoTe no antiferromagnetic ordering has been

Table VIII : Comparison of Néel Temperatures of Divalent Cobalt Compounds

Compound	Crystal type	Lattice constants a, c Å; ∝	Transition temperature °K		
			Heat capacity	Susceptibility	Other methods
CoO	NaCl	4.249	289.7	293	292 (D)
CoTe	NiAs	3.88; 5.37	-	1273	-
CoF_2	Rutile	4.69; 3.19	37.7	-	45 (N) 35 (C)
$CoCl_2$	$CdCl_2$	6.16; 33°26'	24.9; 24.71	25.0	-
$CoBr_2$	CdI_2	3.68; 6.12	-	19.0	-
CoI_2	CdI_2	3.96; 6.65	-	3.0; 12.0	-
$KCoF_3$	Cubic Perovskite	4.069	109.5	114	112 (X)

D = Dialatometric measurements; C = Thermal conductivity;

N = Neutron diffraction; X = X-ray studies.

observed; rather it has been reported[32] to show a ferromagnetic behaviour up to a quite high temperature (1273°K).

The divalent halides show interesting results in the sense that a regular decrease in T_N is observed with the increase in the polarizability of the anion. The spin-orbit interaction due to triagonal symmetry and octahedral crystal field may lower the T_N of these compounds.[33] This may also be explained considering again their crystal structure and superexchange mechanism.

CoF_2 has a tetragonal symmetry and the magnetic ions are separated by a short distance with a single fluorine ion between them. In $CoCl_2$, and $CoBr_2$ and CoI_2, even though they contain increasingly greater polarizable anions, they have layer structures of the $CdCl_2$ and CdI_2 type respectively, with the result that cobalt ions are separated by a much longer distance with two layers of anions (Co - X - X - Co) in between them. Thus there is a relatively much weaker interaction in these cases resulting in a drop in the T_N values. It may be interesting to observe that the T_N values are decreasing even in the series Cl > Br > I which is contrary to what is expected on the basis of their polarizabilities.

In $KCoF_3$ the indirect interaction takes place by way of single fluorine ion, similar to that in CoO and CoF_2. The Néel temperature of $KCoF_3$ is in between that of CoF_2 and CoO . The tetragonal structure of CoF_2 compared to cubic one of $KCoF_3$ may be responsible for the lower T_N.

C H A P T E R - IX

POTASSIUM NICKEL TRIFLUORIDE

A study of the nickel compound, $KNiF_3$, is interesting because of the high symmetry both of the crystal field and of the d-orbitals of nickelous ion ($3d^8$). Though it is believed to be a purely ionic compound, considerable covalent character has been reported by Shulman et al.[34] from nuclear magnetic resonance experiments.

A broad hump in the magnetic susceptibility of $KNiF_3$ has been observed with a maximum at 275°K by Hirakawa et al.[1] A neutron diffraction pattern at 4.2°K by Scatturin et al.[12] indicated antiparallel ordering of the spins of the magnetic ions. In this chapter the heat capacity measurements in the range of 80-300°K of the same are described.

Experimental

The calorimeter is filled with 58.675 g. (0.3790 mole) of $KNiF_3$ and sealed in the usual way after filling with hydrogen gas. Different series of heat capacities measured in the range 80-300°K are given in chronological sequence of measurements in Table IX and the data are presented graphically in fig.6.

Table IX : Heat Capacity of Potassium Nickel Trifluoride (cal./mole.deg.)

Molecular weight : 154.81 $0^{\circ}C$: 273.15°K

T	C_p	T	C_p
SERIES - I			
202.04	23.53	256.37	28.57
208.50	24.32	259.57	26.70
213.28	23.88	262.71	26.61
218.20	24.34	266.56	26.75
222.96	25.02	SERIES - II	
225.95	25.15	237.60	26.90
228.24	25.70	243.08	27.90
230.66	25.79	247.64	29.15
232.54	26.00	249.33	29.55
235.18	26.55	251.92	30.43
236.16	26.49	252.59	30.75
239.71	27.02	253.87	30.67
240.52	27.28	256.06	29.21
243.67	28.40	257.02	27.95
245.12	28.50	259.51	26.53
247.32	29.01	260.96	26.53
249.06	29.48	274.23	26.81
252.56	30.80	277.71	27.03
254.18	30.45	280.99	26.90

contd...

contd...

T	C_p	T	C_p
285.77	27.23	SERIES - IV	
290.43	27.25	96.70	14.14
294.86	27.35	100.12	15.04
298.35	27.30	103.56	15.45
SERIES - III		106.22	15.39
121.70	17.53	108.89	15.98
124.58	17.65	112.72	16.59
127.19	17.24	116.82	17.36
130.77	18.58	120.76	17.34
135.03	18.88	123.68	17.80
140.13	18.72	131.79	18.55
145.03	19.24	135.89	17.95
149.34	19.63	139.08	19.21
155.33	19.81	142.89	19.54
157.06	20.30	150.51	20.40
160.52	20.58	154.38	20.65
165.22	21.49	157.97	20.71
169.00	21.16	161.25	21.19
172.96	22.23	164.93	21.49
180.42	22.24	SERIES - V	
185.90	22.57	79.44	11.95
190.80	23.31	82.01	12.05
195.38	23.11	84.96	12.40

contd...

T	C_p	T	C_p
88.19	13.10	116.99	16.85
92.48	13.50	120.70	17.50
96.59	14.40	124.14	17.95
100.29	14.70	136.72	18.80
103.89	15.50	140.33	19.35
106.95	15.90	145.61	19.80
110.27	16.35	152.16	20.00
114.15	16.67	156.33	20.35

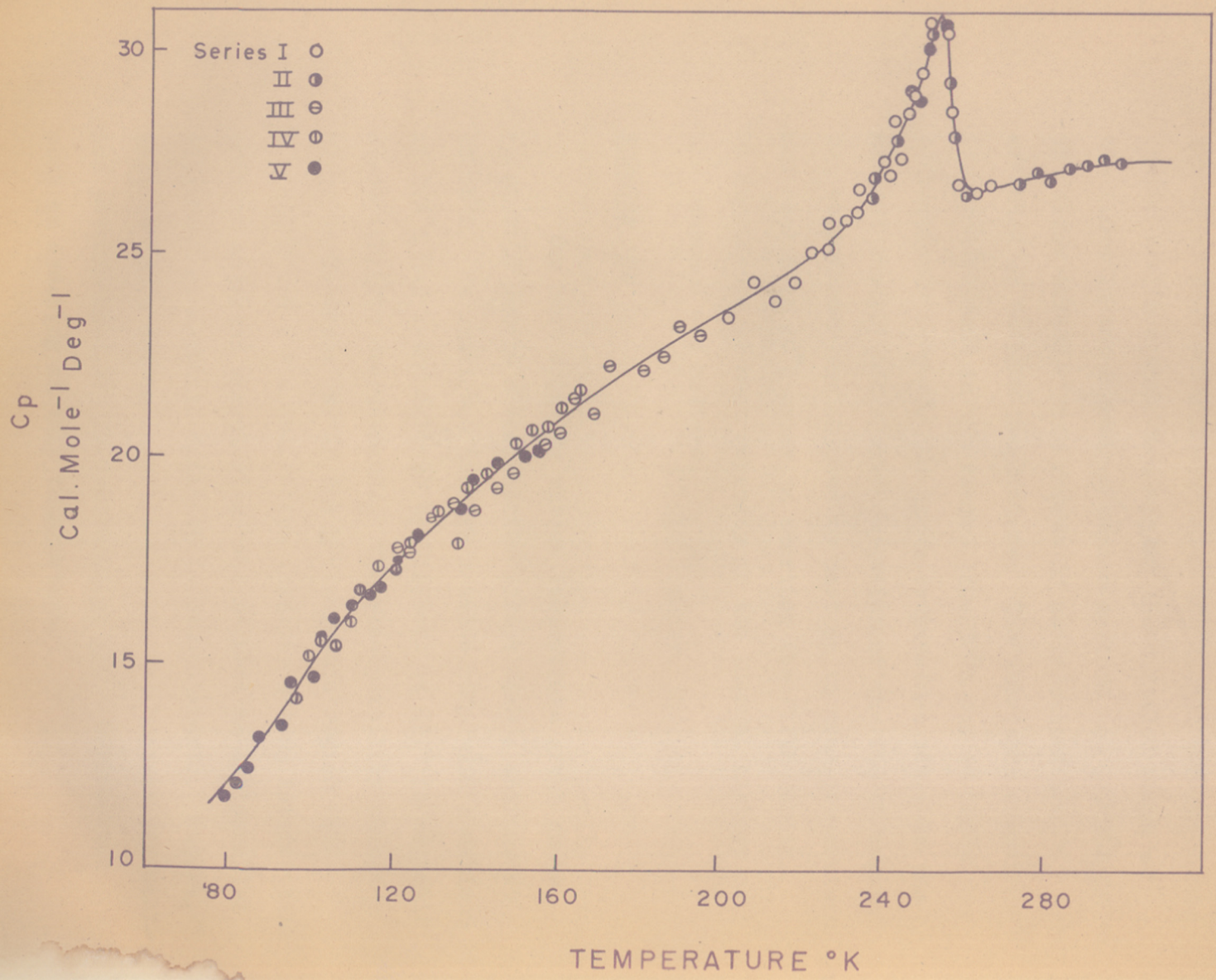

FIG. 6 — HEAT CAPACITY OF POTASSIUM NICKEL TRIFLUORIDE.

The calorimeter was cooled to 200°K and the first series of measurements made upto 266°K. It was recooled to 235°K with a view to studying the detailed shape of the curve in the anomalous region noticed at ~253°K in the first series. This series of measurements was extended up to room temperature. The third and fourth series were done in the ranges 120-200°K and 96-165°K respectively to cover the lower temperature range of the present study. After the completion of the fourth series the calorimeter was allowed to heat up to room temperature and cooled to 80°K prior to starting the fifth series. No dependence of heat capacity on the thermal history of the compound was noticed.

Results

The heat capacity versus temperature graph shows an anomaly due to a cooperative effect with a maximum at 253.5°K. As mentioned earlier a broad hump with a maximum at 275°K has been observed by Hirakawa et al.[1] in magnetic susceptibility measurements. The susceptibility change obeys Curie-Weiss law in the paramagnetic region with θ = 840°K and p = 4.394, which indicate strong interactions between adjacent nickel atoms and suggest an antiparallel alignment of magnetic spins at low temperatures. Superlattice lines due to magnetic ions in the neutron diffraction pattern at 4.2°K by Scatturin et al.[12] corroborate such an ordering at this temperature.

The rapid drop in the heat capacity and the λ-shape of the curve also indicate that the ordered magnetic ions at low temperatures are distributed randomly above the transition temperature. Though the Néel temperature observed by powder susceptibility differs considerably from the present thermal studies, the anisotropic measurements[35] are in excellent agreement with the heat capacity maximum observed by us at 253.5°K. It is surprising to note that the thermal conductivity did not show any anomaly in the relevant temperature region.[14]

No other anomaly has been noticed, unlike in $KMnF_3$, in the entire range of our measurements. The crystallographic data of Okazaki et al.[36] showed that the compound retains its cubic structure down to liquid nitrogen temperature, which is in support of our heat capacity data.

The nickel ion which possesses the $3d^8$ electronic configuration has an orbital degeneracy of one in octahedral field. The spin quantum number of the nickel ion is one and hence a spin degeneracy of $2S+1$ is expected. Thus the maximum entropy that can be acquired at attainable temperatures is $R\ln(2S+1) = R\ln 3$. Since the heat capacity data on the isomorphous diamagnetic salt, $KZnF_3$, are not available, an approximate estimation of the lattice contribution to the heat capacity has been made by using a Debye-Einstien type of function, so that it could be

subtracted from the total observed value to evaluate the magnetic entropy due to the transition. Such an estimation gave a value of 0.64 e.u. at 253°K and 0.94 e.u. at 300°K. These values are again much lower than the expected value of 2.04 e.u. As before, this result at least indicates that short range order persists significantly above the T_N.

The heat capacity has a value of 27.33 cal./deg.mole. at 298.15°K which is the minimum of all the compounds reported in this dissertation. The values of thermodynamic functions viz. entropy, enthalpy and free energy at the same temperature are 36.86 cal./deg.mole, 5308 cal./mole and -5679 cal./mole, respectively.

In Table X the Néel temperatures of several nickel compounds along with that of $KNiF_3$ obtained by various techniques are given with a view to studying their interrelation.

As mentioned earlier, nickel compounds with the cubic octahedral symmetry have a single orbital state and consequently have little spin-orbital interaction similar to that of Mn^{2+} salts. Following the indirect exchange mechanisms of Anderson[18] and Slater,[20] these Néel temperatures can be correlated with the characteristics of the anions.

Table X : Comparison of Néel Temperatures of Divalent Nickel Compounds

Compound	Crystal type	Lattice constants a,c Å; α	Transition temperature °K		
			Heat capacity	Susceptibility	Other methods
NiO	NaCl	4.1684	523	492-647	523 (D)
β-NiS	NiAs	3.39; 5.30	148	150	-
NiSe	NiAs	3.661; 5.256	-	weakly paramagnetic	-
NiTe	NiAs	3.96; 5.35	-	-	-
NiF_2	Rutile	4.6505; 3.084	73.22	-	83 (N)
$NiCl_2$	$CdCl_2$	6.13; 33°36'	52.35	50	-
$NiBr_2$	CdI_2	6.465; 33°20'	-	60	-
NiI_2	$CdCl_2$	6.92; 32°40'	-	75	-
$KNiF_3$	Cubic Perovskite	4.015	253.5	275	253 (A)

D = Dialatometric measurements;
N = Neutron diffraction;
A = Anisotropic measurements.

No regular behaviour in the oxide-telluride series has been observed, which is contrary to that of the Mn^{2+} compounds. Nickel oxide with NaCl structure, has a high Néel temperature (523°K) whereas β-NiS is found to be antiferromagnetic below 150°K. But NiSe and NiTe which have the same NiAs structure as NiS did not show any ordering in the regions 90-750°K and 5-300°K respectively, as reported by various methods.

However, the divalent anhydrous halides behave in somewhat similar way to those of the corresponding manganese salts. As we go down from fluoride to chloride there is a decrease in the Néel temperature but this is much less than that in the Mn^{2+} compounds. Similarly there is a positive increase in T_N from chloride to iodide which may be explained as due to the incressed strength of indirect exchange interaction with the polarizability of the anions in the order Cl < Br < I.

Incidentally it may be noted that the T_N values of the chloride, bromide and iodide did drop to the expected extent from that of the fluoride in comparison with the corresponding manganese salts.

Finally, we may compare the T_N's of NiF_2 and $KNiF_3$. Both the compounds have octahedral ligand fields but $KNiF_3$ has cubic symmetry while NiF_2 has orthorhombic

symmetry. The higher value of $KNiF_3$ compared to NiF_2 may be due to higher symmetry allowing stronger coupling interactions between the magnetic ions. In comparison to NiO a lower value of T_N is expected for $KNiF_3$ or NiF_2 because of the higher electronegativity and less deformability of F^- (weaker field on Ni^{2+}) with respect to O^{2-}.

C H A P T E R - X

POTASSIUM COPPER TRIFLUORIDE

In the divalent copper ($3d^9$) the electronic charge distribution has $d\text{-}\tau$ symmetry. Dunitz and Orgel[37] have shown that in such a case, a distortion of the local octahedron surrounding the Cu^{2+} ion to a tetragonal symmetry is expected due to the Jahn-Teller effect. It has indeed been noticed in $CuCl_2$ by Wells[38]. The metal ion is surrounded by four chlorine ions at a shorter distance and by two at considerably greater distance. A critical account of the Jahn-Teller mechanism in paramagnetic compounds of the iron group has been given by Bose and coworkers.[39,40]

In $KCuF_3$, a distorted fluorine octahedron surrounding the Cu^{2+} ion, with two fluorine ions situated at long, two at medium and two at short distances has been reported by Okazaki et al.[41] from their X-ray studies. A broad peak has been observed in magnetic susceptibility with the maximum value at 243°K by Hirakawa et al.[1] No superstructure line has, however, been observed in neutron diffraction pattern due to magnetic ordering in this salt.[12] As stated earlier, the heat capacity-temperature study also provide a sensitive method of detecting magnetic ordering in a

substance. No such data are available in the literature, which could have been made use of for verifying the above disagreement between the magnetic and neutron diffraction results. In what follows, a report on the measurements of the same over the range 80-300°K has been given.

Experimental

The calorimeter was filled with 71.690 g. (0.448 mole) of the substance and sealed after filling with hydrogen gas to one atmosphere. All the different series of measurements are tabulated in chronological sequence in Table XI.

The calorimeter was cooled to 200°K and the first series of measurements was started and extended up to 300°K. An anomaly was observed at about 235°K. In the second series the calorimeter was cooled to just above the anomalous peak and measurements were repeated in the high temperature range. It was then cooled to 80°K to cover the low temperature region. Series IV and V were done on the low temperature side of the anomaly to determine the shape of the curve more closely in the anomalous region. No thermal hysteresis in the compound has been noticed in the entire range of the present study.

Results

The heat capacity-temperature curve shows an anomalous behaviour with a maximum at 233.2°K. (fig. 7) The peak

Table XI : Heat Capacity of Potassium Copper Trifluoride (cal./mole.deg.)

T	C_p	T	C_p
SERIES - I			
203.23	25.84	251.00	26.86
207.21	25.82	254.73	27.87
210.65	27.43	258.65	27.45
213.18	27.63	262.85	27.05
215.84	28.05	266.97	27.45
218.94	28.53	271.30	27.43
221.75	28.65	275.65	27.89
224.67	29.30	277.67	27.36
227.61	29.95	280.97	28.12
228.59	30.15	284.59	27.87
230.12	30.40	288.10	27.87
231.95	30.52	292.21	28.41
234.27	30.55	295.89	28.36
235.95	30.33	299.59	28.52
236.24	30.25	SERIES - II	
238.70	29.84	238.97	29.47
239.52	29.85	241.70	28.74
241.17	29.20	245.22	27.89
242.54	28.26	248.20	27.25
243.91	28.49	251.10	27.32
246.54	27.87	255.02	27.18
247.42	27.89	258.38	27.47

contd...

T	C_p	T	C_p
263.22	27.29	SERIES - IV	
267.83	27.11	143.83	19.62
271.78	27.49	145.90	19.73
275.53	28.00	148.53	19.63
279.44	28.41	152.04	20.14
SERIES - III		158.33	20.52
85.18	11.58	160.83	21.30
87.46	11.49	165.92	22.15
90.40	12.21	169.95	22.39
94.15	12.59	174.60	22.59
97.97	13.50	178.63	23.14
101.64	13.99	183.22	24.17
106.02	14.17	186.62	24.53
108.95	14.72	190.27	23.93
111.78	15.31	194.91	24.79
115.04	15.73	199.75	25.80
118.40	16.29	203.72	25.80
121.87	16.33	208.30	26.51
126.99	17.27	211.08	26.72
132.64	17.56	214.23	27.54
135.63	18.09	216.33	28.03
142.04	19.21	SERIES - V	
148.48	19.81	104.22	14.21
152.47	20.36	106.54	14.13
156.27	20.74	108.70	14.75

contd...

T	C_p	T	C_p
111.92	15.06	157.04	20.81
114.82	15.22	165.49	21.83
119.47	15.44	171.32	22.32
124.05	16.60	185.85	23.80
127.31	16.80	192.56	24.61
129.73	17.82	198.08	24.92
132.01	17.31	202.39	25.80
134.83	17.88	206.81	25.98
138.73	18.20	209.18	26.75
142.58	19.07	212.73	27.45
146.72	19.72	215.67	28.03
149.50	19.81	219.97	28.85
152.60	20.34	224.62	29.28
153.78	20.38		

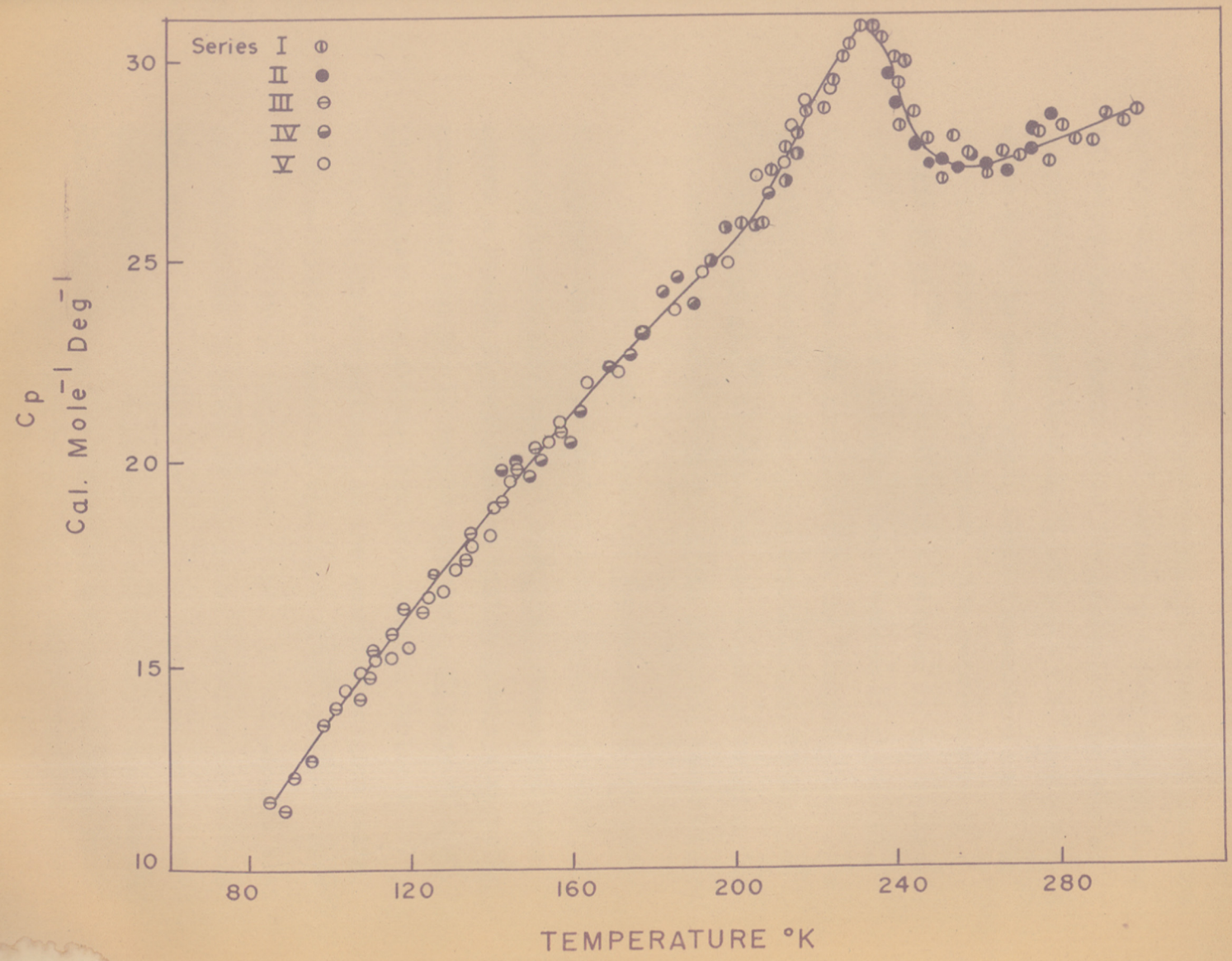

FIG. 7 - HEAT CAPACITY OF POTASSIUM COPPER TRIFLUORIDE.

is, however, a broad one unlike those in the cases of Mn, Co and Ni compounds. Hirakawa et al.[1] indicated that the susceptibility below 243°K decreases slowly with falling of temperature. Curie-Weiss law is applicable only at temperatures higher than 500°K with $\theta = 355^{\circ}$ and $p = 2.16$ where θ is the paramagnetic Curie temperature and p the effective Bohr-magneton number. The measurements by Machin et al.[29] also indicated a maximum in the susceptibility though at a slightly lower temperature (215°K). The lower value was attributed to the contamination by a hydrolysis product. The X-ray crystallographic studies of Okazaki et al.[36] showed that the compound retains its tetragonal structure down to liquid nitrogen temperature.

Cu^{2+} ($3d^9$) has an orbital degeneracy of two and the ground state in octahedral coordination consists of two non-interacting Kramers' doublets. Since the ions assume a random distribution at higher levels a magnetic entropy of $R\ln(2S+1)$ may be expected. In view of our limited data, an attempt has been made to evaluate approximately the entropy in the anomalous region using a Debye-Einstein function viz. $C_p = D(\frac{119}{T}) + 2E(\frac{248}{T}) + 2E(\frac{560}{T})$ over the relevant temperature range. It was assumed that the calculated C_p given by the above function represents the lattice contribution only. The contribution due to the transition was evaluated by subtracting this from the observed total C_p. The evaluated entropy values at 233°

and 250°K are respectively 0.77 e.u. and 1.14 e.u. Since the latter value is of the order of Rln 2 = 1.37 it is suggested that the ground state is a Kramers' doublet. The difference observed may be attributed to an over estimation of the lattice contribution by the approximate Debye-Einstein function.

As mentioned earlier, each Cu^{2+} ion has two fluorine ions at long (2.25 Å), two at medium (1.96 Å) and two at short (1.89 Å) distances. One of the e_g orbitals is completely filled and the other half-filled and therefore the orbital oriented towards the two far off F^- ions (dz^2) should be completely filled. The p-orbital of the F^- ion overlap on each side with a half-filled Cu^{2+} ion in the z' direction, while that of the Cu^{2+} ion is half-filled on one side and completely filled on the other side (x', y' directions). The super-exchange interaction between Cu^{2+} ions on opposite side of F^- ion may be antiferromagnetic for the former and ferromagnetic for the latter as suggested by Kanamori[42] and Goodenough.[43]

Further, Cu^{2+} in $KCuF_3$ has a single unpaired electron in the e_g orbital similar to that in $Mn^{3+}F_3^-$ and $La^{3+}Mn^{3+}O_3^{2-}$. By neutron diffraction, Wollan and coworkers have confirmed the A-type antiferromagnetic structures in MnF_3[44] and $LaMnO_3$.[45] But Scatturin et al.[12] did not observe any superstructure in $KCuF_3$ at low temperatures. However the isostructural $KCrF_3$, which also has a single free electron in

the e_g orbital has been found[12] to have the A-type antiferromagnetic structure.

In the light of the above considerations and the ~~following~~ falling off of susceptibility with the lowering of temperature below the maximum at 243°K and the expected magnetic contribution of Rln2 to entropy in our heat capacity data, we can conclude that the antiferromagnetic ordering exists in $KCuF_3$ at low temperature (< 233.2°K).

Above the Néel temperature, the heat capacity rises slowly and reaches a value of 28.5 cal./mole.deg. The thermodynamic functions calculated at regular intervals of 5°K from the smoothened heat capacity values are reported in Chapter XI. The values of entropy, enthalpy and free energy at 298.15°K are 35.34 cal./mole.deg. and 5387 and 5153 cal./mole, respectively.

The Néel temperatures of several divalent copper compounds are listed in Table XII for a comparative study of the extent of super-exchange interactions in the light of Kramers, Anderson and Slater's theories.

CuO has a monoclinic structure and the Néel temperature was found to be 220°K. This T_N could not be compared with those of sulphide, selenide and telluride of the series as the data for them are not available.

Table XII : Comparison of Néel Temperatures of Divalent Copper Compounds

Compound	Crystal type	Lattice constants a, b, c Å; α	Transition temperature ^{o}K		
			Heat capacity	Susceptibility	Other methods
CuO	Monoclinic	4.635; 3.410; 5.108; $99^{o}22'$	220	230	230 (N)
CuF_2	Monoclinic	4.59; 4.54; 3.32; $96^{o}40'$	-	68.7	69 (P)
$CuCl_2$	Monoclinic	6.70; 3.30; 6.85; 121^{o}	23.9	70.0	-
$CuBr_2$	Monoclinic	7.14; 3.46; 7.18; $121^{o}5'$	-	93	-
$KCuF_3$	Tetragonal	4.14; 3.93	233.2	243 215	-

N = Neutron diffraction;

P = Paramagnetic resonance.

A comparison of the T_N values of the divalent copper halides is interesting in that they show an expected regular increase with the increase in the polarizability of the anions. This is in contrast with that observed in the cases of the halides of Mn, Co and Ni. This can be reconciled with the fact that while the crystal field energy and the symmetry of the anions around the magnetic ion remained more or less the same in the former, these changed considerably in the latter series.

Incidentally, it appears that the low T_N value (23.9°K) observed for $CuCl_2$ by Stout *et al.*[31] from heat capacity-temperature curve needs re-examination in view of its large deviation from the anticipated regularity observed in the magnetic data. They have, however, recorded a very broad hump spreading over the 30-60°K region, which was explained as due to a short range magnetic ordering.

Finally, it may be noted that the T_N of $KCuF_3$ (233°K) is much higher than that of CuF_2 (69°K). The same trend has been observed in all the earlier cases also, though to a different extent. As before, this result can be qualitatively explained on the basis of crystal field symmetry and angular dependence of the Cu-F-Cu coupling interaction.

C H A P T E R - XI

THERMODYNAMIC FUNCTIONS OF THE COMPOUNDS

The thermodynamic functions such as entropy, enthalpy and free energy were evaluated from the smoothened values of experimental heat capacity data. As the measurements were restricted down to 80°K only, it necessitated the extrapolation of heat capacity values to 0°K in order to evaluate the thermodynamic functions. Several methods are available for such an extrapolation.

The extrapolation method suggested by Kelley et al.[46] may be written as

$$C_p \text{ (mole)} = C_{p_o} (A + BT)$$

where C_p and C_{p_o} are the heat capacities of the substance and the standard substance respectively and A and B are constants. As a first approximation the constant B can be assumed to be zero. Hence the equation may be written, for example, for $KMnF_3$, as follows:

$$C_p\ KMnF_3 = A\ (C_p\ KF + C_p\ MnF_2)$$

where the sum of the heat capacities of KF and MnF_2 represent the standard substance.

Kelley et al.[46] used the method essentially for homologous series of organic compounds. Shomate[47] extended it to calculate the heat capacities of hydrates from the measured values of anhydrous salts and water.

Debye has shown that at low temperatures C_v is proportional to T^3 and entropy is equal to $\frac{1}{3} C_v$. But as the present measurements are not extended to low enough temperatures a Debye function for the extrapolation can not be used. Born has proposed a function of the type

$$C_v = \sum D \left(\frac{\theta_D}{T} \right) + \sum_{i=1}^{p-1} E \left(\frac{\theta_{E_i}}{T} \right)$$

where $D(\frac{\theta_D}{T})$ and $E(\frac{\theta_E}{T})$ represent Debye and Einstein functions respectively and p the number of atoms in a molecule of the substance. This equation has been shown[48] to represent heat capacities of several substances over a wide temperature range and permit reasonably accurate extrapolation.

The measured heat capacities were plotted against log T and the curve extrapolated smoothly into a Debye function and was extended to 300°K. Differences between the measured curve and the Debye function were read at convenient intervals. These differences were then plotted against log T and fitted with a series of Einstein functions.

C_p values below 80°K were extrapolated using the following equations for $KCoF_3$, $KNiF_3$ and $KCuF_3$ respectively:

$$C_p\ KCoF_3 = D\left(\frac{87}{T}\right) + 2E\left(\frac{276}{T}\right) + 2E\left(\frac{368}{T}\right)$$

$$C_p\ KNiF_3 = D\left(\frac{97}{T}\right) + 2E\left(\frac{225}{T}\right) + 2E\left(\frac{568}{T}\right)$$

$$C_p\ KCuF_3 = D\left(\frac{119}{T}\right) + 2E\left(\frac{248}{T}\right) + 2E\left(\frac{560}{T}\right)$$

For manganese the same equation as that used for nickel compound represents well.

The values of thermodynamic functions above 80°K calculated at 5° interval from the measured heat capacity data are listed in Tables XIII, XIV, XV and XVI respectively for Mn, Co, Ni and Cu compounds.

Table XIII : Thermodynamic Functions of Potassium Manganese Trifluoride

Temp. °K	C_p cal./mole.deg.	S_T-S_0 cal./mole.deg.	H_T-H_0 cal./mole	$-(F-H_0)$ cal./mole
80	19.40	9.95*	470.3*	325.7
85	20.21	11.28	579.8	378.7
90	16.15	12.30	668.2	439.0
95	15.68	13.15	747.8	501.2
100	15.75	13.96	826.4	569.6
105	16.21	14.74	906.2	640.8
110	16.75	15.51	988.8	717.2
115	17.30	16.26	1073	796.0
120	17.78	17.01	1161	880.0
125	18.24	17.75	1252	967.0
130	18.61	18.47	1344	1057
135	19.08	19.18	1438	1151
140	19.46	19.89	1534	1251
145	19.86	20.58	1636	1349
150	20.21	21.27	1733	1457
155	20.60	21.94	1835	1565
160	20.98	22.60	1938	1678
165	21.57	23.25	2044	1792
170	22.48	23.91	2158	1906
175	24.25	24.58	2271	2030
180	25.23	25.29	2396	2156
185	23.90	25.96	2518	2285

* Extrapolated values.

contd...

Temp. ^{o}K	C_p cal./mole.deg.	S_T-S_0 cal./mole.deg.	H_T-H_0 cal./mole	$-(F-H_0)$ cal./mole
190	23.33	26.59	2636	2417
195	23.30	27.19	2754	2548
200	23.49	27.79	2869	2689
205	23.73	28.37	2987	2830
210	24.00	28.95	3107	2973
215	24.25	29.51	3227	3116
220	24.47	30.08	3348	3268
225	24.67	30.63	3472	3420
230	24.90	31.17	3594	3575
235	25.19	31.71	3721	3731
240	25.45	32.24	3848	3890
245	25.71	32.77	3976	4052
250	25.93	33.29	4104	4218
255	26.19	33.81	4235	4385
260	26.42	34.32	4366	4559
265	26.62	34.82	4499	4729
270	26.83	35.32	4631	4906
273.15	26.94	35.63	4719	5017
275	27.01	35.82	4767	5082
280	27.13	36.31	49,01	5263
285	27.23	36.78	5039	5441
290	27.39	37.26	5174	5626
295	27.48	37.73	5312	5818
298.15	27.50	38.02	5399	5938
300	27.52	38.20	5451	6009

Table XIV : Thermodynamic Functions of Potassium Cobalt Trifluoride

Temp. °K	C_p cal./mole.deg.	S_T-S_0 cal./mole.deg.	H_T-H_0 cal./mole	$-(F-H_0)$ cal./mole
80	12.90	10.11*	480.0*	328.8*
85	14.01	10.92	547.4	380.7
90	15.12	11.75	592.3	465.2
95	16.20	12.60	671.5	525.5
100	18.31	13.49	756.0	593.0
105	20.49	14.43	868.5	647.5
110	22.16	15.43	964.2	733.1
115	18.82	16.22	1064	812.5
120	18.82	17.12	1155	899.0
125	19.44	17.90	1302	936.0
130	20.00	18.67	1400	1027
135	20.56	19.43	1502	1121
140	21.01	20.19	1606	1220
145	21.47	20.94	1713	1323
150	21.89	21.67	1821	1429
155	22.33	22.40	1953	1518
160	22.75	23.11	2043	1655
165	23.15	23.82	2160	1771
170	23.53	24.52	2276	1893
175	23.84	25.20	2394	2016
180	24.07	25.88	2514	2145
185	24.35	26.54	2635	2275

* Extrapolated values

contd...

Temp. °K	C_p cal./mole.deg.	S_T-S_0 cal./mole.deg.	H_T-H_0 cal./mole	$-(F-H_0)$ cal./mole
190	24.66	27.19	2758	2408
195	24.91	27.84	2882	2546
200	25.18	28.48	3007	2689
205	25.39	29.10	3133	2834
210	25.62	29.72	3261	2980
215	25.82	30.32	3388	3130
220	26.09	30.92	3519	3284
225	26.34	31.51	3648	3441
230	26.58	32.09	3782	3597
235	26.79	32.77	3916	3784
240	26.99	33.23	4052	3923
245	27.03	33.79	4186	4093
250	27.39	34.24	4322	4263
255	27.61	34.89	4460	4436
260	27.77	35.42	4598	4610
265	27.91	35.95	4738	4785
270	28.08	36.48	4878	4973
273.15	28.19	36.80	4965	5085
275	28.25	36.99	5019	5151
280	28.39	37.50	5158	5342
285	28.53	38.01	5302	5528
290	28.65	38.50	5445	5715
295	28.76	38.99	5581	5919
298.15	28.84	39.40	5669	6040
300	28.89	39.48	5732	6112

Table XV : Thermodynamic Functions of Potassium Nickel Trifluoride

Temp. °K	C_p cal./mole.deg.	S_T-S_0 cal./mole.deg.	H_T-H_0 cal./mole	$-(F-H_0)$ cal./mole
80	11.90	9.95*	470.3*	325.7
85	12.50	10.90	531.3	395.1
90	13.22	11.43	595.6	433.1
95	14.00	12.17	662.6	492.4
100	14.80	12.91	735.7	555.3
105	15.51	13.65	811.4	621.6
110	16.19	14.38	890.0	691.8
115	16.79	15.12	972.5	766.5
120	17.35	15.85	1058	844.0
125	17.92	16.57	1146	925.0
130	18.35	17.28	1237	1009
135	18.77	17.98	1330	1098
140	19.20	18.67	1425	1188
145	19.58	19.35	1522	1284
150	20.05	20.02	1624	1379
155	20.40	20.63	1722	1476
160	20.83	21.34	1825	1589
165	21.25	21.99	1931	1697
170	21.70	22.63	2038	1809
175	22.10	23.27	2147	1924
180	22.43	23.89	2259	2042
185	22.75	24.51	2372	2163

* Extrapolated values.

contd...

Temp. °K	C_p cal./mole.deg.	S_T-S_0 cal./mole.deg.	H_T-H_0 cal./mole	$-(F-H_0)$ cal./mole
190	23.00	25.12	2486	2287
195	23.27	25.72	2602	2412
200	23.50	26.32	2719	2545
205	23.75	26.90	2837	2679
210	24.00	27.48	2956	2816
215	24.40	28.05	3077	2955
220	24.87	28.62	3200	3096
225	25.25	29.18	3326	3240
230	25.80	29.75	3453	3389
235	26.42	30.30	3584	3536
240	27.30	30.86	3721	3687
245	28.48	31.44	3856	3847
250	29.81	32.02	4002	4003
255	30.00	32.63	4155	4165
260	26.75	33.17	4291	4333
265	26.70	33.68	4424	4499
270	26.71	34.18	4557	4673
273.15	26.78	34.48	4641	4813
275	26.82	34.67	4691	4894
280	26.90	35.15	4825	5017
285	27.10	35.65	4960	5200
290	27.20	36.10	5086	5384
295	27.27	36.57	5222	5558
298.15	27.30	36.86	5308	5679
300	27.33	37.03	5359	5750

*Extrapolated values.

Table XVI : Thermodynamic Functions of Potassium Copper Trifluoride

$T^{\circ}K$	C_p cal./mole.deg.	S_T-S_0 cal./mole.deg.	H_T-H_0 cal./mole	$-(E_T-H_0)$ cal./mole
80	11.00	8.155*	407.3*	245.2*
85	11.60	8.840	463.5	288.0
90	12.20	9.520	522.6	334.1
95	12.95	10.20	585.1	383.9
100	13.60	10.88	651.3	436.7
105	14.25	11.57	720.3	493.7
110	14.90	12.24	793.0	554.0
115	15.55	12.92	870.3	615.7
120	16.20	13.60	948.3	683.7
125	16.90	14.27	1031	752.0
130	17.60	14.95	1117	827.0
135	18.20	15.62	1206	903.0
140	18.75	16.29	1299	981.0
145	19.37	16.96	1394	1066
150	20.00	17.63	1492	1152
155	20.60	18.29	1595	1239
160	21.23	18.96	1689	1345
165	21.77	19.62	1806	1432
170	22.37	20.28	1916	1516
175	22.92	20.94	2030	1634
180	23.42	21.59	2146	1740
185	23.92	22.24	2265	1850

*Extrapolated values.

contd...

$T^{\circ}K$	C_p cal./mole.deg.	S_T-S_0 cal./mole.deg.	H_T-H_0 cal./mole	$-(F_T-H_0)$ cal./mole
190	24.35	22.88	2386	1961
195	24.85	23.52	2509	2077
200	25.38	24.15	2625	2204
205	26.06	24.79	2754	2329
210	26.86	25.42	2896	2441
215	27.60	26.07	3032	2572
220	28.38	26.70	3174	2699
225	29.37	27.35	3318	2837
230	30.36	28.02	3468	2977
235	30.50	28.68	3620	3121
240	29.25	29.31	3770	3264
245	27.87	29.90	3913	3413
250	27.38	30.46	4051	3564
255	27.25	31.00	4187	3718
260	27.30	31.53	4324	3874
265	27.45	32.05	4461	4031
270	27.57	32.56	4598	4194
273.15	27.65	32.86	4685	4291
275	27.70	33.07	4736	4357
280	27.90	33.57	4875	4524
285	28.08	34.07	5015	4692
290	28.20	34.56	5165	4855
295	28.40	35.04	5298	5042
298.15	28.47	35.34	5387	5153
300	28.52	35.52	5442	5208

C H A P T E R - XII

GENERAL DISCUSSION

The crystal field theory[37] together with the Jahn-Teller effect predict that ions with orbitally degenerate electron configurations distort their environment so as to remove the degeneracy. For transition metal ions the d-orbitals are split by an octahedral field into a lower triplet, t_{2g}, and an upper doublet e_g. When the degeneracy occurs in the antibonding orbitals the distortions from the cubic symmetry will be large, while in the non-bonding, t_{2g}, they are small. More refined treatments show that the strong spin-orbit coupling reduces the degeneracy of Co^{2+} to a Kramers doublet which cannot be split by configurational distortions of the Jahn-Teller type. Thus in the present series of compounds containing Mn ($3d^5$), Co ($3d^7$), Ni ($3d^8$) and Cu ($3d^9$) no distortions can be expected except in $KCuF_3$ where large distortion of the Jahn-Teller type due to the d^9 configuration may be anticipated.

In accordance with the theoretical prediction, it has been found that $KMnF_3$, $KCoF_3$ and $KNiF_3$ crystallize in the cubic perovskite structures (space group O_h^1 $P_m 3_m$) and their lattice constants do not differ radically (p.64, Table IV). $KCuF_3$ shows a tetragonal structure which can

be looked upon as distorted from the cubic symmetry.

The compounds are paramagnetic at room temperature. There is an appreciable contribution to the entropy arising from a change of completely ordered low temperature form of the magnetic ions to a high temperature form where there is a random distribution among several electronic states. The entropy is lost at low temperatures by a cooperative process of antiferromagnetic ordering involving interactions between the neighbouring magnetic ions.

The magnetic ordering of the compounds can be accounted for on the basis of indirect exchange interactions. The cation e_g orbitals overlap with the p-orbitals of the intervening anions and hence these orbitals would be expected to be associated with the indirect magnetic exchange coupling in these compounds. Thus the half-filled orbitals of two magnetic cations in $KMnF_3$, $KCoF_3$ and $KNiF_3$ overlap respectively the two p-orbitals of the anion (F^-) and the octahedral symmetry of the e_g orbitals lead to the observed G-type antiferromagnetism.

In $KCuF_3$, the overlapped Cu^{2+} ion is half-filled on one side of the F^- ion and completely filled on the other side. Thus the super-exchange interaction between Cu^{2+} ions on opposite side of the F^- ion may be antiferromagnetic for the former and ferromagnetic to the latter

i.e. an A-type antiferromagnetism may be expected below the Néel temperature.

Recently the extent of super-exchange interaction in these compounds has been investigated theoretically as well as experimentally by Shulman et al.[34] and Hirakawa.[49] They determined the fraction of unpaired spins, f_s, $f_\sigma - f_\pi$ in the 2s and 2p orbitals of F^- ions where the subscripts s, σ, and π refer to s, p_σ and p_π orbitals respectively. While the f_s values remain small and nearly constant (~ 0.5 %), the $(f_\sigma - f_\pi)$ values change remarkably from one compound to another.

In Mn^{2+} with half-filled orbitals a very small value of $(f_\sigma - f_\pi)$ viz. 0.18 % has been observed as a result of the cancellation of nearly same values of $f_\sigma - f_\pi$. In the case of Ni^{2+} where t_{2g} orbitals are completely filled but e_g orbitals are half-filled a positive value of 5% is expected because $f_\pi \sim 0$. Experimentally a value of 4.95 % has been observed. Applying the same considerations, an intermediate value for Co^{2+} where t_{2g} orbitals are partially filled, is anticipated. However, a value of 5.7 %, which is higher than that of Ni^{2+}, has been found. After accounting for the partial quenching in the cubic field of the orbital, a value of 4.9% was obtained which is within the expected order.

The heat capacity measurements on the compounds indicated anomalous regions with maxima at 83.3°, 109.5°,

253.5 and 233.2 °K respectively for the Mn, Co, Ni and Cu compounds. The rapid drop in the heat capacity on the high temperature side of the anomaly and the λ-shape of the curves clearly indicate the characteristic antiferromagnetic ordering of the magnetic moments of these cations. A comparison of the maxima observed in the present measurements with the corresponding Néel temperatures reported in the literature from various other studies is given in Table XVII.

Table XVII

Comparison of Néel Temperatures of the Present Measurements with other Determinations

Compound	Néel temperature °K		
	Heat capacity measurements (Present work)	Magnetic susceptibility	Other studies
$KMnF_3$	83.3	88	88 (C)
$KFeF_3$	-	113	-
$KCoF_3$	109.5	114; 135	112 (X) 114 (C) 119 (A)
$KNiF_3$	253.5	275; 280	253 (A)
$KCuF_3$	233.2	243; 215	243 (X)

C = Thermal conductivity;
X = X-ray diffraction;
A = Magnetic anisotropy.

It is seen that the agreement in general is satisfactory. It may interesting to note that the heat capccity maxima

observed are lower than those given by magnetic susceptibility measurements. The higher values in magnetic studies has been explained as due to statistical effects.[1,50]

As the transitions occur at sufficiently high temperatures in these compounds, the lattice contribution form an important fraction of the total heat capacity and it must be estimated with considerable accuracy in order to calculate the entropy changes associated with the magnetic ordering. Assuming that the lattice heat capacity of UO_2 equals that of isomorphous, diamagnetic ThO_2, Osborne and Westrum[51] estimated the magnetic contribution in UO_2 by subtracting the heat capacity of ThO_2 from the observed value for UO_2. Catalano and Stout,[52] however, have shown that such an assumption fails in NiF_2 since the observed heat capacity at higher temperatures is considerably lower than that of the isomorphous diamagnetic ZnF_2. So they used the data on the diamagnetic salt together with a corresponding states argument[31] to estimate the lattice contributions of such compounds.

Since such an estimation is not possible at this stage, as mentioned earlier, Debye-Einstein type of function was used to evaluate the vibrational heat capacity. Admittedly such an estimation is not accurate since it over-estimates the lattice contribution but still can be used for an approximate evaluation. The difference

between the observed heat capacity and that given by the Debye-Einstein function may be taken to be that due to the magnetic transition. The values of magnetic entropy obtained for $KCoF_3$, $KNiF_3$ and $KCuF_3$ are 0.82, 0.64 and 0.77 e.u. respectively at the Néel temperatures. These values are, however, much lower than the values expected from their spin configurations viz. $R\ln(2S+1)$. This, however, can be taken as a clear indication of the persistence of short range order above the Néel temperatures. That there is always a considerable magnetic heat capacity in the short range order region above the maximum is also expected from more elaborate statistical theories of the antiferromagnetic transitions. But there is as yet no theory which agrees quantitatively with experiment.

The smoothened heat capacity-temperature curves of all the compounds are given in fig.8 for direct comparison. $KCoF_3$ is having a higher heat capacity than that of all other compounds of the series, throughout the range of the present measurements. $KMnF_3$ and $KNiF_3$ are having almost the same value except near the transition regions. $KCuF_3$ is having the lowest value in low temperature region and then rises steadily because of the transition. A comparison of C_p, ΔH, ΔS, and $-\Delta F$ of these compounds at 298.15°K are given in Table XVIII.

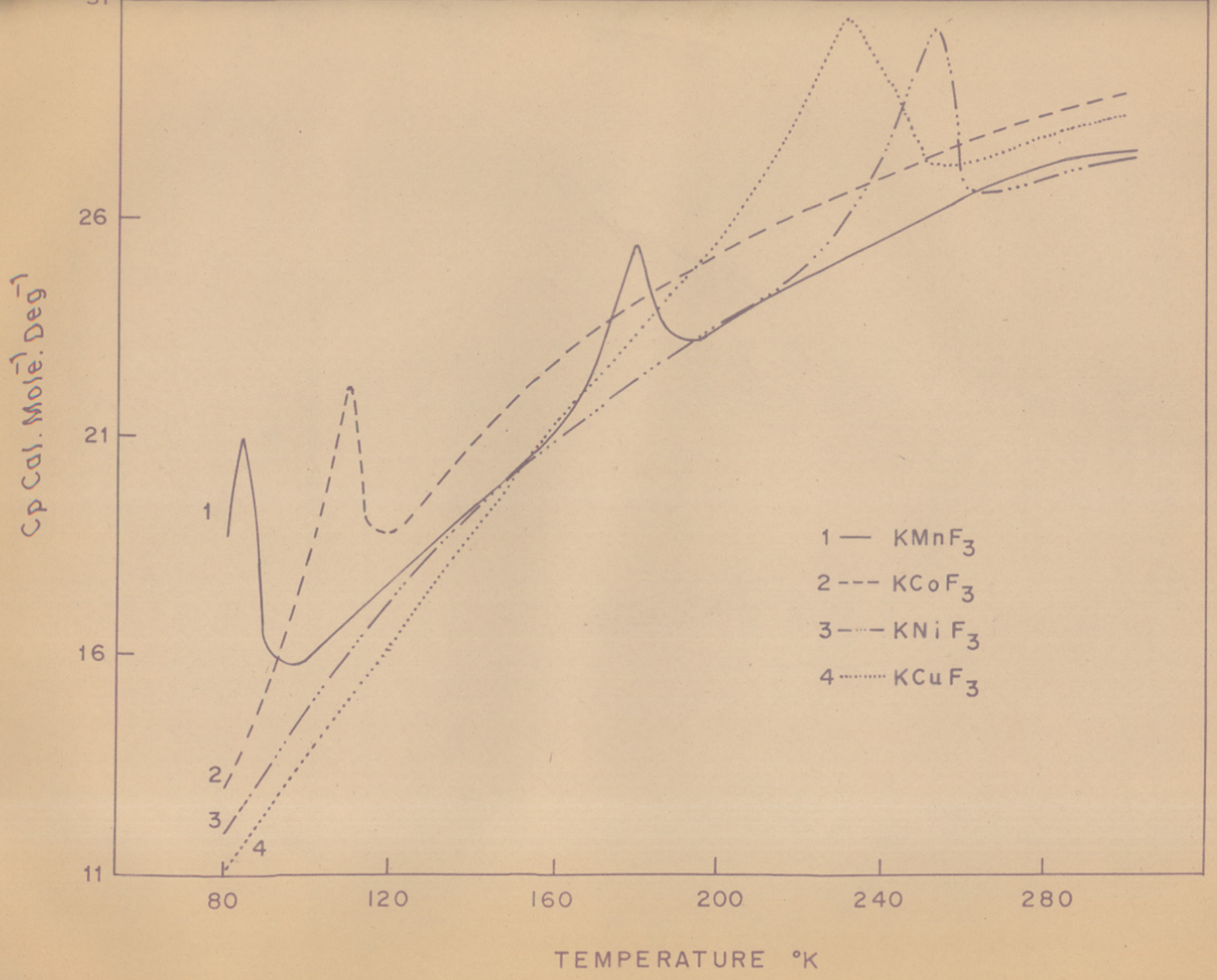
Cp Cal. Mole^{-1}. Deg^{-1}
26
21
16
11
80
120
160
200
240
280
TEMPERATURE °K
1
2
3
4
1 — $KMnF_3$
2 --- $KCoF_3$
3 — · — $KNiF_3$
4 ····· $KCuF_3$

FIG. 8

Table XVIII

Standard Values of C_p, ΔH, ΔS and $-\Delta F$ of Some Related Divalent 3d Transition Group Compounds at 298.15°K

Compound	C_p cal./mole.deg.	ΔH cal./mole	ΔS cal./mole.deg.	$-\Delta F$ cal./mole.deg.
$KMnF_3$	27.50	5399	38.02	19.92
$KCoF_3$	28.84	5669	39.40	20.50
$KNiF_3$	27.20	5308	36.86	19.04
$KCuF_3$	28.47	5387	35.34	17.29
MnF_2	16.23	-	22.25	-
CoF_2	16.44	3008	19.69	9.67
NiF_2	15.31	2729	17.59	8.44
MnO	10.54	-	14.27	-
CoO	13.20	-	12.66	-
NiO	10.46	-	9.08	-
CuO	10.11	569	10.19	4.50

It can be seen the value for $KCuF_3$ is in between that of $KCoF_3$ and $KNiF_3$. The latter has the lowest heat capacity at room temperature. These observations are in general agreement with those of other divalent series of compounds, for example, oxides and fluorides of the iron group as noted in the Table XVIII.

CoO and CoF_2 also have higher heat capacities at higher temperatures than the corresponding Mn, Ni and Cu compounds. The oxides of Mn and Ni have nearly the same values at room temperature. NiF_2 has the lowest value of the series as in the case of the double fluorides. CuO has higher heat capacity than NiO at lower temperatures but lower near room temperature which is different from that in the trifluorides.

A comparison of the Néel temperatures of the present series with other similar series of compounds such as MF_3, Mo, is worth mentioning. In general, there is a successive increase in the Néel temperatures with increase in the number of delectrons as can be seen in Table IXX. The transition temperatures observed in KMF_3 group may be divided into two viz. the low and a high temperature groups. Compounds with $t_{2g}^5 e_g^2$ (i.e. Co^{2+}) configuration or that with lesser number of electrons viz. $Mn^{2+}(t_{2g}^3 e_g^2)$ form the lower whereas $Ni^{2+}(t_{2g}^6 e_g^2)$ and $Cu^{2+}(t_{2g}^6 e_g^3)$ with more electrons form the other group. $KFeF_3$ with $t_{2g}^4 e_g^2$ has been reported[1] to show a transition at 113°K from magnetic studies in consistence with the above grouping.

In view of the more or less the same crystal field potential in the cases of the oxides as well as of the double fluorides a proportional rise in T_N may be expected in the order Mn < Co < Ni. However, it is observed that for

Table IXX : Comparison of Néel Temperatures with Various Other Similar Compounds in °K.

Series	d^4	d^5	d^6	d^7	d^8	d^9
$LaMO_3$	$LaMnO_3$	$LaFeO_3$	$LaCoO_3$	-	-	-
	100	750	80			
MF_3	MnF_3	FeF_3	CoF_3	-	-	-
	43	394	460			
Sr_2MSbO_6	Sr_2MnSbO_6	Sr_2FeSbO_6	Sr_2CoSbO_6	-	-	-
	10	21	35			
Sr_2MWO_6	-	Sr_2MnWO_6	Sr_2FeWO_6	Sr_2CoWO_6	Sr_2NiWO_6	-
		10	16	22	54	
MO	-	MnO	FeO	CoO	NiO	CuO *
		118	189	290	520	230
KMF_3	-	$KMnF_3$	$KFeF_3$	$KCoF_3$	$KNiF_3$	$KCuF_3$ **
		83.3	-	109.5	253.2	233.2

* Monoclinic complicated structure.

** Tetragonally distorted perovskite structure.

Co compounds the T_Ns are smaller than anticipated, the lowering being much greater in the fluoride. This may be ascribed to weaker coupling caused by spin-orbit interaction. Compared with the oxide the weaker crystalline field present in the $KCoF_3$ system may have caused a further lowering of T_N.

REFERENCES

(1) Hirakawa, K., Hirakawa, K. and Hashimoto, T., J. Phys. Soc. Japan, 15, 2063-68 (1960).

(2) Beckman, O. and Knox, K., Phys. Rev., 121, 376-80 (1961).

(3) Martin, R.L., Nyholm, R.S. and Stephenson, N.C., Chem. and Indus., 3, 83-85 (1956).

(4) Bizette, H., Squire, C.F. and Tsai, B., Comptes Rendus, 207, 449-50 (1938).

(5) Shull, C.G., Strauser, W.A. and Wollan, E.O., Phys. Rev., 83, 333 (1951).

(6) Roth, W.L., Phys. Rev., 110, 1333-41 (1958).

(7) Miller, R.W., J. Am. Chem. Soc., 50, 1875-83 (1928).

(8) Todd, S.S., Bonnickson, K.R., J. Am. Chem. Soc., 73, 3894 (1951).

(9) Bizette, H., J. Phys. Rad., 12, 161-169 (1951).

Bizette, H. and Tsai, B., Comptes Rendus, 209, 205-6 (1939);

de Hass, W.J., Schultz, B.H. and Koolhaas, Physica, 7, 57 (1940);

Murray, R.B. and Roberts, L.D., Phys. Rev., 100, 1067-70 (1955).

(10) Wollan, E.O., Koehler, W.C. and Wilkinson, M.K., Phys. Rev., 110, 638-46 (1958);

Erickson, R.A., Phys. Rev., 90, 779-85 (1953).

(11) Anderson, C.T., J. Am. Chem. Soc., 53, 476-83 (1931);
Murray, R.B., Phys. Rev., 100, 1071-74 (1955);
Kelley, K.K., J. Am. Chem. Soc., 61, 203-207 (1939);
Hadley, W.B. and Stout, J.W., J. Chem. Phys., 39, 2205 (1963);
Stout, J.W. and Adams, H.E., J. Am. Chem. Soc., 64, 1535-38 (1942);

(12) Scatturin, V., Corliss, L., Elliott, N. and Hastings, J., Acta Cryst., 14, 19-26 (1961).

(13) Rao, R.V.G., Das, C.D., Keer, H.V. and Biswas, A.B., Proc. Phys. Soc. London, 81, 191-2 (1963).

(14) Suemune, Y. and Ikawa, H., J. Phys. Soc. Japan, 19, 1686-90 (1964).

(15) Heeger, A.J., Beckman, O. and Portis, A.M., Phys. Rev., 123, 1652-60 (1961).

(16) Geller, S., J. Chem. Phys., 24, 1236-39 (1956).

(17) Kramers, H.A., Physica, 1, 182-92 (1934).

(18) Anderson, P.W., Phys. Rev., 79, 350-56 (1950).

(19) van Vleck, J.H., J. Phys. Rad., 12, 262-74 (1951).

(20) Slater, J.C., Quart. Prog. Report, M.I.T., 15, 1 (1953); Rev. Mod. Phys., 25, 199 (1953).

(21) Kanamori, J., Prog. Theor. Phys., 17, 197-222 (1957).

(22) Nakamura, T. and Taketa, H., Prog. Theor. Phys., 13, 129-47 (1955).

(23) Anderson, P.W., Phys.Rev., 115, 2-13 (1959).

(24) Rooksby, H.P. and Tombs, N.C., Nature, 167, 364 (1951).

(25) La Blanchetais, C.H., J. Phys. Rad., 12, 765-71 (1951).

(26) King, E.G., J. Am. Chem. Soc., 79, 2399-400 (1957).

(27) Bizette, H., Ann. Phys., (12) 1, 295 (1946).

(28) Stout, J.W. and Matarrese, L.M., Rev. Mod. Phys., 25, 338 (1953);

Catalano, E. and Stout, J.W., J. Chem. Phys., 23, 1803-8 (1955).

(29) Machin, D.J., Martin, R.L. and Nyholm, R.S., J. Chem. Soc., 1490-1500 (1963).

(30) Okazaki, A., Suemune, Y. and Fuchikami, T., J. Phys. Soc. Japan, 14, 1823-24 (1959).

(31) Stout, J.W. and Catalano, E., J. Chem. Phys., 23, 2013-22 (1955);

Stout, J.W. and Chisholm, R.C., J. Chem. Phys., 36, 979-91 (1962).

(32) Uchida, E., J. Phys. Soc. Japan, 10, 517-22 (1955).

(33) Kanamori, J., Prog. Theor. Phys., 17, 177-96 (1957).

(34) Shulman, R.G. and Sugano, S. Phys. Rev., 130, 506-11 (1963);

Knox, K., Shulman, R.G. and Sugano, S., Phys. Rev., 130, 512-16 (1963).

Sugano, S. and Shulman, R.G., Phys. Rev., 130, 517-30 (1963).

(35) Hirakawa, K., Hashimoto, T. and Hirakawa, K., J. Phys. Soc. Japan, 16, 1934-39 (1961).

(36) Okazaki, A. and Suemune, Y., J. Phys. Soc. Japan, 16, 671-75 (1961).

(37) Dunitz, J.D. and Orgel, L.E., J. Phys. Chem. Solids, 3, 20-9 (1957).

(38) Wells, A.F., J. Chem. Soc., 1670-75 (1947).

(39) Bose, A. and Mitra, S.C., Ind. J. Phys., 26, 393-426; 546-62 (1952); 27, 95-108 (1953).

(40) Bose, A., Mitra, S.C. and Dutta, S.K., Proc. Roy. Soc. London, A239, 165-83 (1957).

(41) Okazaki, A. and Suemune, Y., J. Phys. Soc. Japan, 16, 176-83 (1961).

(42) Kanamori, J., J. Appl. Phys., 31, 14S-23S (1960).

(43) Goodenough, J.B., J. Phys. Rad., 20, 155-59 (1959).

(44) Woolan, E.O., Child, H.R., Koehler, W.C. and Wilkinson, M.K., Phys. Rev., 112, 1132-36, (1958).

(45) Koehler, W.C. and Wollan, E.O. J. Phys. Chem. Solids, 2, 100-6 (1957).

(46) Kelley, K.K., Parks, G.S. and Huffman, H.M., J. Phys. Chem., 33, 1802-5 (1929).

(47) Shomate, C.H., J. Am. Chem. Soc., 67, 765-7 (1945); 67, 1096-98 (1945).

(48) King, E.G., J. Phys. Chem., 60, 410-12 (1956);

Shomate, C.H. and Kelley, K.K., J. Am. Chem. Soc., 66, 1490-92 (1944).

(49) Hirakawa, K., J. Phys. Soc. Japan, 19, 1678-85 (1964).

(50) Nagai, O., J. Phys. Soc. Japan, 18, 510-15 (1963).

(51) Osborne, D.W. and Westrum, E.F., J. Chem. Phys., 21, 1884-87 (1953).

(52) Catalano, E. and Stout, J.W., J. Chem. Phys., 23, 1284 (1955).

S U M M A R Y

Low temperature calorimetric studies have always aroused considerable interest among scientific workers, as such information are of fundamental importance in developing and explaining theories of the structure of the condensed phases and elucidation of solid state properties. Furthermore, the increased requirement of basic and applied research workers for thermodynamic properties has led to a demand for accurate tabulation of thermodynamic data of substances over a broad temperature range.

In a programme of studies of the thermal properties and phase transitions of materials of fundamental and technological interest, a low temperature isothermal calorimeter has been constructed with some modifications to those described in the literature, to suit our limited workshop and laboratory facilities.

An all-glass apparatus has also been constructed for the calibration of copper-constantan thermocouples at some fixed points for precise temperature measurement. The calorimeter heater-wire used as a combined resistance thermometer-heater, is calibrated continuously during the heat capacity runs every time.

To show the performance and reliability of the apparatus and to check the temperature scale, heat capacity of standard benzoic acid has been determined in the range of temperature 78-300°K. These data and derived thermodynamic properties such as entropy and enthalpy are compared with National Bureau of Standards values.

Recently the compounds with perovskite-like structures are becoming very important as they show many interesting solid state properties. The crystal structure and magnetic properties of these have been investigated experimentally and theoretically in detail by various workers. We have been interested in the thermodynamic properties of a series of KMF_3 type compounds, where M denotes divalent 3d transition group element such as Mn, Co, Ni and Cu. They also belong to the same group and show antiferromagnetic ordering at low temperatures. In these materials one may expect plenty of information about magnetic interactions and phase transition mechanism since the M^{2+} ions are arranged more or less in a simple cubic lattice with F^- ions in the centre of the adjacent M^{2+} ions. The magnetic and crystallographic studies of these compounds have been reported but no thermal data are available. The heat capacities and derived thermodynamic properties

of some of these compounds, viz. $KMnF_3$, $KCoF_3$, $KNiF_3$ and $KCuF_3$ have been reported in this thesis.

The heat capacity-temperature study of $KMnF_3$ shows two transitions, one at 83.3°K and the other at 179.0°K. The former is lambda shaped due to an antiferromagnetic ordering below this temperature. Thermal conductivity, susceptibility and neutron diffraction data are consistent with our results. The latter hump is attributed to a crystallographic transition where the compound changes from a low temperature tetragonal to a cubic perovskite structure. The instability of the $KMnF_3$ lattice indicated by the low value of the Goldschmidt tolerance factor ($t = 0.88$) might be responsible for this structural change.

$KCoF_3$ and $KNiF_3$ exhibit peaks in heat capacity versus temperature curve, at 109.5°K and 253.5°K respectively. These also correspond to antiferromagnetic transitions. X-ray, neutron diffraction and thermal conductivity studies lend support to our finding of the Néel point of $KCoF_3$, whereas only anisotropic measurements agree with our data on $KNiF_3$.

Similarly, $KCuF_3$ reveals a hump at 233.2°K, due to an antiferromagnetic ordering of the atomic moments of Cu^{2+} ions below this temperature. This Néel

temperature is slightly lower than that reported from susceptibility measurements while neutron diffraction studies have failed to observe magnetic ordering in this salt.

An attempt has been made to evaluate the magnetic entropy associated with antiferromagnetic transitions in these compounds. Lower values than the expected $R\ln(2S + 1)$ have been obtained in all cases which may be attributed to the persistence of short-range order above the Néel temperature.

The Néel temperatures of these compounds have been compared with those of the related types reported in the literature and correlated on the basis of the super-exchange coupling mechanism given by Anderson and Slater.

The thermodynamic functions such as entropy, enthalpy and Gibbs energy have also been calculated at $5^{\circ}K$ increments of the functions in the range $80\text{-}300^{\circ}K$. Since the experimental measurements are limited down to $80^{\circ}K$ only, the heat capacities below this temperature have been extrapolated using a Debye-Einstein type of function.

The values of C_p, S_T-S_0, H_T-H_0 and $-(F_T-H_0)$ for the compounds at 298.15°K along with their Néel points (T_N) are given below:

Compound	T_N °K	C_p cal./deg.mole	S_T-S_0 cal./deg.mole	H_T-H_0 cal./mole	$-(F_T-H_0)$ cal./mole
$KMnF_3$	83.3	27.50	38.02	5399	5938
$KCoF_3$	109.5	28.84	39.40	5669	6040
$KNiF_3$	253.5	27.30	36.86	5308	5679
$KCuF_3$	233.2	28.47	35.34	5387	5153

These general trend of heat capacities have also been compared with those of the related systems such as MO and MF_2.

Appendix I : Temperature T versus Thermo-e.m.f. E values

$T^{\circ}K$	E Microvolts	dE/dT	$T^{\circ}K$	E Microvolts	dE/dT
74	- 5576	16	118	- 4722	24
76	- 5544	17	120	- 4674	24
78	- 5510	17	122	- 4626	24
80	- 5476	17	124	- 4578	24
82	- 5442	17	126	- 4530	24
84	- 5408	18	128	- 4482	24
86	- 5372	18	130	- 4434	24
88	- 5336	18	132	- 4386	24
90	- 5300	18	134	- 4338	24
92	- 5264	18	136	- 4290	24
94	- 5228	20	138	- 4242	24
96	- 5192	20	140	- 4194	24
98	- 5152	20	142	- 4146	24
100	- 5112	20	144	- 4098	25
102	- 5072	20	146	- 4048	25
104	- 5032	21	148	- 3998	25
106	- 4992	21	150	- 3948	26
108	- 4950	21	152	- 3896	26
110	- 4908	21	154	- 3844	26
112	- 4862	23	156	- 3792	26
114	- 4816	23	158	- 3740	26
116	- 4770		160	- 3688	

contd...

T°K	E Microvolts	dE/dT	T°K	E Microvolts	dE/dT
		26			32
162	- 3636		208	- 2296	
		28			32
164	- 3582		210	- 2232	
		28			32
166	- 3528		212	- 2168	
		28			32
168	- 3472		214	- 2104	
		28			32
170	- 3416		216	- 2040	
		28			32
172	- 3360		218	- 1976	
		28			32
174	- 3304		220	- 1912	
		28			32
176	- 3248		222	- 1848	
		28			32
178	- 3192		224	- 1784	
		29			34
180	- 3134		226	- 1716	
		29			34
182	- 3076		228	- 1648	
		29			34
184	- 3018		230	- 1580	
		29			35
186	- 2960		232	- 1510	
		29			35
188	- 2902		234	- 1440	
		29			35
190	- 2844		236	- 1370	
		29			35
192	- 2786		238	- 1300	
		29			35
194	- 2728		240	- 1230	
		29			35
196	- 2670		242	- 1160	
		30			35
198	- 2610		244	- 1090	
		31			35
200	- 2548		246	- 1020	
		31			36
202	- 2486		248	- 948	
		31			37
204	- 2424		250	- 874	
		32			37
206	- 2360		252	- 800	

contd...

$T^{o}K$	E Microvolts	dE/dT	$T^{o}K$	E Microvolts	dE/dT
		38			38
254	- 724		278	184	
		38			38
256	- 648		280	260	
		38			38.5
258	- 572		282	337	
		38			38.5
260	- 496		284	414	
		38			39.
262	- 420		286	492	
		38			39
264	- 344		288	510	
		38			39
266	- 268		290	648	
		38			39.5
268	- 192		292	727	
		38			39.5
270	- 116		294	806	
		38			40
272	- 44		296	886	
		38			40.5
274	32		298	967	
		38			40.5
276	108		300	1048	

A P P E N D I X - II

PUBLISHED WORK* OF THE AUTHOR NOT INCLUDED IN THIS THESIS

S.No.	Title of the publication	Reference
1.	Vapour Pressure and Intermolecular Energy Constants of Liquids.	Z. Physik. Chem., 220, 71-8 (1962).
2.	Cohesive Energies of Alkali Halides.	Ind. J. Phys., 37, 238-40 (1963).
3.	Lattice Energies and Other Properties of Some Ionic Crystals.	Z. Physik. Chem., 224, 377-83 (1963).
4.	Imperfect Vapour Phase, Compressibility and Force Constants of Liquids.	Ind. J. Chem., 2, 27-8 (1964).
5.	A Finite Virial Expansion of Fluid State.	Ind. J. Chem., 2, 29-30 (1964).

* Reprints attached.

Sonderdruck aus „Zeitschr. für Physikalische Chemie“ **220,** 71–78, 1962

Vapour Pressure and Intermolecular Energy Constants of Liquids

By

R. V. Gopala Rao, H. V. Keer and **C. D. Das**

With 1 figure and 1 table

(Received 10. November 1961)

AKADEMISCHE VERLAGSGESELLSCHAFT
GEEST & PORTIG K.-G., LEIPZIG
1962

National Chemical Laboratory, Poona

Vapour Pressure and Intermolecular Energy Constants of Liquids

By

R. V. Gopala Rao, H. V. Keer and C. D. Das[1]

With 1 figure and 1 table

(Eingegangen am 10. November 1961)

Abstract

From the idea of continuity of states a relation between the pressure change of the bulk modulus of rigidity, i.e. $\left[\frac{d(1/\beta)}{dP}\right]_T$, and vapour pressure has been formulated by using the well known virial equation. The relationship between $C_1 \equiv \left[\frac{d(1/\beta)}{dP}\right]_T$ and intermolecular energy force constants has been discussed. The derived equation has been applied to a number of liquids and was found to be very satisfactory especially when considering the simplicity of treatment of the fluid state.

The discovery by ANDREWS [1] of the critical phenomenon and the idea of corresponding states have greatly contributed to the realisation of the idea of continuity of states especially between a vapour and its liquid. KAMERLINGH, ONNES [2] and various others [3, 4] have extensively used the so-called virial equation to represent the behaviour of imperfect gases. From the idea of continuity of states one can extend the representation to liquid state as well. By such a representation and by using thermodynamic arguments important conclusions [5] can be arrived at. Therefore we write the equation of state for the fluids as

$$P = \frac{RT}{V} + \sum_{n=2}^{m} \frac{Bn}{Vn} \tag{1}$$

That is to say the pressure of a fluid can be adequately expressed as a polynomial of $1/V$. The Bn are the so-called virial coefficients which are functions of temperature and intermolecular forces only [6, 7].

At this point it may be remarked that equation (1) is not purely empirical because it was shown by MAYER and others [8, 9, 10, 11, 12, 13] with the help of statistical mechanics that P can be expressed as an inverse power of V.

[1] Dr. R. V. Gopala Rao, H. V. Keer and C. D. Das, Poona/India, National Chemical Laboratory.

Communication No. 480 from the National Chemical Laboratory, Poona – 8 (India).

MAYER's theory actually predicts the phenomenon of condensation and further it accounts for the constancy of pressure when the gas actully begins to liquid. However there is still much controversy about exactly how the change of state is associated with the singularities, even though it may be admitted that MAYER's theory is a far greater advancement in formulating an equation of state. Further it is rather difficult to calculate the higher virial coefficients from the so-called cluster integrals [8]. But one can get greater satisfaction to-day from the fact that equation (1) is not purely empirical in nature.

For the process of actual vaporisation MAXWELL's theorem states [14, 15] that

$$P(V_g - V_\varrho) = \int_{V_\varrho}^{V_g} P\,dV \tag{2}$$

where P is the vapour pressure of the liquid and V_g and V_ϱ are the molal volumes of the gas and liquid phases respectively. Further, if the virial coefficients in equation (1) can be related to the derivatives $\left(\frac{dP}{dV}\right)_T$ for both liquid and gas the vapour pressure can be related to these derivatives which are properties of individual phases and are not related to equilibrium. Therefore through the idea of continuity of states, the equilibrium properties of the two phases can be predicted from the properties of the individual phases in question. However, because of the limitations of the available accurate data of compressibility, the practical realisation may not be as good as desired.

Relation between vapour pressure and pressure change of bulk modulus of rigidity

As a first approximation we make the assumption that $m = 5$ can represent the state of fluids adequately and hence equation (1) can be written for fluids as

$$P = \frac{RT}{V} + \frac{B_2}{V^2} + \frac{B_3}{V^3} + \frac{B_4}{V^4} + \frac{B_5}{V^5} \tag{3}$$

Hence for the volume of the gas and liquid we can write

$$P = \frac{RT}{V_g} = \frac{B_2}{V_g^2} + \frac{B_3}{V_g^3} + \frac{B_4}{V_g^4} + \frac{B_5}{V_g^5} \tag{4}$$

$$P = \frac{RT}{V_\varrho} + \frac{B_2}{V_\varrho^2} + \frac{B_3}{V_\varrho^3} + \frac{B_4}{V_\varrho^4} + \frac{B_4}{V_\varrho^5} \tag{5}$$

By substituting equation (3) in equation (2) we get

$$P(V_g - V_\varrho) = RT \ln\left(\frac{V_g}{V_\varrho}\right) + B_2\left(\frac{1}{V_\varrho} - \frac{1}{V_g}\right) + \frac{1}{2} B_3\left(\frac{1}{V_\varrho^2} - \frac{1}{V_g^2}\right) + \frac{1}{3} B_4\left(\frac{1}{V_\varrho^3} - \frac{1}{V_g^3}\right) + \frac{1}{4} B_5\left(\frac{1}{V_\varrho^4} - \frac{1}{V_g^4}\right) \tag{6a}$$

Since compressibility is defined as $\beta = -1/V(dV/dP)_T$, we get from equation (5) for the compressibility of the liquid the following expression:

$$\frac{1}{\beta} = \frac{RT}{V_\varrho} + \frac{2B_2}{V_\varrho^2} + \frac{3B_3}{V_\varrho^3} + \frac{4B_4}{V_\varrho^4} + \frac{5B_5}{V_\varrho^5} \tag{7}$$

Further, if the vapour pressure is not high, it is reasonable to assume that the vapour phase of the fluid obeys the ideal gas law. Therefore equation (4) becomes

$$0 = B_2 + \frac{B_3}{V_g} + \frac{B_4}{V_g^2} + \frac{B_5}{V_g^3} \tag{8}$$

Under ideal gas law conditions we also have $V_g \gg V_\varrho$. Hence V_ϱ can be neglected in comparison with V_g; so that equation (6a) reduces to

$$RT - RT\ln\left(\frac{RT}{pV_\varrho}\right) = \frac{B_2}{V_\varrho} + \frac{B_3}{2V_\varrho^2} + \frac{B_4}{3V_\varrho^3} + \frac{B_5}{4V_\varrho^4} \tag{6}$$

In the case of non-polar liquids, it was shown by MOELWYN-HUGHES [16] by thermodynamic arguments that the pressure change of bulk modulus of rigidity is a constant, i.e.

$$C_1 \equiv \left[\frac{\mathrm{d}(1/\beta)}{\mathrm{d}P}\right]_T = \text{constant}$$

Further he showed that [16]

$$C_1 = \frac{1}{3}(n + m + 6)$$

where n and m are the exponents for repulsion and attraction in the well known bireciprocal function of LENNARD-JONES [17, 18]. Even in the case of polar liquids a three constant potential function of the type [19]

$$\Phi = Aa^{-n} - Ba^{-m} - Ca^{-p}$$

adequately represents the potential of a polar molecule. Here A, B and C are constants and the first term is due to repulsion while the second and third terms are due to van der WAALS' forces and dipole-dipole interactions, respectively. It can be shown [20] that

$$C_1 \equiv \left[\frac{\mathrm{d}(1/\beta)}{\mathrm{d}P}\right]_T = \frac{1}{3}\left\{\frac{Rm(n-m)(n+m+6) + p(n-p)(n+p+6)}{Rm(n-m) + p(n-p)}\right\}$$

$$= \text{constant}$$

and

$$R = \frac{(na_s^{p-m-n}\sigma^{-p} - pa_s^{-m}\sigma^{-n})}{(ma_s^{-m}\sigma^{-n} - na_s^{-n}\sigma^{-m})}$$

where a_s and σ are the equilibrium distance and collision diameter respectively. That is, in the case of liquids in general the pressure change of bulk modulus

of rigidity is a constant. Therefore from equation (7) we can easily evaluate C_1 which comes out to be

$$\frac{C_1}{\beta} = \frac{RT}{V_\varrho} + \frac{4B_2}{V_\varrho^2} + \frac{9B_3}{V_\varrho^3} + \frac{16B_4}{V_\varrho^4} + \frac{25B_5}{V_\varrho^5} \tag{9}$$

Then from equations (5), (6), (7), (8) and (9) we can solve for C_1 and get

$$C_1 = \frac{\begin{vmatrix} 0 & 1 & 1/V_g & 1/V_g^2 & 1/V_g^3 \\ p-(RT/V_\varrho) & 1/V_\varrho^2 & 1/V_\varrho^3 & 1/V_\varrho^4 & 1/V_\varrho^5 \\ RT-RT\ln x & 1/V_\varrho & 1/2V_\varrho^2 & 1/3V_\varrho^3 & 1/4V_\varrho^4 \\ (1/\beta)-(RT/V_\varrho) & 2/V_\varrho^2 & 3/V_\varrho^3 & 4/V_\varrho^4 & 5/V_\varrho^5 \\ RT/V_\varrho & -4/V_\varrho^2 & -9/V_\varrho^3 & -16/V_\varrho^4 & -25/V_\varrho^5 \end{vmatrix}}{\begin{vmatrix} 0 & 1 & 1/V_g & 1/V_g^2 & 1/V_g^3 \\ 0 & 1/V_\varrho^2 & 1/V_\varrho^3 & 1/V_\varrho^4 & 1/V_\varrho^5 \\ 0 & 1/V_\varrho & 1/2V_\varrho^2 & 1/3V_\varrho^3 & 1/4V_\varrho^4 \\ 0 & 2/V_\varrho^2 & 3/V_\varrho^3 & 4/V_\varrho^4 & 5/V_\varrho^5 \\ 1/\beta & -4/V_\varrho^2 & -9/V_\varrho^3 & -16/V_\varrho^4 & -25/V_\varrho^5 \end{vmatrix}}$$

where $x = \dfrac{RT}{pV_\varrho} = V_g/V_\varrho$.

Neglecting V_ϱ in comparison with V_g we can simplify the above determinant in a straightforward way and get

$$C_1 = -36\beta\left[p - \frac{25RT}{18V_\varrho} - \frac{2RT\ln x}{3V_\varrho} - \frac{11}{36\beta}\right] \tag{10}$$

If the vapour pressure is small, the first term is negligible in comparison with the remaining terms. Hence we have

$$\frac{11-C_1}{\beta} = 2px(12\ln x - 25) \tag{11}$$

Equation (11) is surprisingly simple and is convenient for evaluating C_1 and hence the intermolecular potential energy constants from single values of β and x.

In order to have an idea about the order of magnitude of the errors involved in neglecting V_ϱ in comparison with V_g we can take the example of benzene. The vapour pressure of benzene at 20 °C is 74.8 mm *Hg*. At this vapour pressure and temperature, to a first approximation, one mole of benzene vapour occupies 22.4 litres and its molal volume in the liquid state at the same temperature is about 89 c.c. Therefore $V_g/V_\varrho \cong 2500$ and hence

$V_g \gg V_\varrho$. Further, in equation (10) p is neglected in comparison with the other terms because p is in general a fraction of unity while the other terms run into hundreds and thousands.

For example, again for benzene at 20 °C, $p = 0{,}099$ atm, while

$$\frac{25\,RT}{18\,V_\varrho} = 375\,\text{atm}, \quad \frac{2\,RT\ln x}{3\,V_\varrho} = 1425\,\text{atm} \quad \text{and} \quad \frac{11}{36\,\beta} = 2900\,\text{atm}$$

Equation (11) has been applied to a number of liquids and the calculated values are given in Table I, column 6, while the experimental values [19, 21, 22, 23] are obtained from the slope of the graphs of $1/\beta$ vs. P and are given in column 7.

Table I

Liquid	Temp. °C	V ml	p mm 21, 23	[21, 22, 25] $\beta \cdot 10^6$ atm^{-1}	[21, 22, 25] C_1(cal.)	[19, 21, 22] C_1 (Exp.)
1. Hydrocarbons						
a) Pentane	20	112	183.7	176	6.74	–
b) Hexane	23	131	139.3	159	7.58	7.75
c) Heptane	20	147	41.4	144	7.65	–
d) Octane	23	163	12.5	121	7.96	8.5
e) Benzene	20	89	74.8	95	7.41	8.0
f) Toluene	20	106	22.2	92	7.56	8.0
2. Esters						
a) Methyl acetate	20	79.3	169.8	101	7.23	8.0
b) Ethyl acetate	20	98.0	72.8	105	7.44	8.0
c) Ethyl propionate	20	115.0	27.8	102	7.64	8.0
d) Methyl butrate	20	113.0	24.5	98	7.64	8.5
e) Ethyl butrate	20	132.0	11.3	101	7.61	8.5
3. Alcohols						
a) Methyl alcohol	0	40	30.0	90	2.0	8.8
b) Ethyl alcohol	0	57	12.2	100	3.4	5.4
c) Amyl alcohol	20	108	2.5	91	5.7	6.0
d) Isoamyl alcohol	20	109	2.3	99	6.2	8.7
e) n-butyl alcohol	20	92	4.3	97	5.7	9.0
f) Tertiary butyl alcohol	20	74.1	30.6	108	6.7	10.0
4. Miscellaneous						
a) Carbon tetrachloride	20	97	91.6	106	7.5	8.6
b) Mercury	0	14.8	$1.9 \cdot 10^{-4}$	3.9	8.1	6.8
c) Ethylene bromide	20	86.0	10.2	59	7.9	–
d) Carbon disulphide	20	60	298	87	7.0	7.5
e) Acetone	20	73	185	105	6.7	6.5
f) Chloroform	20	80	160	102	7.2	8.2

The agreement in most cases can be considered as very good especially when considering that we are dealing with the pressure change of bulk modulus of rigidity which contains the derivative of pressure with respect to volume. However, in the case of alcohols (especially those with low molecular weights) the calculated values of C_1 are in poor agreement with the experimental values, which is also the case even in the theoretical evaluation of compressibility coefficient [5]. The reason for this deviation is most probably due to the fact that higher order virial coefficients ($m > 5$) may have to be taken into account. That means the pressure of a fluid has to be represented by considering a greater number of virial coefficients in the polynomial expression (1). But this introduces a large number of unknowns which are to be eliminated in order to correlate the physical properties of the fluids.

In the case of non-polar liquids, C_1 is simply related to n and m, and by London's theory of dispersion [24] m can be taken as equal to 6 and hence n can be evaluated. In the case of polar liquids it is reasonable to take [20] $m = 6$ and $p = 3$, and in order to evaluate n one still requires a knowledge of the collision diameter σ and equilibrium distance a_s. At any rate equation (11) should be useful in checking the experimental value of C_1 i.e. the pressure change of bulk modulus of rigidity.

A General Correlation between Vapour Pressure and Intermolecular Energy Force Constants

It was shown [5] that

$$\beta p x(6 \ln x - 11) = 1 \tag{13}$$

where β, p and x have their usual significance, when the pressure of a fluid is expressed by

$$p = \frac{RT}{V} + \sum_{n=2}^{4} \frac{Bn}{V^n}$$

This suggests that a plot of $\log x$ against $V_g/\beta T$ should be a straight line for all liquids at all temperatures. It is obvious that this is not the case. The reason probably is that the representation of the pressure of fluids as a polynomial of $1/V$ is inadequate, as has already been stated [5], and higher virial coefficients ought to be considered to get better agreement with experiment. Now, in the derivation of equation (11) it is assumed that $m = 5$, i.e. one more virial coefficient, namely B_5, has been taken into account in expressing the pressure of fluids. Equation (11) can be put in the following form

$$\frac{V_g}{\beta T} = \frac{24 R \ln x}{11 - C_1} - \frac{50 R}{11 - C_1} \tag{14}$$

Equation (14) implies that a plot of $\log x$ against $V_g/\beta T$ should be a straight line at all temperatures for a particular liquid only, as shown in figure 1, in the region where the approximation holds, namely $V_g \gg V_0$, since the slope

of the graph contains C_1 which is a constant characteristic of a particular liquid and related to its intermolecular force constants, thus scoring definite edge over the inexplicable situation met with in the former case [vide equation (13)].

The authors are grateful to Dr. A. B. Biswas, Assistant Director, for his interest in this work.

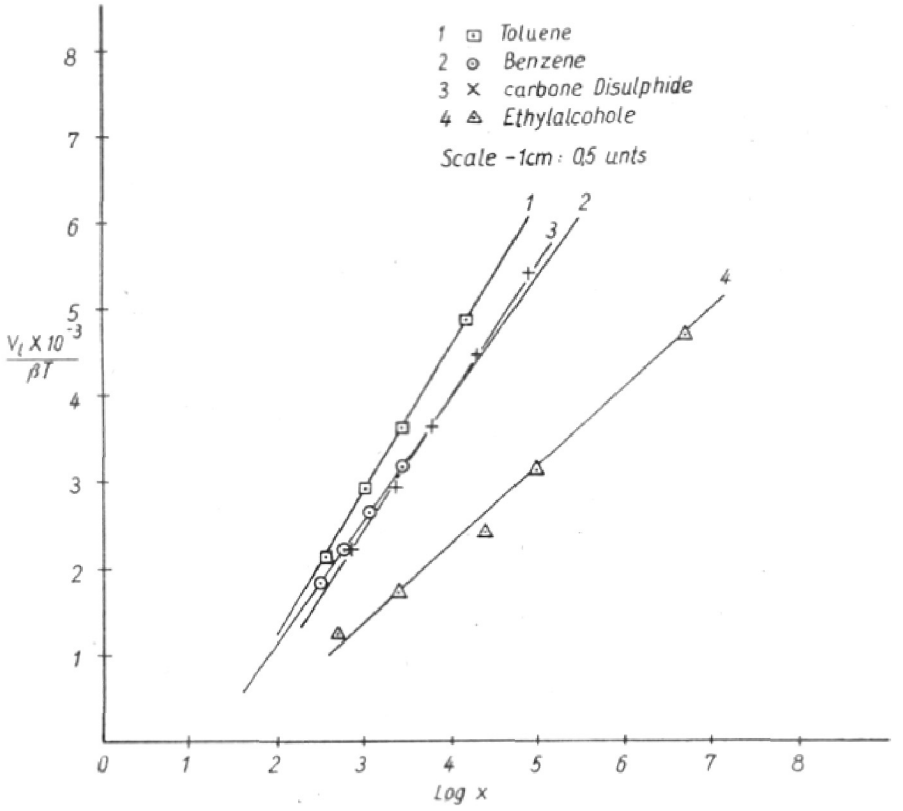

Fig. 1

References

[1] Andrews: Phil. Mag. **4** (1870) 39, 150.
[2] Onnes, H. K.: Proc. Kon. Ned. Acad. Wet. **4** (1902) 125.
[3] Clausius, R.: Ann. Phys. **141** (1870) 124.
[4] Holborn, L., and J. Otto: Z. Phys. **33** (1925) 1.
[5] Rao, R. V. G., and J. C. M. Li: Z. phys. Chem. **213** (1960) 166.
[6] Ter Harr: Elements of Statistical Mechanics, Rinehart & Company Inc. (1954) 177.
[7] Squire, C. F.: Low Temperature Physics, McGraw-Hill Books Company Inc. (1953) 32.
[8] Mayer, J. E., and M. G.: Statistical Mechanics, John Wiley & Sons Inc., New York (1940), chapters 13 and 14.
[9] Mayer, J. E.: J. Chem. Phys. **5** (1937) 67.
[10] Mayer, J. E., and P. G. Ackermann: J. Chem. Phys. **5** (1937) 74.
[11] Mayer, J. E., and S. F. Harrison: J. Chem. Phys. **6** (1938) 87.

[12] MAYER, J. E., and S. F. HARRISON: Z. Chem. Phys. **6** (1938) 101.
[13] MAYER, J. E.: J. Chem. Phys. **19** (1951) 1024.
[14] WALL, F. T.: J. Chem. Phys. **16** (1948) 508.
[15] TERRELL L. HILL: Statistical Mechanics, Principles and selected applications, McGRAW-HILL Book Company Inc., New York (1956) 165.
[16] MOELWYN-HUGHES, E. A.: J. Chem. Phys. **55** (1951) 1246.
[17] LENNARD-JONES: Proc. Roy. Soc., A **106** (1924) 463.
[18] GLASSTONE, S.: Theoretical Chemistry, D. van-Nostrand Company Inc. (1944) 424.
[19] MOELWYN-HUGHES, E. A.: Physical Chemistry, Pergamon Press (1957) 324, 325.
[20] RAO, R. V. G., and H. V. KEER: Communicated to Z. physik. Chemie, Leipzig.
[21] International Critical Tables, McGRAW-HILL Book Company Inc., New York and London (1928) Vol. III, 40.
[22] Physikalische Chemie, LANDOLT-BORNSTEIN, Roth and Scheel, Photo Lithoprint Reproduction of Edwards Brothers Inc., Michigan (1943), 5th Edition, Part I, 88.
[23] JORDAN, J. E.: Vapour pressure of organic compounds Interscience Publishers, New York (1954).
[24] London, Z. Phys. **63** (1930) 245.
[25] Liquids and Liquid Mixtures, J. S. ROWLINSON, Butterworths Scientific Publications, London (1959) Edition, 37, 55.

Reprinted from the Indian Journal of Physics Vol. XXXVII, No. 4, April 1963, pp. 238—240.

4

COHESIVE ENERGIES OF ALKALI HALIDES

R. V. GOPALA RAO, H. V. KEER AND C. DEENADAS

NATIONAL CHEMICAL LABORATORY, POONA-8 (INDIA)

(*Received June* 22, 1962, *Resubmitted Dec* 17, 1962)

The principal interactions in ionic lattices which are Coulomb interaction, van der Waals' interaction and overlap force, are two body forces. In the case of simple ions possessing spherical symmetry and rare gas structures, the cohesive energy can be represented as a function of their distance apart. For the ionic crystals a number of observable properties can be calculated using a bireciprocal Lennard-Jones potential function coupled with a coulombic term. Recently the cohesive energies of ionic crystals have been calculated (Sharma and Madan, 1961) using a (12 : 6) potential function. It was pointed out that the discrepancy with the experimental data was more pronounced for lighter alkali halides. Hence the authors presently aim to propose an appropriate (9:6) potential function for such alkali halides. This is reasonable in the light of the fact that the values of the repulsion constant 'n' obtained by Pauling's rules (1927, 1928) derived from a theoretical treatment of the interaction of closed shell electronic configurations, lie in the vicinity of 9 (Sherman, 1932).

Hence the energy per cell is represented by

$$\phi_{(r)} = -\frac{\alpha e^2}{r} + \frac{B}{r^9} - \frac{C}{r^6} + \epsilon_0 \qquad (1)$$

where α is the Madelung's constant, e is the electron charge, r is the distance between closest ion centres and ϵ_0 is the zero point energy. B and C are the coefficients for repulsive and van der Waals terms.

Here interactions between dipole-quadrupole and other than the nearest neighbours are neglected as their contribution is very small.

By the use of thermodynamic relations it can be easily shown that first and second derivatives of lattice energy can be expressed in terms of directly observable quantities. The equations are :

$$\frac{d\phi_{(r)}}{dr} = \frac{3vT}{r\beta}\left(\frac{1}{V}\cdot\frac{\partial V}{\partial T}\right)_P \qquad \ldots (2)$$

$$\frac{d^2\phi_{(r)}}{dr^2} = \frac{9v}{r^2\beta}\left[1+\frac{T}{\beta}\left\{\left(\frac{\partial\beta}{\partial T}\right)_P + \frac{1}{V}\left(\frac{\partial V}{\partial T}\right)_P \frac{1}{\beta}\left(\frac{\partial\beta}{\partial P}\right)_T\right\} + \frac{2T}{3V}\left(\frac{\partial V}{\partial T}\right)_P\right] \ldots (3)$$

TABLE I

Cohesive energy in K. Cal/mole

Compound	Repulsion constant	Experimental	Calculated (present work)	Calculated (12 : 6)	
LiF	6.0	246[a]	264.6	273.1	246.8
NaF	7.0	218[a]	227.3	236.6	218.7
LiCl	7.0	201.5[b]	199.8	212.6	202.0
LiBr	7.5	191.5[b]	189.9	200.0	190.7
NaCl	8.0	184.3[a]	182.8	192.8	185.9
KF	8.0	193.0[a]	195.8	205.8	194.4
LiI	8.5	180.0[a]	174.8	184.3	176.8
NaBr	8.5	176.0[b]	172.1	182.1	176.7
RbF	8.5	—	177.9	191.6	185.9
KCl	9.0	167.8[a]	163.8	174.1	169.4
NaI	9.5	166.0[a]	159.3	168.8	165.4
KBr	9.5	160.0[a]	154.8	164.8	162.4
RbCl	9.5	162.0[a]	155.8	166.8	164.0
RbBr	10.0	157.0[a]	149.6	159.1	157.5
KI	10.5	152.0[a]	145.0	155.0	153.0

a. Plendl (1961) b. Born and Huang (1954) c. Cubicciotti (1961)

Using Equation (3) the repulsive parameter B can be evaluated and hence the cohesive energy. The experimental data used have been taken from Huggins (1937), Seitz (1940) and Spangenberg (1956), Spangenberg *et. al.* 1957). The values of cohesive energy are compared with the observed values and also with other determinations. The values calculated with (12 : 6) potential function are also given. All values are listed in Table I.

In the case of lighter halides, the 'n' value is less than the assumed value of 9. Thus for the lightest one, namely LiF, the 'n' value is around 6 (Sherman, 1932) and hence cohesive energy is higher. Better agreement can be obtained using the value of 'n' as 7. As we go down the group of alkali halides the agreement becomes better. This is explicable since in all these cases, the 'n' values are either 9 or very near 9. For heavier crystals, the calculated values are lower and the discrepancy increases as we proceed towards still heavier compounds. Incidentally the 'n' value increases to 10.5 and (12 : 6) potential function becomes more appropriate.

The authors are grateful to Dr. A. B. Biswas for his interest in this work and one of us (C. Deenadas) to the Council of Scientific and Industrial Research, New Delhi, for the award of a Junior Research Fellowship.

REFERENCES

Born and Huang, 1954, *Dynamical Theory of Crystal Lattices*, 26.
Cubicciotti, D., 1961, *J. Chem. Phy.*, **34**, 2189.
Huggins, M. L., 1937, *J. Chem. Phys.*, **5**, 143.
Pauling, L., 1927, *Proc. Roy. Soc.*, **114**, 181.
1927, *J. Am. Chem. Soc.*, **49**, 765.
1928, *Z. Krist.*, **67**, 377.
Plendl, J. N., 1961, *Phy. Rev.*, **123**, 1174.
Seitz, F., 1940, *The Modern Theory of Solids*, 88.
Sharma, M. N. and Madan, M. P., 1961, *Ind. J. Phys.*, **35**, 596.
Sherman, J., 1932, *Chem. Rev.*, **11**, 93.
Spangenberg, K., 1956, *Naturwissenschaften.*, **43**, 394.
Spangenberg, K. and Haussuhl S., 1957, *Z. Krist.*, **109**, 422.

National Chemical Laboratory, Poona (India)

Lattice Energy and other Properties of some Ionic Crystals

By **C. D. Das, H. V. Keer** and **R. V. G. Rao**[1]

With 2 Tables (Received 24 May 1963)

Abstract

Lattice energies of some ionic crystals at 0 °K have been calculated using an inverse type of potential function with revised value of electronic charge. Compressibilities are evaluated and compared with experimental observations. An equation has been derived for thermal expansion coefficient with the potential function used and the room temperature values have been calculated.

Introduction

It is customary to represent the interaction energy of ions possessing spherical symmetry and rare gas structures as a function of their distance apart. Hence the authors presently aim to use an inverse type of potential function for calculating certain properties of some simple ionic crystals. In general the value of the repulsion constant for alkali halides and alkaline earth chalcogenides obtained by PAULING's rules [1] derived from a theoretical treatment of the interaction of the closed shell electronic configurations is about nine [2]. FOWLER [3] has actually calculated the lattice energies and compressibilities of some of these compounds using a constant value of nine for the repulsion constant. In his calculations he neglected the dipolequadrupole interaction and zero-point vibrational energy. Since then an important change has been made in the value of the electronic charge which not only affects the coulombic term directly but also changes the repulsive parameter indirectly [4, 5]. Hence it is felt necessary to recalculate the properties of these crystals using the revised value of the electronic charge and including the neglected terms with a uniform value of nine for the repulsion constant. The interactions between other than nearest neighbours have been neglected as their contribution is considered very small. The experimental data used have been taken from the available literature [5–8].

Lattice Energy

The lattice energy per cell in ergs can be written as

$$\varphi_{(r_0)} = -\frac{\alpha e^2 z^2}{r_0} + \frac{B}{r_0^9} - \frac{C}{r_0^6} - \frac{D}{r_0^8} + \varepsilon_0 \qquad (1)$$

The symbols in equation (1) have the usual significance.

[1] Dr. R. V. G. RAO, C. D. DAS and H. V. KEER, National Chemical Laboratory, Poona 8 (India). Communication. NO: 541.

Table 1. Lattice Energies and Compressibility Coefficients

Compound	Lattice energy in Kcal/mole				Compressibility $\times 10^{12}$ cm^2/dynes		
	Calculated	Fowler [3]	Observed [10—12]	H & S [6]	Calculated	Observed [5, 6]	H & S [6]
LiF	253.3	–	245.9	–	0.65	1.43	–
Cl	200.8	–	201.5	–	2.35	3.17	–
Br	187.9	–	191.5	–	3.09	3.90	–
I	173.2	–	180.0	–	4.03	5.30	–
NaF	221.0	228.2	218.8	–	1.30	2.06	–
Cl	182.8	190.1	184.7	–	3.54	3.97	–
Br	173.0	181.4	175.9	–	4.41	4.75	–
I	160.2	170.8	166.3	–	5.90	6.21	–
KF	192.8	198.4	194.3	–	2.36	3.14	–
Cl	164.8	173.1	163.0	–	5.20	5.50	–
Br	157.5	166.3	160.0	–	6.35	6.45	–
I	147.2	158.8	151.0	–	8.23	8.07	–
RbF	184.6	187.1	186.3	–	4.40	3.66	–
Cl	158.2	165.7	159.0	–	6.78	6.16	–
Br	151.5	160.6	157.0	–	7.95	7.38	–
I	142.5	153.5	148.0	–	10.00	9.00	–
CsF	173.8	176.9	–	–	5.95	4.25	–
Cl	148.3	157.3	157.8	–	6.40	5.55	–
Br	142.8	153.5	152.3	–	7.35	6.28	–
I	134.6	147.7	141.0	–	8.71	7.83	–
BeO	1172.3	–	–	1082	0.17	0.27	0.37
S	917.7	–	–	893	0.44	–	0.66
Se	868.6	–	–	855	0.55	–	0.75
Te	793.4	–	–	795	0.79	–	0.94
MgO	979.1	976.0	–	938	0.27	0.42, 0.59	0.48
S	792.5	766.0	–	788	0.63	0.69	0.82
Se	755.9	743.0	–	757	0.76	0.75	0.91
Te	687.9	–	–	699	1.36	–	1.62
CaO	858.1	876	–	841	0.46	0.71, 0.88	0.69
S	725.9	714	–	726	0.89	0.98, 2.8	1.09
Se	697.3	700	–	701	1.05	1.04, 2.2	1.21
Te	650.3	648	–	662	1.39	2.40	1.46
SrO	801.4	829	–	792	0.60	0.83	0.84
S	686.6	688	–	692	1.11	3.80	1.28
Se	663.0	675	–	671	1.29	2.50	1.40
Te	621.2	626	–	635	1.67	2.10	1.68
BaO	747.0	780	–	746	0.79	1.74	1.00
S	648.1	662	–	659	1.41	2.90	1.50
Se	627.2	652	–	639	1.61	2.90	1.65
Te	591.2	609	–	608	2.03	3.30	1.96

Following HILDEBRAND's considerations [9] one finds that the first derivative with respect to γ of equation (1) becomes zero at 0 °K.

$$\gamma_0 \left[\frac{d\varphi}{d\gamma}\right]_{\gamma=\gamma_0} = 0 = \frac{\alpha e^2 z^2}{\gamma_0} - \frac{9B}{\gamma_0^9} + \frac{6C}{\gamma_0^6} + \frac{8D}{\gamma_0^8} \tag{2}$$

Using equations (1) and (2) repulsive parameter B and hence lattice energy are calculated. The values together with experimental and other determinations are given in Table 1.

The values are in better agreement with observed values than those of FOWLER [3].

Compressibility

From the second derivative of equation (1), we get

$$\beta = \frac{9K\gamma_0^3 \varkappa}{\gamma_0^2 \left(\frac{d^2\varphi}{d\gamma^2}\right)_{\gamma=\gamma_0}} \tag{3}$$

where β is the compressibility coefficient,
K is a constant given by $V/N\gamma_0^3$,
V is the molar volume,
N is Avogadro's number

and

$$\varkappa = 1 + \frac{T}{\beta}\left[\left(\frac{\partial\beta}{\partial P}\right)_T + \frac{1}{V}\left(\frac{\partial V}{\partial T}\right)_P \cdot \frac{1}{\beta}\left(\frac{\partial\beta}{\partial P}\right)_T\right] + \frac{2}{3}\frac{T}{V}\left(\frac{\partial V}{\partial T}\right)_P$$

The calculated values of compressibility coefficients are given together with experimental and other determinations in Table 1. $\varkappa$ is assumed to be unity for alkaline earth chaleogenides [6]. In the case of alkaline earth chaleogenides it was pointed out [13] that the observed values are unreliable and generally too high. Nevertheless it is gratifying to note that the values are in general in good agreement with those of HUGGINS and SAKAMOTO [6].

Thermal Expansion coefficient

Assuming that the oscillators vibrate independently of each other with the same frequency it was shown [14] that

$$\alpha' = -\frac{c_v}{2a\gamma_0} \cdot \frac{1}{\nu} \cdot \frac{d\nu}{d\gamma} \tag{4}$$

where α' is the linear thermal expansion coefficient,
c_v the specific heat at constant volume,
ν the frequency of vibration,

and

$$a = \frac{1}{2}\left(\frac{\mathrm{d}^2\varphi}{\mathrm{d}\gamma^2}\right)_{\gamma=\gamma_0}$$

Now the frequency of vibration for linear harmonic oscillator is

$$\nu = \left[\left(\frac{\mathrm{d}^2\varphi}{\mathrm{d}\gamma^2}\right)_{\gamma=\gamma_0} \Big/ 4\pi^2 m\right]^{\frac{1}{2}} \tag{5a}$$

where "m" is the reduced mass of the oscillating ions.

Near the equilibrium position

$$\frac{1}{\nu}\cdot\frac{\mathrm{d}\nu}{\mathrm{d}\gamma} = \frac{1}{4\pi\nu m^{\frac{1}{2}}}\left(\frac{\mathrm{d}^2\varphi}{\mathrm{d}\gamma^2}\right)^{-\frac{1}{2}}_{\gamma=\gamma_0}\left(\frac{\mathrm{d}^3\varphi}{\mathrm{d}\gamma^3}\right) \tag{5b}$$

Using equations (1), (4), (5a) and (5b) an expression has been derived which comes out to be

$$\alpha' = 2C_v\left[\frac{\left(\frac{26\alpha e^2 z^2}{\gamma_0} + \frac{81C}{\gamma_0^6} + \frac{40D}{\gamma_0^8}\right)}{\left(\frac{8\alpha e^2 z^2}{\gamma_0} + \frac{18C}{\gamma_0^6} + \frac{8D}{\gamma_0^8}\right)^2}\right] \tag{6}$$

Equation (6) gives α' in terms of C_v and potential energy constants. However, for solids generally Cp, the heat capacity at constant pressure, is available as a function of temperature. So in order to use the available Cp data we make the following readjustment.

It is well known from thermodynamics that

$$Cp - Cv = (3\alpha')^2\,\mathrm{VT}/\beta$$

Let

$$A = 2\left[\left(\frac{26\alpha e^2 z^2}{\gamma_0} + \frac{81C}{\gamma_0^6} + \frac{40D}{\gamma_0^8}\right)\Big/\left(\frac{8\alpha e^2 z^2}{\gamma_0} + \frac{18C}{\gamma_0^6} + \frac{8D}{\gamma_0^8}\right)^2\right]$$

So from equation (6) we have $\alpha' = ACv$

Hence

$$Cp = \frac{\alpha'}{A} + \frac{9(\alpha')^2\mathrm{VT}}{\beta} \tag{7}$$

Solving for α' from equation (7) and neglecting the negative root we have

$$\alpha' = \frac{\beta}{18\mathrm{VTA}}\left[-1 + (1+\delta)^{\frac{1}{2}}\right],$$

Table 2. Thermal Expansion Coefficient

Compound	Cp. Sp. heat at 298 °K Kcal deg.$^{-1}$ mole^{-1} [15—18]	$\frac{1}{4}\delta = \frac{9\,VTCpA^2}{\beta} \times 10^2$	Coefficient of Linear thermal expansion $\times 10^6$ at 298 °K/deg.	
			Calculated	Observed [6, 14]
LiF	10.04	3.65	27.80	34.0
Cl	12.20	6.07	39.80	44.0
Br	12.40	7.00	42.60	50.0
I	13.00	8.00	47.60	49.0
NaF	11.00	5.00	33.20	36.0
Cl	11.88	8.50	44.10	40.0
Br	12.50	8.50	46.00	43.0
I	13.00	9.80	49.10	48.3
KF	11.73	7.20	39.20	36.70
Cl	12.31	9.40	46.80	38.30
Br	12.82	10.55	50.20	40.00
I	13.16	12.00	54.00	45.00
RbF	12.20	10.70	40.60	—
Cl	12.30	10.30	47.50	36.00
Br	12.68	11.00	51.00	38.00
I	12.50	12.20	52.60	43.00
CsCl	12.62	12.50	50.00	56.00
BeO	6.10	0.45	3.7	5.3
MgO	8.87	0.58	6.5	10.3
CaO	10.20	0.86	8.4	11.6
SrO	10.76	1.44	9.5	13.7
BaO	11.10	0.99	10.4	13.0
CaS	11.35	0.83	11.1	—

where

$$\delta = \frac{36\,VTCpA^2}{\beta}$$

The average value of δ for the alkali halides is 0.35 and that for the alkaline earth chalcogenides is 0.03. Hence expanding $(1 + \delta)^{\frac{1}{2}}$ and neglecting terms higher than the quadratic which causes an error of less than 1 per cent and simplifying we have

$$\alpha' = ACp\left(1 - \frac{1}{4}\delta\right) \tag{8}$$

Thus for alkali halides by using Cv instead of Cp one makes an error of 5–10 per cent and of 0.5–1.5 per cent for alkaline earth chalcogenides if thermal expansion

coefficients are calculated at room temperature. To avoid this the accurate equation (8) has been used for the calculation of α'. The calculated values together with experimental observations are given in Table 2.

To account for the polarization of ions KUMAR [14] used in his calculations certain empirical factors. It may however be noted that even though the authors have not resorted to any such empirical factors the agreement with observed values is satisfactory.

Gruneisen Constant

From equations (4), (5a) and (5b) we can write

$$\alpha' = -\frac{C_v}{2\gamma_0} \cdot \frac{(d^3\varphi/d\gamma^3)}{(d^2\varphi/d\gamma^2)^2}$$

It is well known that the Gruneisen constant is

$$\gamma = \frac{3\alpha' v}{c_v \beta}$$

Substituting the value of α' we get

$$\gamma = -\frac{3v}{2\beta\gamma_0} \cdot \frac{(d^3\varphi/d\gamma^3)}{(d^2\varphi/d\gamma^2)^2}$$

But $\beta = +(gv/\gamma_0^2)(d^2\varphi/d\gamma^2)^{-1}$ assuming $\varkappa$ to be unity in equation [3].

$$\gamma = -\frac{1}{6}\gamma_0 \frac{(d^3\varphi/d\gamma^3)}{(d^2\varphi/d\gamma^2)}$$

An identical relation was obtained by MEINCKE [19] from quantum mechanical considerations.

Acknowledgement

The authors are thankful to Dr. A. B. BISWAS for his critical comments on and helpful suggestions for this paper. One of us (C. D. DAS) is thankful to the Council of Scientific and Industrial Research Organization, India, for the award of a Junior Research Fellowship while this work was being done.

References

[1] PAULING, L.: Proc. Roy. Soc. **114** (1927) 181; J. Amer. Chem. Soc. **49** (1927) 765; Z. Krist. **67** (1928) 377.
[2] SHERMAN, J.: Chem. Rev. **11** (1932) 93.
[3] FOWLER, R. H.: Statistical Mechanics, Cambridge University Press 1955.
[4] MOLIERE, K.: Landolt Bodenstein, Springer-Verlag, Berlin 1955, Vol. **1**, Part IV, p. 534.

[5] CUBBICCIOTTI, D.: J. Chem. Phys. **31** (1959) 1646.
[6] HUGGINS, M. L., and Y. Sakamoto: J. Phys. Soc. Japan **12** (1957) 241.
[7] SEITZ, F.: The Modern Theory of Solids, McGraw Hill, New York 1940.
[8] HUGGINS, M. L.: J. Chem. Phys. **5** (1937) 143; **15** (1947) 212.
[9] HILDEBRAND, J. H.: Z. Phys. **67** (1931) 127.
[10] MAYER, J. E.: Z. Phys. **61** (1930) 798.
[11] MAYER, J. E., and L. HELMHOLTZ: Z. Phys. **75** (1932) 19.
[12] MOELWYN HUGHES, E. A.: States of Matter, Oliver and Boyd, Edinburgh and London 1961.
[13] BRIDGMAN, P. W.: Phys. Rev. **57** (1940) 237.
[14] KUMAR, S.: Proc. Nat. Inst. Sci. India **25A** (1959) 364.
[15] Selected Values of Chemical Thermodynamic Properties (1952). Circ. No. 500 U.S. Bur. Stand.
[16] KELLEY, K. K.: Bull. U.S. Bur. Min. (1934) 371; J. Amer. Chem. Soc. **61** (1939) 1217.
[17] PARKS, G. S., and K. K. KELLEY: J. Phys. Chem. **30** (1926) 47.
[18] ANDERSON, C. T.: J. Amer. Chem. Soc. **57** (1935) 429; **53** (1931) 476.
[19] MEINCKE, P. P. M.: Canad. J. Phys. **40** (1962) 283.

Reprinted from the *Indian Journal of Chemistry*, 1964, Vol. 2, No. 1, pp. 27, 28

Imperfect Vapour Phase, Compressibility & Force Constants of Liquids*

R. V. Gopala Rao, H. V. Keer & C. D. Das
National Chemical Laboratory, Poona 8

Manuscript received 30 *August* 1963

Assuming the vapour phase of fluids to be imperfect, a relation between vapour pressure, compressibility coefficient and intermolecular energy constant (C_1) of liquids has been derived from the idea of continuity of states by using the virial equation. The derived relation has been applied to a number of liquids and the calculated values of C_1 are in good agreement with observed values.

IT is well known from statistical mechanical methods[1-6] that the pressure can be expressed as an inverse power of volume. Actually the pressure of a fluid as a polynomial of $1/V$ has been successfully used in correlating a number of physical properties of fluids by the present authors[7,8]. In the previous paper[8], assuming the vapour phase to be ideal, an equation was derived for $C_1 \equiv \left[\frac{\partial(1/\beta)}{\partial P}\right]_T$ which has been proved to be a constant for non-polar as well as polar liquids and related to intermolecular energy constants[9,10]. Although the agreement was excellent for non-polar liquids, the deviations for polar liquids were marked. In the present communication it is shown how a consideration of the imperfection of the vapour phase can improve the agreement in the case of polar liquids as well.

Assuming the polynomial to be of the 5th order, the following equations can be written:

$$P = \frac{RT}{V_g} + \frac{B_2}{V_g^2} + \frac{B_3}{V_g^3} + \frac{B_4}{V_g^4} + \frac{B_5}{V_g^5} \quad \ldots\ldots\ldots (1)$$

$$P = \frac{RT}{V_l} + \frac{B_2}{V_l^2} + \frac{B_3}{V_l^3} + \frac{B_4}{V_l^4} + \frac{B_5}{V_l^5} \quad \ldots\ldots\ldots (2)$$

$$P(V_g - V_l) = RT\ln\left(\frac{V_g}{V_l}\right) + B_2\left(\frac{1}{V_l} - \frac{1}{V_g}\right) + \frac{B_3}{2}\left(\frac{1}{V_l^2} - \frac{1}{V_g^2}\right) + \frac{B_4}{3}\left(\frac{1}{V_l^3} - \frac{1}{V_g^3}\right) + \frac{B_5}{4}\left(\frac{1}{V_l^4} - \frac{1}{V_g^4}\right) \quad \ldots (3)$$

*Communication No. 620 from the National Chemical Laboratory, Poona 8.

$$\frac{1}{\beta} = \frac{RT}{V_l} + \frac{2B_2}{V_l^2} + \frac{3B_3}{V_l^3} + \frac{4B_4}{V_l^4} + \frac{5B_5}{V_l^5} \quad \ldots\ (4)$$

$$\frac{C_1}{\beta} = \frac{RT}{V_l} + \frac{4B_2}{V_l^2} + \frac{9B_3}{V_l^3} + \frac{16B_4}{V_l^4} + \frac{25B_5}{V_l^5} \quad \ldots\ (5)$$

Assuming that the vapour phase of fluids does not obey the ideal gas law, it can be represented as

$$P = \frac{RT}{V_g} + \frac{B_2}{V_g^2}$$

Hence equation (1) reduces to

$$O = B_3 + \frac{B_4}{V_g} + \frac{B_5}{V_g^2} \quad \ldots\ (6)$$

and equation (3) to

$$(RT - PV_l) = RTln\left(\frac{V_g}{V_l}\right) + B_2\left(\frac{1}{V_l} - \frac{2}{V_g}\right) + \frac{B_3}{2}\left(\frac{1}{V_l^2} - \frac{1}{V_g^2}\right) + \frac{B_4}{3}\left(\frac{1}{V_l^3} - \frac{1}{V_g^3}\right) + \frac{B_5}{4}\left(\frac{1}{V_l^4} - \frac{1}{V_g^4}\right)$$

Therefore, neglecting V_l in comparison with V_g, we get

$$RT - RTln\left(\frac{V_g}{V_l}\right) = \frac{B_2}{V_l} + \frac{B_3}{2V_l^2} + \frac{B_4}{3V_l^3} + \frac{B_5}{4V_l^4} \quad \ldots\ (7)$$

Calculation of $ln(V_g/V_l)$

Since $P = RT/V_g + B_2/V_g^2$

$$\therefore V_g = \tfrac{1}{2}\left[\frac{RT}{P} + \sqrt{\left(\frac{R^2T^2}{P^2} + \frac{4B_2}{P}\right)}\right]^*$$

$$= \tfrac{1}{2}\left[\frac{RT}{P} + \frac{RT}{P}\left(1 + \frac{4B_2P}{R^2T^2}\right)^{\frac{1}{2}}\right]$$

Since $4B_2P/R^2T^2 \ll 1$ by expanding and neglecting higher terms we have

$$V_g = \tfrac{1}{2}\left[\frac{RT}{P} + \frac{RT}{P}\left(1 + \frac{2B_2P}{R^2T^2}\right)\right]$$

$$\frac{V_g}{V_l} = \frac{RT}{PV_l}\left(1 + \frac{B_2P}{R^2T^2}\right)$$

$$ln\left(\frac{V_g}{V_l}\right) = ln\left(\frac{RT}{PV_l}\right) + ln\left(1 + \frac{B_2P}{R^2T^2}\right)$$

Again expanding the last logarithmic term in the above equation and neglecting higher terms we get

$$ln\left(\frac{V_g}{V_l}\right) = ln\left(\frac{RT}{PV_l}\right) + \frac{B_2P}{R^2T^2} \quad \ldots\ (8)$$

Substituting equation (8) in equation (7)

$$RT(1 - lnx) = B_2\left(\frac{1}{V_l} + \frac{P}{R^2T^2}\right) + \frac{B_3}{2V_l^2} + \frac{B_4}{3V_l^3} + \frac{B_5}{4V_l^4} \quad \ldots\ (9)$$

where $x = RT/PV_l$. Solving the determinant for C_1 from Eqs. (2), (4), (5), (6) and (9) and neglecting minor terms as in the previous case[8], we get

$$(10 - C_1) = \beta Px(12lnx - 31) \quad \ldots\ (10)$$

The above equation has been applied to both polar and non-polar liquids.

*The other root is not considered since it is negative which cannot be the case.

Table 1 — Calculated and Experimental Values of C_1 for Different Fluids

Liquid	Present work	Exp.	Previous work
Hydrocarbons			
Pentane	8·09	—	6·74
Hexane	8·47	7·75	7·58
Heptane	8·47	—	7·65
Octane	8·60	8·5	7·96
Benzene	8·36	8·0	7·40
Toluene	8·41	8·0	7·56
Ethers			
Methyl acetate	8·30	8·0	7·23
Ethyl acetate	8·37	8·0	7·44
Ethyl propionate	8·44	8·0	7·64
Methyl butyrate	8·45	8·5	7·64
Ethyl butyrate	8·49	8·5	7·61
Alcohols			
Water	3·70	4·6	2·3
Methyl alcohol	5·75	8·8	2·0
Ethyl alcohol	6·47	5·4	3·4
Amyl alcohol	7·93	6·0	5·7
Isoamyl alcohol	7·76	8·7	6·2
n-Butyl alcohol	7·52	9·0	5·7
tert-Butyl alcohol	7·30	10·0	6·7
Miscellaneous			
Carbon tetrachloride	8·41	8·6	7·5
Mercury	9·88	6·8	8·1
Carbon disulphide	8·20	7·5	7·0
Chloroform	8·28	8·2	7·2
Valeric acid	7·54	9·5	—

The agreement between calculated and observed values of C_1 appears to have been improved considerably.

Further, it may be pointed out that Eq. (10) gives, in general, higher values while the previous equation with ideal gas assumption gave lower values[8]. Thus it appears that the assumption of non-ideality appears to give better agreement with experiment as expected because as is well known highly polar vapours are imperfect in the vapour phase even at lower pressures. The present calculated values, and the experimental and previous calculated values[8] are given in Table 1.

The authors are thankful to Dr A. B. Biswas for his keen interest in this work.

References

1. Mayer, J. E. & Mayer, M. G., *Statistical mechanics* (John Wiley & Sons Inc., New York), 1940.
2. Mayer, J. E., *J. chem. Phys.*, **5** (1937), 67.
3. Mayer, J. E. & Ackermann, P. G., *J. chem. Phys.*, **5** (1937), 74.
4. Mayer, J. E. & Harrison, S. F., *J. chem. Phys.*, **6** (1938), 87.
5. Mayer, J. E. & Harrison, S. F., *J. chem. Phys.*, **6** (1938), 101.
6. Mayer, J. E., *J. chem. Phys.*, **19** (1951), 1024.
7. Rao, R. V. G. & Li, J. C. M., *Z. phys. Chem.*, **213** (1960), 166.
8. Rao, R. V. G., Keer, H. V. & Das, C. D., *Z. phys. Chem.*, **220** (1962), 71.
9. Moelwyn Hughes, E. A., *J. chem. Phys.*, **55** (1951), 1246.
10. Rao, R. V. G. & Keer, H. V., *Z. phys. Chem.*, **219** (1962), 321.

Reprinted from the *Indian Journal of Chemistry*, 1964, Vol. 2, No. 1, pp. 29, 30

A Finite Virial Expansion of Fluid State*

R. V. Gopala Rao, C. D. Das & H. V. Keer
National Chemical Laboratory, Poona 8

Manuscript received 30 *August* 1963

A method has been outlined to extend the virial equation so as to include a finite number of higher virial coefficients. An equation has been derived between

$$C_1 \equiv \left[\frac{\partial(1/\beta)}{\partial P}\right]_T$$

vapour pressure and compressibility coefficient using the virial equation up to the seventh virial coefficient. The equation has been applied to a number of polar liquids and the calculated values of C_1 are in good agreement with the observed values.

IT is customary to represent the pressure (P) of a fluid as a polynomial of V^{-1} so as to correlate the various equilibrium properties of fluids[1,2]. It is also known that the complete equation of fluids must be of odd degree in V, for the volume increases with diminishing pressure at both ends of the P-V curve. Further, the equation must be of at least third degree in volume since a certain pressure may correspond to more than one volume. Thus the famous van der Waals equation satisfying these conditions has been of great use in interpreting the relations of liquid and vapour. In the previous paper[2] the equation of the fifth degree in volume has been successfully used to obtain a relation between vapour pressure and intermolecular energy constants of liquids. In the present communication it is demonstrated how such a representation can be extended to use the higher powers of volume.

Thus by adopting the method previously described by the authors[1,2] and extending it up to the seventh power, the following equations can be written:

$$P = \frac{RT}{V_g} + \frac{B_2}{V_g^2} + \frac{B_3}{V_g^3} + \frac{B_4}{V_g^4} + \frac{B_5}{V_g^5} + \frac{B_6}{V_g^6} + \frac{B_7}{V_g^7} \quad \ldots\ldots (1)$$

$$P = \frac{RT}{V_l} + \frac{B_2}{V_l^2} + \frac{B_3}{V_l^3} + \frac{B_4}{V_l^4} + \frac{B_5}{V_l^5} + \frac{B_6}{V_l^6} + \frac{B_7}{V_l^7} \quad \ldots\ldots (2)$$

$$RT(1-lnx) = \frac{B_2}{V_l} + \frac{B_3}{2V_l^2} + \frac{B_4}{3V_l^3} + \frac{B_5}{4V_l^4} + \frac{B_6}{5V_l^5} + \frac{B_7}{6V_l^6} \quad (3)$$

$$1/\beta = \frac{RT}{V_l} + \frac{2B_2}{V_l^2} + \frac{3B_3}{V_l^3} + \frac{4B_4}{V_l^4} + \frac{5B_5}{V_l^5} + \frac{6B_6}{V_l^6} + \frac{7B_7}{V_l^7} \quad \ldots (4)$$

$$\frac{C_1}{\beta} = \frac{RT}{V_l} + \frac{4B_2}{V_l^2} + \frac{9B_3}{V_l^3} + \frac{16B_4}{V_l^4} + \frac{25B_5}{V_l^5} + \frac{36B_6}{V_l^6} + \frac{49B_7}{V_l^7} \quad (5)$$

where R is universal gas constant; T, temperature in absolute degrees; V_g, volume of gas; V_l, volume of liquid; $B_2, B_3 \ldots B_7$, the virial coefficients; β, the compressibility coefficient; $C_1 \equiv \left[\frac{\partial(1/\beta)}{\partial P}\right]_T$; and $x = RT/PV_l$.

It has been shown[3,4] that both for non-polar as well as polar liquids, the pressure change of bulk modulus is constant and was related to intermolecular energy constants (C_1). Hence Eq. (5) can be differentiated and further equations can be obtained to solve for higher virial coefficients in any finite virial expansion.

Thus if we differentiate Eq. (5) twice we get the following two equations:

$$\frac{C_1^2}{\beta} = \frac{RT}{V_l} + \frac{8B_2}{V_l^2} + \frac{27B_3}{V_l^3} + \frac{64B_4}{V_l^4} + \frac{125B_5}{V_l^5} + \frac{216B_6}{V_l^6} + \frac{343B_7}{V_l^7} \quad \ldots\ldots (6)$$

$$\frac{C_1^3}{\beta} = \frac{RT}{V_l} + \frac{16B_2}{V_l^2} + \frac{81B_3}{V_l^3} + \frac{256B_4}{V_l^4} + \frac{625B_5}{V_l^5} + \frac{1296B_6}{V_l^6} + \frac{2401B_7}{V_l^7} \quad \ldots\ldots (7)$$

This procedure can be extended to include higher virial coefficients by differentiating Eq. (7) and so on.

From Eqs. (1) to (7) one can solve for $1/\beta$ in a straightforward way and get

$$C_1^3 - 24C_1^2 + 221C_1 - 954 = \frac{RT\beta}{V_l}(1764 - 720lnx) - 1800P\beta$$

In deriving the above relation it was assumed that the vapour behaves ideally and that the volume of liquid is negligible in comparison with that of vapour. In the above equation the term $1800P\beta$ is of the order of 10^{-3} whereas the other terms are very large and hence can be safely neglected. Therefore, the above equation reduces to

$$C_1^3 - 24C_1^2 + 221C_1 - 954 = \frac{RT\beta}{V_l}(1764 - 720lnx) \quad \ldots (8)$$

Thus Eq. (8) gives a relation between compressibility, vapour pressure and C_1. Since the equation is cubic in C_1, it has three possible values. The solution actually gives one real and two imaginary roots† and hence only the real value is considered.

Eq. (8) has been applied to a number of liquids and the calculated values of C_1 are found to be in

TABLE 1 — EXPERIMENTAL AND CALCULATED VALUES OF C_1

Liquid	Temp. °C.	V_l ml.	P mm. (ref. 5, 6)	βX (10^6 atm.$^{-1}$) (ref. 5, 7, 8)	C_1 Calc.	C_1 Exp. (ref. 5, 7, 9)
Water	20	18·0	17·50	47·0	4·07	4·60
Methyl alcohol	0	40·0	30·00	90·0	6·40	8·80
Ethyl alcohol	0	57·0	12·20	100·0	7·80	5·40
Amyl alcohol	18	108·0	2·50	91·0	10·43	6·00
Isoamyl alcohol	20	109·0	2·30	99·0	10·18	8·70
n-Butyl alcohol	20	92·0	4·30	97·0	9·83	9·00
tert-Butyl alcohol	20	74·1	30·60	108·0	9·48	10·00
Ethyl chloride	0	70·0	485·00	135·0	8·70	10·14
Ethyl bromide	20	76·2	386·00	114·6	9·47	10·45
Isobutyl alcohol	20	92·5	8·70	105·3	9·90	12·60
n-Propyl alcohol	20	75·0	14·50	89·6	9·85	8·90
Ethyl iodide	20	80·6	108·50	98·8	10·76	9·60
Valeric acid	20	108·0	0·45	90·0	9·84	9·50

*Communication No. 616 from the National Chemical Laboratory, Poona 8.

†A cubic equation of the type $y^3 + py^2 + qy + r = 0$ can be reduced to the form $X^3 + aX + b = 0$, with $y = x - p/3$, $a = 1/3(3q - p^2)$ and $b = 1/27(2p^3 - 9pq + 27r)$. So if $b^2/4 + a^3/27 > 0$ then there will be one real and two conjugate imaginary roots which is the case with Eq. (8).

good agreement with the experimental values in the case of polar liquids (Table 1). It may be pointed out at this stage that even though a method has been outlined in this paper for using higher virial coefficients, the procedure may not give accurate results since successive differentiations of Eq. (5) make Eqs. (6) and (7) approximate as any slight inaccuracies in the experimental values will be exaggerated. Unfortunately Eq. (8) has been found to give higher values in the case of non-polar liquids. However, it is important to realize that in principle one can find a method of using higher virial coefficients for finding equilibrium properties provided accurate data of compressibility are available.

The authors are thankful to Dr A. B. Biswas for his keen interest in this work.

References

1. Rao, R. V. G. & Li, J. C. M., *Z. phys. Chem.*, **213** (1960), 166.
2. Rao, R. V. G., Keer, H. V. & Das, C. D., *Z. phys. Chem.*, **220** (1962), 71.
3. Moelwyn Hughes, E. A., *J. chem. Phys.*, **55** (1951), 1246.
4. Rao, R. V. G. & Keer, H. V., *Z. phys. Chem.*, **219** (1962), 321.
5. *International critical tables*, Vol. III (McGraw-Hill Book Co. Inc., New York), 1928, 40.
6. Jordan, J. E., *Vapour pressures of organic compounds* (Interscience Publishers Inc., New York), 1954.
7. Landolt, Bodenstein, Roth & Scheel, *Physikalische chemie*, Part I (Edwards Brothers Inc., Michigan), 1943, 88.
8. Rowlinson, J. S., *Liquids and liquid mixtures* (Butterworths Scientific Publications, London), 1939.
9. Moelwyn Hughes, E. A., *Physical chemistry* (Pergamon Press Ltd, Oxford), 1957, 324.

A C K N O W L E D G E M E N T

The author wishes to express his sincere appreciation to Dr. A.B. Biswas for his suggestion and supervision of this research.

He is indebted to Dr. R.V. Gopala Rao for his keen interest and valuable advice during the course of this work.

He is grateful to all his colleagues, in particular to Sri H.V. Keer and Sri S.G. Sankar for their ungrudging cooperation and to Sri K.B. Kaushal for fabricating the high-vacuum glass system.

He wishes to acknowledge his indebtedness to the Director, National Chemical Laboratory, Poona-8 for his kind permission to submit this work in the form of a thesis and to the Council of Scientific and Industrial Research, New Delhi for the award of a research fellowship during the period 1961-63.

S Deenadas